

DOI: 10.31891/2079-1372

THE INTERNATIONAL SCIENTIFIC JOURNAL

***PROBLEMS
OF
TRIBOLOGY***

Volume 28

No 1/107-2023

МІЖНАРОДНИЙ НАУКОВИЙ ЖУРНАЛ

ПРОБЛЕМИ ТРИБОЛОГІЇ

PROBLEMS OF TRIBOLOGY

INTERNATIONAL SCIENTIFIC JOURNAL

Published since 1996, four time a year

Volume 28 No 1/107-2023

Establishers:

Khmelnitskiy National University (Ukraine)
Lublin University of Technology (Poland)

Associated establisher:

Vytautas Magnus University (Lithuania)

Editors:

O. Dykha (Ukraine, Khmel'nitskiy), **M. Pashechko** (Poland, Lublin), **J. Padgurskas** (Lithuania, Kaunas)

Editorial board:

V. Aulin (Ukraine, Kropivnitskiy),
P. Blau (USA, Oak Ridge),
B. Bhushan (USA, Ohio),
V. Voitov (Ukraine, Kharkiv),
Hong Liang (USA, Texas),
E. Ciulli (Italy, Pisa),
V. Dvoruk (Ukraine, Kiev),
M. Dzimko (Slovakia, Zilina),
M. Dmitrichenko (Ukraine, Kiev),
L. Dobzhansky (Poland, Gliwice),
G. Kalda (Ukraine, Khmel'nitskiy),
T. Kalaczynski (Poland, Bydgoszcz),
M. Kindrachuk (Ukraine, Kiev),
Jeng-Haur Horng (Taiwan),
L. Klimentenko (Ukraine, Mykolaiv),
K. Lenik (Poland, Lublin),

O. Mikosianchyk (Ukraine, Kiev),
R. Mnatsakanov (Ukraine, Kiev),
J. Musial (Poland, Bydgoszcz),
V. Oleksandrenko (Ukraine, Khmel'nitskiy),
M. Opielak (Poland, Lublin),
G. Purcek (Turkey, Karadeniz),
V. Popov (Germany, Berlin),
V. Savulyak (Ukraine, Vinnitsa),
A. Segall (USA, Vancouver),
T. Skoblo (Ukraine, Kharkiv),
M. Stechyshyn (Ukraine, Khmel'nitskiy),
M. Chernets (Poland, Lublin),
V. Shevelya (Ukraine, Khmel'nitskiy),
Zhang Hao (China, Peking),
M. Śniadkowski (Poland, Lublin),
D. Wójcicka-Migasiuk (Poland, Lublin)

Executive secretary: O. Dytyuk

Editorial board address:

International scientific journal "Problems of Tribology",
Khmelnitskiy National University,
Institutskaia str. 11, Khmel'nitskiy, 29016, Ukraine
phone +380975546925

Indexed: CrossRef, DOAJ, Ulrichsweb, Google Scholar, Index Copernicus

E-mail: tribology@khnmu.edu.ua

Internet: <http://tribology.khnmu.km.ua>

ПРОБЛЕМИ ТРИБОЛОГІЇ

МІЖНАРОДНИЙ НАУКОВИЙ ЖУРНАЛ

Видається з 1996 р.

Виходить 4 рази на рік

Том 28

№ 1/107-2023

Співзасновники:

Хмельницький національний університет (Україна)
Університет Люблінська Політехніка (Польща)

Асоційований співзасновник:

Університет Вітовта Великого (Литва)

Редактори:

О. Диха (Хмельницький, Україна), М. Пашечко (Люблін, Польща),
Ю. Падгурскас (Каунас, Литва)

Редакційна колегія:

В. Аулін (Україна, Кропивницький),
П. Блау (США, Оук-Ридж),
Б. Бхушан (США, Огайо),
В. Войтов (Україна, Харків),
Хонг Лян (США, Техас),
Е. Чуллі (Італія, Піза),
В. Дворук (Україна, Київ),
М. Дзимко (Словачія, Жиліна)
М. Дмитриченко (Україна, Київ),
Л. Добжанський (Польща, Глівіце),
Г. Калда (Україна, Хмельницький),
Т. Калачинські (Польща, Бидгощ),
М. Кіндрачук (Україна, Київ),
Дженг-Хаур Хорнг (Тайвань),
Л. Клименко (Україна, Миколаїв),
К. Ленік (Польща, Люблін),

О. Микосянчик (Україна, Київ),
Р. Мнацаканов (Україна, Київ),
Я. Мушял (Польща, Бидгощ),
В. Олександренко (Україна, Хмельницький),
М. Опеляк (Польща, Люблін),
Г. Парсек (Турція, Караденіз),
В. Попов (Германія, Берлін),
В. Савуляк (Україна, Вінниця),
А. Сігал (США, Ванкувер),
Т. Скобло (Україна, Харків),
М. Стечишин (Україна, Хмельницький),
М. Чернець (Польща, Люблін),
В. Шевеля (Україна, Хмельницький),
Чжан Хао (Китай, Пекин),
М. Шнядковський (Польща, Люблін),
Д. Войцицька-Мігасюк (Польща, Люблін),

Відповідальний секретар: О.П. Дитинюк

Адреса редакції:

Україна, 29016, м. Хмельницький, вул. Інститутська 11, к. 4-401
Хмельницький національний університет, редакція журналу "Проблеми трибології"
тел. +380975546925, E-mail: tribology@khmnu.edu.ua

Internet: <http://tribology.khnu.km.ua>

Зареєстровано Міністерством юстиції України
Свідоцтво про держреєстрацію друкованого ЗМІ: Серія КВ № 1917 від 14.03. 1996 р.
(перереєстрація № 24271-1411 ППР від 22.10.2019 року)

Входить до переліку наукових фахових видань України
(Наказ Міністерства освіти і науки України № 612/07.05.19. Категорія Б.)

Індексується в МНБ: CrossRef, DOAJ, Ulrichsweb, Google Scholar, Index Copernicus

Рекомендовано до друку рішенням вченої ради ХНУ, протокол № 12 від 23.02.2023 р.

© Редакція журналу "Проблеми трибології (Problems of Tribology)", 2023



Problems of Tribology, V. 28, No 1/107-2023

Problems of Tribology

Website: <http://tribology.khnu.km.ua/index.php/ProbTrib>

E-mail: tribosensor@gmail.com

CONTENTS

A. Milanenko. Influence of microgeometry in the point contact zone of rest friction on fatigue life for friction bearing units.....	6
V.D. Makarenko, O.I.Kliuiev, O.A.Voitovych, Yu. Ye. Mieshkov, Yu.V. Makarenko. Study of frictional properties, long-term (cyclic) strength of materials of brake pads of motor vehicles.....	13
M.S. Stechishyn, M.Ye. Skyba, A.V. Martynyuk, D.V. Zdorenko. Wear resistance of structural steels nitrided in a cyclically switched discharge with dry friction.....	20
A.V. Voitov. Mathematical model of running-in of tribosystems under conditions of boundary lubrication. Part 1. Development of a mathematical model.....	25
O.A. Ilina, O.O. Mikosianchyk, O. P. Yashchuk, R.H. Mnatsakanov, N.M. Berezivskiy. Tribomonitoring of the quality of aviation hydraulic oils according to lubricity and rheological indicators.....	34
K. Holenko, O. Dykha, J. Padgurskas, O. Babak. Thermal and stress-strain state of friction pairs in ventilated disc brakes of lightweight vehicles.....	41
E.K. Solovykh, I.V. Shepelenko*, M.I. Chernovol, S.O. Mahopets, A.E. Solovuch, S.E. Katerynych. Optimization of the technology for applying discrete coatings in restoration of bronze parts by electrospark alloying.....	51
O.V. Berezyuk, V.I. Savulyak, V.O. Kharzhevskiy. Establishing the peculiarities of tire wear of garbage trucks during the transportation of municipal solid waste.....	59
D.D. Marchenko, K.S. Matvyeyeva. Increasing the Wear Resistance of Restored Car Parts by Using Electrospark Coatings.....	65
A. Lopata, I. Smirnov, M. Holovashchuk, V. Lopata. Investigation of the properties of coatings obtained by electric arc spraying.....	73
V.V. Aulin, S.V. Lysenko, A.V. Hrynkyv, A.A. Tykhyi, O.V. Kuzyk, O.M. Livitskyi. The regularity of the change in the coefficient of friction of the coupling of "shaft-sleeve" parts using polymeric materials.....	81
Rules of the publication	92



ЗМІСТ

Міланенко О.А. Вплив мікрогеометрії в зоні точкового контакту на втомну довговічність в умовах тертя спокою для підшипникових вузлів тертя.....	6
Макаренко В. Д., Ключев О. І., Войтович О. А., Мешков Ю. Є., Макаренко Ю.В. Дослідження фрикційних властивостей, тривалої (циклічної) міцності матеріалів гальмових колодок автотранспорту.....	13
Стечишин М.С., Скиба М.Є., Мартинюк А.В., Здоренко Д.В. Зносостійкість конструкційних сталей, азотованих в циклічно-комутованому розряді при сухому терті.....	20
Войтов А.В. Математична модель припрацювання трибосистем в умовах граничного навантаження. Частина 1. Розробка математичної моделі.....	25
Льбіна О. А., Мікосянчик О. О., Ящук О. П., Мнацаканов Р.Г., Березівський Н.М. Трибомоніторинг якості авіаційних гідравлічних олиव за змащувальними та реологічними показниками.....	34
Іголенко К.Е., Диха О.В., Падгурскас Ю., Бабак О.П. Термічний та напружено-деформований стан пар тертя вентиляованих дискових гальм легких транспортних засобів.....	41
Солових Е.К., Шепеленко І.В., Черновол М.І., Магопець С.О., Солових А.Е., Катеринич С.Е. Оптимізація технології нанесення дискретних покриттів при відновленні бронзових деталей електроіскровим легуванням.....	51
Березюк О.В., Савуляк В.І., Харжевський В.О. Встановлення закономірностей зносу шин сміттєвозів під час транспортування твердих побутових відходів.....	59
Марченко Д.Д., Матвеева К.С. Підвищення зносостійкості відновлених деталей автомобілів шляхом застосування електроіскрових покриттів.....	65
Лопата О.В., Смирнов І.В., Головащук М.В., Лопата В.М. Дослідження властивостей покриттів, отриманих електродуговим напиленням.....	73
Аулін В.В., Лисенко С.В., Гриньків А.В., Тихий А.А., Кузик О.В., Лівіцький О.М. Закономірність зміни коефіцієнта тертя спряження деталей "вал-втулка" з використанням полімерних матеріалів.....	81
Вимоги до публікацій	92



Influence of microgeometry in the point contact zone of rest friction on fatigue life for friction bearing units

A. Milanenko¹

¹*National Transport University, Kyiv, Ukraine*

**E-mail: milanmasla@gmail.com*

Received: 11 December 2022; Revised: 20 January 2023; Accept: 02 February 2023

Abstract

A comprehensive methodology has been developed to assess the maximum contact stresses and deformations in the point contact zone and the maximum tangential stresses, including their position in the subsurface zone in depth and in the rolling direction when the microgeometry of the rest contact.

Key words: Point contact zone, fatigue life, friction bearing units (bearing assemblies), maximum contact stresses and deformations, maximum tangential stresses, microgeometry.

Introduction

One of the most important factors limiting the durability of bearing units is fatigue damage, namely pitting, which occurs during repeated cyclic loading. Since metal elements are damaged, fatigue is usually associated with the problem of metal stability and microgeometry of the contact zone. While fatigue life has been significantly increased by controlling the type and size of non-metallic inclusions, heat treatment and the introduction of alloying additives to the base metal, little or no thorough research has been paid to the influence of microgeometry in the contact zone, especially for bearing assemblies.

In any case, a comprehensive calculation methodology is needed that would allow to take into account the influence of microgeometry on the fatigue life of bearing units.

The purpose of the work

To develop a comprehensive methodology for assessing the influence of microgeometry on the maximum contact stresses and deformations in point contact, the maximum tangential stresses and their penetration position in the subsurface zone along the depth and direction of rolling under resting friction conditions.

1. Technique for researching the properties of coatings for the influence of microgeometry.

The method of calculating the maximum stresses, deformations, position and value of the maximum subsurface tangential stress is necessary to assess the fatigue life of friction bearing units [1].

Hydrodynamic lubrication is characterized by surfaces that fit well together, that is, surfaces that have a high degree of geometric similarity, and the load is transferred over a relatively larger plane. In addition, the actual plane for such surfaces remains virtually constant with increasing load.

But many bearings do not have a very good surface fit. The full load falls on a relatively small plane. As a rule, the actual contact area increases significantly with increasing load, but still remains small compared to surfaces that fit well together. The loads per unit area for adjacent bearings are relatively small, about 1 MPa and rarely 7 MPa. But the load per unit area in contacts with non-adjacent surfaces, like to the contacts of ball bearings, usually exceeds 700 MPa even with a moderate load on the bearing. Such high pressures lead to elastic deformation of the materials, resulting in elliptical contacts that can support these loads. Therefore, appropriate simplified calculations of stresses and deformations in the contacts of non-adjacent surfaces are required.

To model a real friction unit, it is necessary to know the field of static contact of interacting bodies. Determination of the properties of static contact of interacting parts in non-conformal (with local contact) nodes



is reduced to determining the type and type of contact field, maximum contact and tangential stresses and strains in the field and within the contact field (Fig. 1).

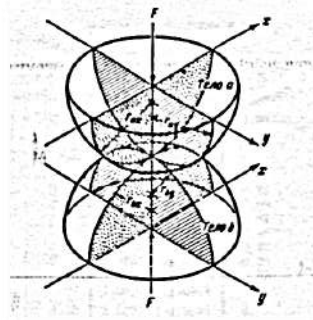


Fig. 1 - Geometry with point contact friction

In general, the geometry of undeformed contacting bodies can be represented by pressing two ellipsoids. Two bodies with different radii of curvature in the two principal planes (x and y), passing through the contact between the bodies, touch at one point at zero load. This state is called point contact, in which the radii of curvature are denoted by r (see Fig. 1). It is assumed that convex bodies have positive curvature and concave bodies have negative curvature. Thus, if the center of curvature lies inside the body, the radius of curvature is positive, otherwise it is negative.

It is important to note that if the choice of x and y coordinates satisfies the condition:

$$\frac{1}{r_{ax}} + \frac{1}{r_{bx}} \geq \frac{1}{r_{ay}} + \frac{1}{r_{by}}, \tag{1}$$

then the x-coordinate determines the direction of the minor semi-axis and the y-coordinate determines the major semi-axis of the contact ellipse that occurs when the load is applied. The direction of motion is always given along the x-axis. The sum of curvatures (reduced radius of curvature), which is necessary in the analysis of contact stresses and strains, is determined by the following formula:

$$\frac{1}{R} = \frac{1}{R_x} + \frac{1}{R_y}, \tag{2}$$

where:

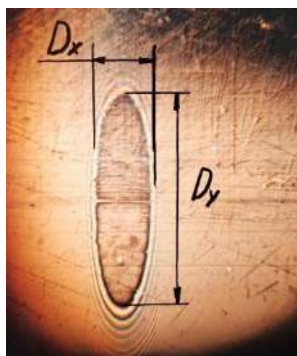
$$\frac{1}{R_x} = \frac{1}{r_{ax}} + \frac{1}{r_{bx}}, \tag{3}$$

$$\frac{1}{R_y} = \frac{1}{r_{ay}} + \frac{1}{r_{by}}. \tag{4}$$

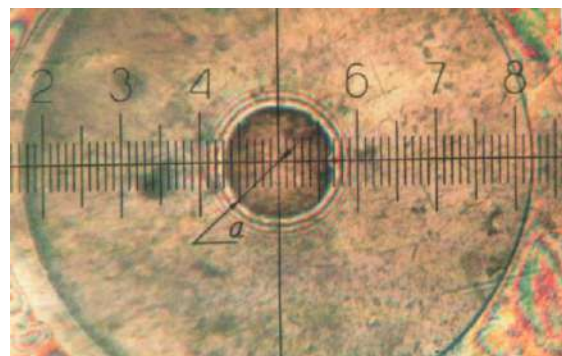
The ratio of radii of curves α is determined by the following formula:

$$\alpha = \frac{R_y}{R_x}. \tag{5}$$

The shape of the plane of such contacts is called point contacts. Point contacts can be elliptical (Fig. 2, a), when the ratio of radii of curvature $\alpha \neq 1$, or circular (Fig. 2, b), when $\alpha = 1$, since $r_{ax} = r_{ay}$ and $r_{bx} = r_{by}$, then according to expressions (3) and (4), it turns out that the radii of curvature $R_x = R_y = r/2$. If the radii of curvature r_{ay} and r_{by} are infinite, the initial linear contact is transformed into a rectangular contact under load.



a – elliptical contact



b – circular contact

Fig. 2 a, b. Shape of friction point contact at change of microgeometry, made by optical interferometry

The ellipticity parameter k is defined as the ratio of the diameter of the elliptical contact in the y direction (transverse direction) to the diameter in the x direction (direction of movement):

$$k \equiv \frac{D_y}{D_x}. \quad (6)$$

If condition (6) is satisfied and $\alpha \geq 1$, then the contact ellipse will be oriented with a large diameter across the direction of movement (see Fig. 2, *a*), i.e., $k \geq 1$, which is characteristic of the contact form formed in ball bearings with an outer ring and tubular roller bearings. Circular contact (see Fig. 2, *b*), where $\alpha = 1$, $k = 1$, is characteristic of ball bearings with self-aligning outer ring. In the elliptical contact, in which $\alpha < 1$, $k < 1$, the contact ellipse, on the contrary, will be oriented with a small diameter across the direction of movement and is characteristic of some gears and locomotive wheel contact on the rail (this option was not considered in this work).

If two elastic bodies are brought into contact under load, a plane appears, the shape and size of which depends on the applied load, the elastic properties of the materials and the microgeometry of the contact.

Under conditions of elastohydrodynamic (EHD) lubrication, two surfaces are separated by a lubricating layer, the thickness of which has the shape shown in Fig. 3.

With the usual parabolic approximation for the shape of an undeformed film, the thickness of the lubricating layer under deformation will be as follows:

$$h(x; y) = h_0 + \frac{x^2 + y^2}{2 \cdot R} + d(x; y) - d(0; 0), \quad (7)$$

where $x; y$ - Cartesian coordinates.

The total normal deformation $d(x_1; y_1)$ of two surfaces is defined by the following equation:

$$d(x_1; y_1) = \frac{1}{\pi \cdot E'} \iint_A \frac{p(x; y) \cdot dx \cdot dy}{((x - x_1)^2 + (y - y_1)^2)^{\frac{1}{2}}}, \quad (8)$$

where the reduced modulus of elasticity E' is equal:

$$E' = \frac{2}{\left(\frac{1 - \nu_1^2}{E_1} + \frac{1 - \nu_2^2}{E_2} \right)}, \quad (9)$$

where E_1 and E_2 are the elastic modulus of the 1st and 2nd bodies in contact with each other; $\nu_1; \nu_2$ are the Poisson's ratios of the 1st and 2nd bodies, respectively; $x_1; y_1$ are the nodal points along the x and y axes.

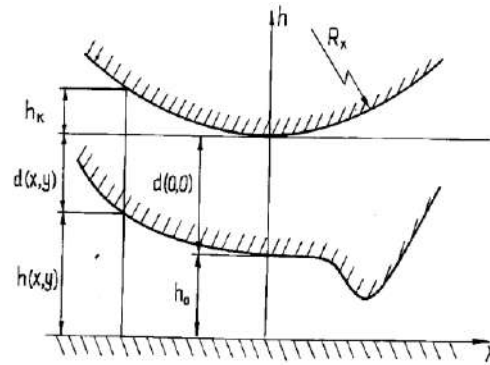


Fig. 3. Microgeometry of circular friction contact taking into account elastic deformations:

h_0 - central thickness of the lubricating layer; $d(0; 0)$ - the value of elastic deformation in the central contact area; $h(x; y)$, $d(x; y)$ - current value of thickness and deformation; $h_k = (x^2 + y^2)/2R$ - current value of thickness at $h_0 = 0$; R_x - equivalent radius of curvature in the X plane.

For an approximate calculation of deformations and stresses in point contact, a simplified calculation of stresses and deformations can be used according to the method [2], which allows solving the classical Hertz problem without the use of complex mathematical calculations on a computer using simplified formulas.

The classical Hertzian solution for deformations requires the calculation of the ellipticity parameters k and the calculation of elliptic integrals of the first ψ and second ϵ kind. For point friction contact, the parameters ψ and ϵ as functions of α are simplified by means of approximating curves. These parameters make it possible to determine the deformation δ in the center of contact with a small loss of accuracy, but without the use of complex mathematical calculations when using diagrams, as well as the maximum contact stress σ_{\max} in the center of contact depending on the ratio of the radii of the curves α .

The maximum contact stress in the center of the point contact σ_{\max} is calculated by the following formulas:

- for circular contact:

$$\sigma_{max} = \frac{3 \cdot F}{2 \cdot \pi \cdot a^2}, \quad (10)$$

where F is the applied load, N;

$a = \left(\frac{6 \cdot \varepsilon \cdot F \cdot R}{\pi \cdot E'} \right)^{\frac{1}{3}}$ – circumferential contact radius, m.

- for elliptical contact:

$$\sigma_{max} = \frac{6 \cdot F}{\pi \cdot D_y \cdot D_x}, \quad (11)$$

where F is the applied load, N;

$D_y = 2 \cdot \left((6 \cdot k^2 \cdot \varepsilon \cdot F \cdot R) / \pi \cdot E' \right)$ – diameter of the major axis of the elliptical contact, m (see Fig. 2, a);

$D_x = 2 \cdot \left((6 \cdot \varepsilon \cdot F \cdot R) / \pi \cdot k \cdot E' \right)$ – diameter of the small axis of the elliptical contact, m (see Fig. 2, a).

The maximum deformation in the central contact zone δ is calculated by the following formulas:

- for circular contact:

$$\delta = \psi \cdot \left[\left(\frac{4,5}{\varepsilon \cdot R} \right) \cdot \left(\frac{F}{\pi \cdot E'} \right)^2 \right]^{\frac{1}{3}}, \quad (12)$$

- for elliptical contact:

$$\delta = \psi \cdot \left[\left(\frac{4,5}{\varepsilon \cdot R} \right) \cdot \left(\frac{F}{\pi \cdot k \cdot E'} \right)^2 \right]^{\frac{1}{3}}. \quad (13)$$

One of the causes of wear is material fatigue caused by cyclic strong and elastic deformations on the surface. Fatigue cracks are formed at a certain depth in the plane parallel to the rolling direction. Therefore, special attention is paid to the amplitude of the tangential stress in the part of the plane where it reaches a maximum.

The value of the maximum tangential stress of the point contact max is determined by the formula:

$$\tau_{max} = \sigma_{max} \cdot \frac{\sqrt{2 \cdot t - 1}}{2 \cdot t \cdot (t + 1)}, \quad (14)$$

where $t = 1 + 0,16 \cdot \operatorname{csch}(\alpha^{2\pi}/2)$ – a reduced auxiliary parameter.

It should be noted that max represents the maximum half-amplitude of the subsurface orthogonal tangential stress.

Taking into account that the stresses are referred to a rectangular coordinate system with the origin at the center of contact, the z - axis coinciding with the internal normal of the body under consideration, the x - axis along the rolling direction and the y - axis perpendicular to it, we find the position of the maximum point (depth) max in the xz- plane:

- for the circular contact:

$$|Z_0| = \frac{a}{(t+1) \cdot \sqrt{2t-1}}; \quad (15)$$

$$|X_0| = \frac{t}{t+1} \cdot \sqrt{\frac{2t+1}{2t-1}} \cdot a, \quad (16)$$

- for elliptical contact:

$$|Z_0| = \frac{D_x}{2 \cdot (t+1) \cdot \sqrt{2t-1}}; \quad (17)$$

$$|X_0| = \frac{t}{t+1} \cdot \sqrt{\frac{2t+1}{2t-1}} \cdot \frac{D_x}{2}. \quad (18)$$

Results of calculations for the influence of microgeometry

Below are the input parameters of microgeometry, materials and values of elliptic integrals of the 1st and 2nd kinds for simplified calculation of stresses and strains of friction point contacts (respectively for circular and elliptic contacts) in the range $\alpha \leq 100$ (Table 1) for two selected bearings.

Table 1

The input parameters of microgeometry, materials and values of elliptic integrals of the 1st and 2nd kinds

Input and initial design parameters	Circular contact, $\alpha = 1$	Elliptical contact, $\alpha = 6$
1. The reduced radius of curvature, R_x , mm	6,35	15,24
2. Ellipticity parameter, k	1	5
3. Ellipticity parameter of the 1st kind, $\psi = \frac{\pi}{2} + \left(\frac{\pi}{2} - 1\right) \cdot \ln \alpha$	1,5708	2,5935
4. Ellipticity parameter of the 2nd kind, $\varepsilon = 1 + \left(\frac{\pi}{2} - 1\right) / \alpha$	1,5708	1,0951
5. Auxiliary parameter t	1,307	1,070
6. Modulus of elasticity E_1 , Pa	$2,07 \cdot 10^{11}$	$2,07 \cdot 10^{11}$
7. Modulus of elasticity E_2 , Pa	$0,757 \cdot 10^{11}$	$0,757 \cdot 10^{11}$
8. Poisson's ratio ν_1	0,30	0,30
9. Poisson's ratio ν_2	0,25	0,25

The results of a simplified calculation of the maximum contact stresses, deformations, maximum tangential subsurface stresses and its position in the xz - plane with an increase in the applied load for two bearing units with different microgeometry of contact are presented graphically in Fig. 4 - 8.

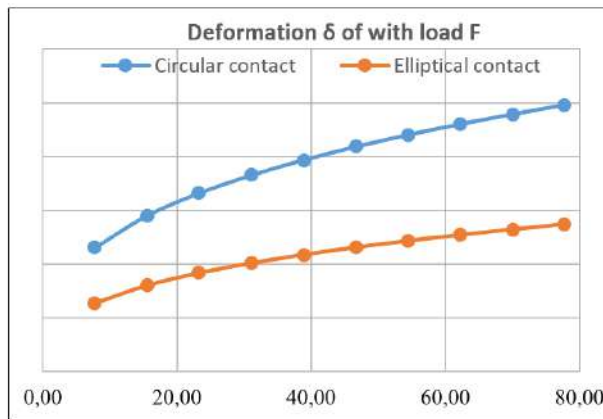


Fig. 4. Influence of microgeometry in the point contact zone on the deformation δ of contacting friction surfaces of bearing units with increasing load F

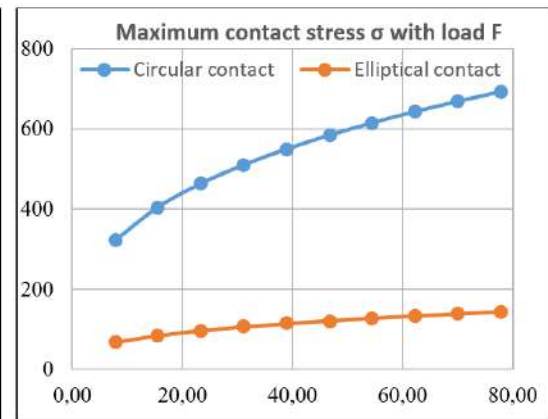


Fig. 5. Influence of microgeometry in the point contact zone on the change in contact stress σ for friction bearing units with increasing load F

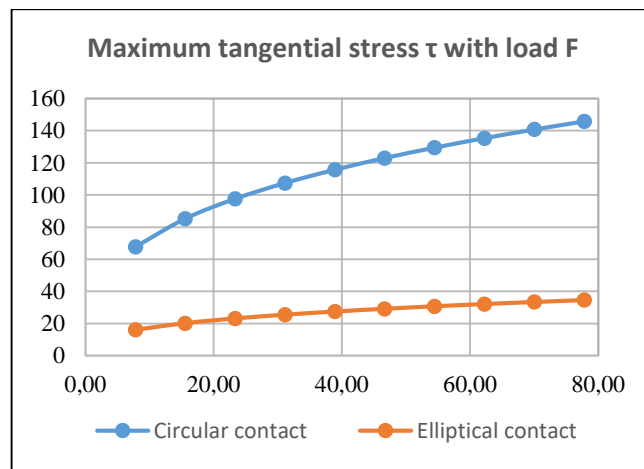


Fig. 6. Effect of microgeometry in the point contact zone on the change in tangential stress τ for friction bearing units with increasing load F

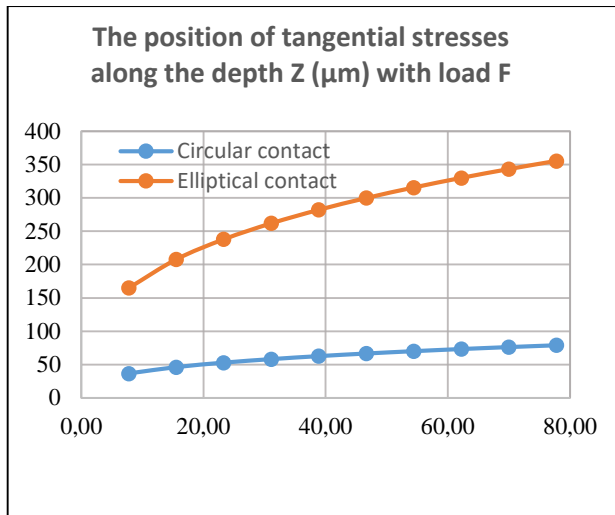


Fig. 7. Influence of microgeometry on the position of penetration of tangential stresses τ in the subsurface zone of point contact along the depth z - (μm) for friction bearing units with increasing load F

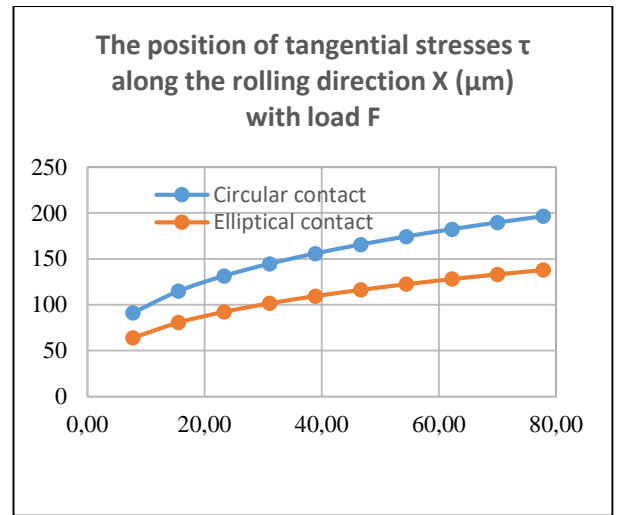


Fig. 8. Influence of microgeometry on the position of penetration of tangential stresses τ in the subsurface zone of point contact along the rolling direction x - (μm) for friction bearing units with increasing load F

Conclusions

An alternative method of calculation to the classical Hertz solution for local stresses and strains of two elastic contacting bodies is presented, i.e., the need to solve transcendental equations to establish the influence of microgeometry in the contact zone is eliminated.

References

- 1 Dmitrichenko N.F. The Elastohydrodynamics: Theory and Practice / N.F. Dmitrichenko. - Lviv: Publishing house of National University "Lviv Polytechnic", 2000. – 224p.
2. Dmytrychenko M.F. Lubricating action of oils in conditions of elastohydrodynamic lubrication / M.F.Dmytrychenko, O.A.Milanenko - K.: Informavtodor, 2009. 184p.

Міланенко О.А. Вплив мікрогеометрії в зоні точкового контакту на втомну довговічність в умовах тертя спокою для підшипникових вузлів тертя.

Представлена альтернативна методика розрахунку класичному рішенню Герца для локальних напружень і деформацій двох пружних контактуючих тіл, тобто, усувається необхідність вирішувати трансцендентні рівняння для встановлення впливу мікрогеометрії в зоні контакту.

За допомогою спрощених формул можна безпосередньо розрахувати максимальні контактні напруження, деформації, підповерхневі дотичні напруження, а також їх положення по глибині та за напрямом кочення та встановити вплив мікрогеометрії.

Максимальні контактні й дотичні напруження, а також максимальні деформації прогнозовано вище за величиною для упорних (осьових) кулькових підшипниках з коловим контактом тертя в порівнянні з радіальними підшипниками, які мають еліптичну форму контакту.

Для радіальних підшипників кочення з характерною еліптичною формою контакту положення проникнення дотичних напружень по глибині (вісь z) значно перевищує дане положення для упорних (осьових) підшипників з коловим контактом при рівних умовах дослідження, що опосередковано вказує на меншу втомну довговічність радіальних підшипників у зв'язку з нерівномірним розподіленням тиску в зоні локального контакту.

Ключові слова: Точковий контакт тертя, втомна довговічність, підшипники кочення, максимальні контактні напруження, максимальні дотичні напруження, мікрогеометрія, тертя спокою.



Study of frictional properties, long-term (cyclic) strength of materials of brake pads of motor vehicles

V.D. Makarenko¹, O.I.Kliuiev¹, O.A.Voitovych¹, Yu. Ye. Mieshkov¹, Yu.V. Makarenko²

¹*Kherson National Technical University, Ukraine*

²*Manitoba Medical University, Winnipeg, Canada*

*E-mail: mieshkov.yuri@gmail.com

Received: 14 December 2022; Revised: 22 January 2023; Accept: 12 February 2023

Abstract

Fractogram analysis shows that deep scratches, particles of titanium and chromium carbides and other elements were found on the friction surfaces. Moreover, in the braking devices there was damage to the large size of the brake pads of trucks. The transfer of particles of borides and carbides to the surface of the wheels can be explained by the processes of metal flooding with their subsequent embrittlement, which inevitably leads, as a rule, to the destruction of friction wheel pairs. It is established that such types of wear as fretting corrosion significantly (by 1.5-2 times) reduce the fatigue limit of parts. Also significantly reduce the cyclic strength of metal friction pairs oxide films on their surface in the absence of lubricant. The service life of friction wheel pairs has a particularly strong impact on fatigue strength. The main reason for the decrease in endurance due to the processes of setting on the working surfaces of friction units is a high concentration of stresses caused by deep tears, cuts, microcracks. The process of destruction of brake pads from fatigue begins from the surface of the part. In this regard, the quality of the surface, its structural-phase composition, physical and mechanical properties of the surface layer in most cases are decisive for the intensity of the development of wear processes of parts from fatigue of the tribosystem (friction wheel pairs), which are operated under cyclic loads. The peculiarity of the influence of friction and wear processes on the fatigue strength of metal is that at the time of running-in there is a change in surface roughness, structure and properties of surface layers. As the analysis of literature sources has shown, the effectiveness of the influence of friction and wear processes on the characteristics of fatigue resistance in the case of repeatedly alternating (cyclic) loads is essential, and therefore ignoring this effect during the traditional assessment of the reliability of parts by individual criteria, for example, wear resistance, often leads to an incorrect assessment of the operational durability of the elements of the tribological system of road or rail transport. The long-term (cyclic) strength of brake pads was determined on a specialized unit model 1251 by Instron company (Great Britain). The basis for spraying and surfacing of different types of coatings was normalized steel 35. Tensile-compressive deformations at zero average stress and a cycle frequency of 20 Hz were studied on the laboratory unit. Most of the tests were carried out in salt solutions (NaCl of industrial purity was used). The process of destruction of brake pads from fatigue begins with the surface of the part. In this regard, the quality of the surface, its structural-phase composition, physical and mechanical properties of the surface layer in most cases are decisive for the intensity of the development of wear processes of parts from fatigue of the tribosystem (friction wheel pairs), which are operated under cyclic loads. Endurance limits in the case of simultaneous exposure to friction forces and cyclic loads will depend on the sliding speed of the tangent surfaces of the normal contact load, which determines the friction force, and the composition of the environment.

Keywords: fractograms, friction, destruction, wear, structural-phase composition, physical and mechanical properties, wheel pair, tribology, cyclic strength, microcracks.

Introduction

Currently, the industrial industry of Ukraine faces the problem of creating the basic foundations for the development of transport technology, in particular, the issues of friction and wear in transport machines. The relevance is due to the fact that the current state of development of technology is characterized by harsh operating



conditions of various transport systems, which is associated with an increase in: specific loads; increase in power; speed; the effect of complex loads of static cyclic and dynamic nature; the influence of various corrosive environments and temperatures. It is known from operational practice that the violation of normal functioning or complete failure of technical systems by 70-80% is caused by the failure of elements of their tribosystems due to surface destruction as a result of wear and other related processes - erosion, fretting, etc. Therefore, increasing the durability of friction units has been and remains one of the most important technical problems of our time in terms of increasing the reliability and extending the service life of transport machines. Despite the large volume of publications on this subject, it can be noted that the diversity of a large amount of experimental material, uncertainty and inconsistency of information about the tribological properties of the material involved in friction and wear pairs leads to the need to find additional resources to improve the wear resistance of brake pads, in particular transport trucks.

Therefore, we have conducted additional studies of the friction properties of brake pads in the conditions of experimental benches that were closest to the real kinematic and dynamic conditions of operation of transport trucks.

The purpose and objectives of the study – conducting systematic experimental studies of the frictional properties of brake linings made of different materials.

Materials and methods of the study

In the experiments, an improved unit of the MFK-1 model was used, which is schematically shown in Figure 1, (which does not show the information system for determining the necessary information and computer processing). To select the material of brake linings, express dry friction tests were carried out together with the specialists of NPO "Powder Metallurgy" and the Institute of Electric Welding named after E.O. Paton of the National Academy of Sciences of Ukraine (a possible case of braking wheelset operation in dry friction mode was simulated on the stand). Tests of samples of coated linings for wear resistance at dry friction were carried out for 45 minutes at a specific pressure of 0.6 MPa and a counterbody rotation speed of 80 min⁻¹, the counterbody was a disk made of hardened steel 40HN. The reference sample of brake linings was steel 45. The lining was made of three types: FMK-8 - metal-ceramic friction (based on iron); "carbon - carbon" - composite materials CCCM and powders of eutectic alloys of the TH system (for coating used powders of eutectic alloys of the 12X18H9T-TiB system). Moreover, it should be noted that the metal matrix of the alloy corresponds to steel 12X18H9T, and the strengthening compounds are titanium and chromium borides. Spraying was carried out by plasma method. The fractograms of the friction surface, which were subjected to wear, were studied by X-ray spectral analysis using a scanning electron microscope model "JSM-35CF" of the company "Geol" (Japan).

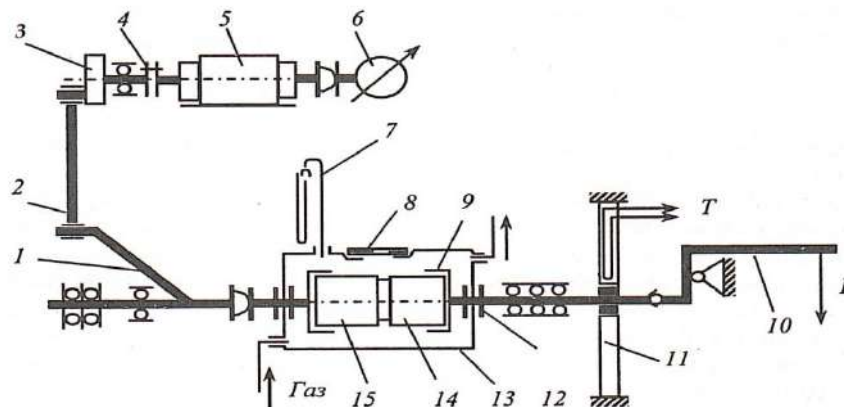


Fig.1. Schematic diagram of MFKU-1 unit:

1 - horizontal connecting rod, 2 - vertical connecting rod, 3 - adjustable eccentric, 4 - coupling, 5 - electric motor, 6 - counter of the number of cycles, 7 - pressure gauge, 8 - inspection window, 9 - collet, 10 - loading device, 11 - strain beam, 12 - seal, 13 - camera, 14 - fixed sample, 15 - moving sample.

Long-term (cyclic) strength of brake pads was determined on a specialized model 1251 unit of the Instron company (Great Britain). Normalized steel 35 served as the basis for filing and surfacing various types of coatings. Tensile-compressive deformations at zero average stress and a cycle frequency of 20 Hz were studied on a laboratory unit. Most of the tests were carried out in salt solutions (NaCl of industrial purity (above 99%) was used).

The results of experimental studies are shown in Figures 2-10.

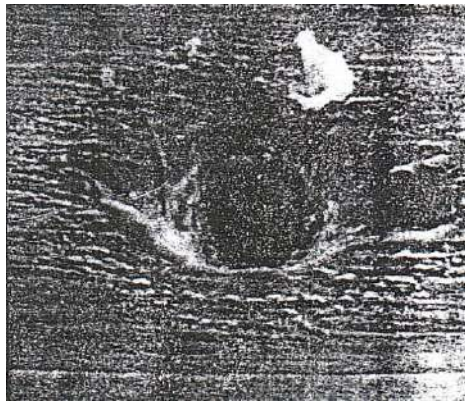


Fig.2. Microstructure of plasma TN coating (cross grinding - base carbon steel U7 - x400).



Fig.3. Microstructure of plasma coating of TN type (general view of the coating surface - base steel 35 (x500))

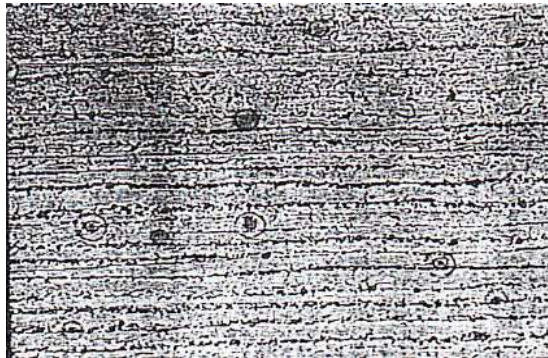


Fig.4. Microstructure of plasma deposited TN coating (x300). Titanium boride inclusions are circled.

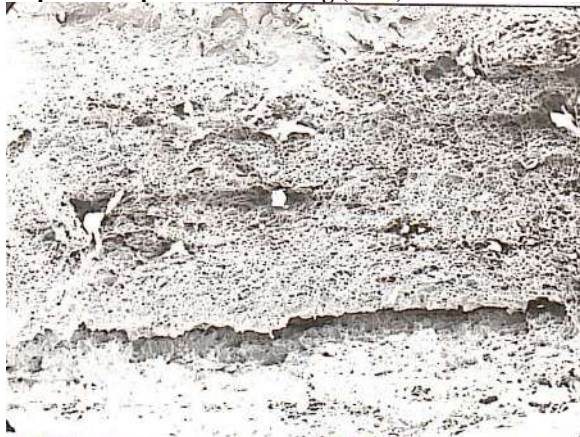


Fig. 5. Fractogram of the surface with surfacing composite coating CCCM. Base - steel 45
The results of tests of brake pads for cyclic (long-term) strength are shown in Figures 6 and 7.

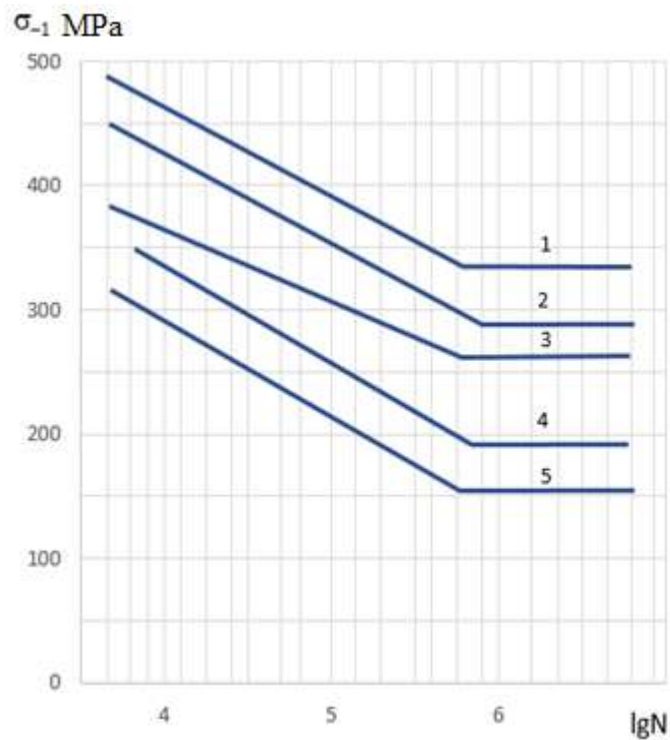


Fig.6. Cyclic strength (fatigue) curves of carbon steel 35 samples.
 1 - unused steel; 2 - service life is 5 years; 3 - service life is 10 years; 4 - service life is 15 years; 5 - service life is 20 years.

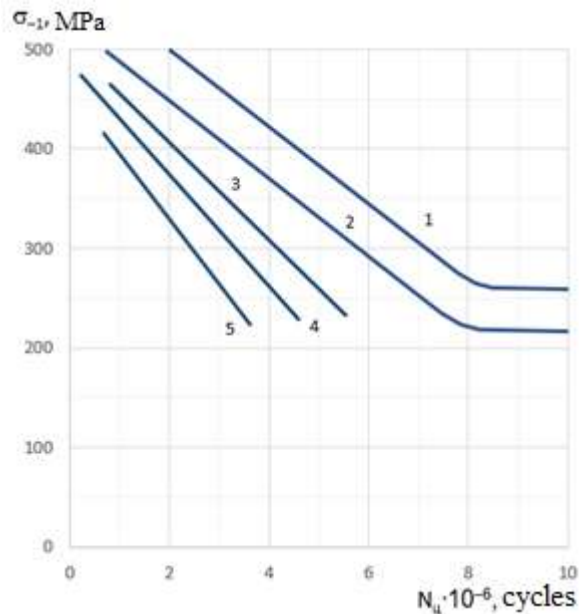


Fig.7. Effect of fretting corrosion on fatigue (cyclic) strength of carbon normalized steel 35.
 1 - fatigue curve without fretting corrosion (service life is 5 years); 2 - fatigue curve without fretting corrosion (service life is 10 years); 3-5 - fatigue curves with fretting corrosion (service life is 5, 10 and 15 years, respectively).

The process of destruction of brake pads from fatigue begins with the surface of the part. In this regard: the quality of the surface; its structural-phase composition; physical and mechanical properties of the surface layer in most cases are decisive for the intensity of the development of wear processes of tribosystem parts (friction wheel pairs) from fatigue, which are operated under cyclic loads. Many parts of motor vehicles operate in such conditions. A feature of the influence of friction and wear processes on the fatigue strength of metal is that at the time of running-in, there is a change in surface roughness, structure and properties of surface layers. As the analysis of literary sources [18,19,20] has shown, the effectiveness of the influence of friction and wear processes on the characteristics of fatigue resistance in the case of repeatedly variable (cyclic) loads is essential, and therefore ignoring this effect during the traditional assessment of the reliability of parts according to certain criteria, for

example, wear resistance, often leads to an incorrect assessment of the operational durability of elements of the tribological system of road or rail transport.

The endurance limits in the case of simultaneous exposure to friction forces and cyclic loads will depend on: sliding speed; contact surfaces; normal contact load, which determines the friction force; composition of the environment.

The data of Figure 6 shows that such types of wear as fretting corrosion significantly (by 1.5-2 times) reduce the fatigue limit of parts. Also significantly reduce the cyclic strength of metal friction pairs oxide films on the surface of friction pairs in the absence of lubricant. Especially strong influence on fatigue strength has the service life of friction wheel pairs (Fig.6).

The main reason for the decrease in endurance due to the processes of setting on the working surfaces of friction units is a large concentration of stresses caused by deep tears, cuts, microcracks (Fig.2 and 5).

The decrease in fatigue strength of steel 35 is characterized by the data in Figure 7. According to the recommendations of Prof. Kindrachuk M.V. [19], if we extrapolate the fretting fatigue curves to the abscissa axis corresponding to the limited endurance based on $N=107$ cycles, and then project the intersection points onto the fatigue curve without fretting corrosion, we obtain the value of the equivalent stress. The higher the values of these equivalent stresses compared to the nominal stress, the more fatigue (cyclic) strength is reduced by fretting corrosion.

So, for example, according to the curves, we have the following σ_{eq} value: $\sigma_2 = 255\text{MPa}$; $\sigma_3 = 151\text{MPa}$; $\sigma_4 = 248\text{MPa}$; $\sigma_5 = 245\text{MPa}$ ($\sigma_{-1} = 200\text{MPa}$), that is, the excess of equivalent stresses over σ_{-1} is in the range from 20 to 40%.

Analysis of the fractograms presented in Figures 3 and 4 shows that deep scratches, particles of titanium and chromium carbides and other elements were found on the friction surfaces. Moreover, in the braking devices there was damage to the large size of the brake pads of trucks. The transfer of particles of borides and carbides to the surface of the wheels can be explained by the processes of flooding the metal with their subsequent embrittlement, which inevitably leads, as a rule, to the destruction of friction wheel pairs.

Conclusions

1. Fractogram analysis shows that deep scratches, particles of titanium and chromium carbides and other elements were found on the friction surfaces. Moreover, in the braking devices there was damage to the large size of the brake pads of trucks. The transfer of particles of borides and carbides to the surface of the wheels can be explained by the processes of flooding the metal with their subsequent embrittlement, which inevitably leads, as a rule, to the destruction of friction wheel pairs.

2. It is established that such types of wear as fretting corrosion significantly (by 1.5-2 times) reduce the fatigue limit of parts. Also significantly reduce the cyclic strength of metal friction pairs oxide films on their surface in the absence of lubricant. The service life of friction wheel pairs has a particularly strong impact on fatigue strength. The main reason for the decrease in endurance due to the processes of setting on the working surfaces of friction units is a high concentration of stresses caused by deep tears, cuts, microcracks.

3. The process of destruction of brake pads from fatigue begins with the surface of the part. In this regard, the quality of the surface, its structural-phase composition, physical and mechanical properties of the surface layer in most cases are decisive for the intensity of the development of wear processes of parts from fatigue of the tribosystem (friction wheel pairs), which are operated under cyclic loads. The peculiarity of the influence of friction and wear processes on the fatigue strength of metal is that at the time of running-in there is a change in surface roughness, structure and properties of surface layers. As the analysis of literature sources has shown, the effectiveness of the influence of friction and wear processes on the characteristics of fatigue resistance in the case of repeatedly alternating (cyclic) loads is essential, and therefore ignoring this effect during the traditional assessment of the reliability of parts by individual criteria, for example, wear resistance, often leads to an incorrect assessment of the operational durability of the elements of the tribological system of road or rail transport.

4. The long-term (cyclic) durability of brake pads was determined on a specialized installation model 1251 of the company "Instron" (Great Britain). The basis for spraying and surfacing of different types of coatings was normalized steel 35. On the laboratory unit was investigated under tensile-compressive deformation at zero average stress and cycle frequency of 20 Hz. Most of the tests were carried out in salt solutions (NaCl of industrial purity was used).

References

1. Gavriilyuk V.P. Tribology of casting alloys.– K:– 2007.– 428c
2. Dmytrychenko M.F. Tribotechnics based on the reliability of machines//K.:–INFORMAVTODOR. – 2006.– 216p
3. Zaporozhets V.V. Diagnostics of friction units and special machines//K.: – KIIGA. – 1987. – 163p
4. Kogaev V.P. Durability and durability of machine parts// M.: Higher school. – 1991.–309p
5. Kuzmenko A.G. Contact, friction and wear of lubricated surfaces. – Khmelnytskyi: KhNU. – 2007. – 344p

6. Labunets V.F. Boride wear resistance is covered. –K.: Technology. – 1989.– 169p
7. Surface strength of materials under friction / B. I. Kostetskyi, I. G. Nosovsky, A. K. Karaulov et al.// K.: Technika. – 1976. – 296p
8. Friction, wear and lubrication. Reference book: In 2 books // Ed. I.V. Kragelskogo, V.V. Anisin. – M.: Machine building. – Book 1-1978. – 400 p.; Book 2. – 1979. – 358 p
9. Shevelya V.V. Tribochemistry and rheology of wear resistance. -Khmelnyskyi: KhNU. –2006. – 278 p
10. Trucbon M.R., Crolet J.I. Experimental limits of sourer service for tubular steels //SSC Symposium. – Saint-Cloud. – 21. – 2013.
11. Stardisco J.B., Pitts R.E. Corrosion of Iron in H₂S-CO₂-H₂O System, Mechanism of Sulfide Film Formation and Kinetics of Corrosion // Corrosion.-2014. – №9. – P.245-253.
12. Galis M.F.J., Orlans B.J., Gunts G.C. Study of metallurgical parameters influencing the behavior of line pipes in H₂S medium // SSC Symposium. – 1991. – 17 p.
- 13.F.Francis, A.M Edwards, R.J..Espiner and G.Senior. Applying Structural Reliability Method to Aging Pipelines. Paper. C57I-/011./99//. IMcchE Conference on Aging Pipelines. Newcastle., UK, October. – 1999.
14. Henderson RL. Hopkins P. Cosham A. Extending the Life of Aging Pipelines. – The Offshore Pipeline Technology Conference. TX OPT USA 2001 Oct. 22-23. Houston.
15. Makarenko V.D., Maksymov S.Yu., Bilyk S.I. etc. Corrosive destruction of sewage systems of Ukraine//Kyiv: NUBiP of Ukraine. – 2021. – 272p
16. Makarenko V.D., Paly R.V., Halychenko E.N. etc. Physico-mechanical basis of hydrogen sulfide corrosion destruction of industrial pipelines. - Chelyabinsk: Izd-vo TsNTI.—2002.–412 p
17. Stepanov M.N. Statistical methods of processing the results of mechanical tests/ Handbook// Machine building. -1985
18. Dmytrychenko M.F. Tribotechnics and the basics of machine reliability: training. Manual// Kyiv: InformAvtoDor. – 2006.– 216p.
19. Tribology /M.V.Kindrachuk, V.F.Labunets, M.I.Pashechko, E.V.Korbut// Kyiv: National Publication. aviation "NAU-Druk" University. – 2009.– 392p
20. Golego N.L. Fretting corrosion of metals// Kyiv: Technika. – 1994. – 272p

Макаренко В. Д., Клюєв О. І., Войтович О. А., Мешков Ю. Є., Макаренко Ю.В. Дослідження фрикційних властивостей, тривалої (циклічної) міцності матеріалів гальмових колодок автотранспорту

Аналіз фрактограм показує, що на поверхнях тертя було виявлено глибокі подряпини, частинки борідів (карбідів) титану і хрому та інших елементів. Причому, у гальмових пристроях мали місце пошкодження великих розмірів гальмових колодок вантажних автомобілів. Перенесення частинок борідів та карбідів на поверхню коліс можна пояснити процесами наводнення металу з подальшим їх окрихненням, що неминуче спричиняє, як правило, руйнування колісних пар тертя. Встановлено, що такі види зношування як фретинг-корозія значно (в 1,5-2 рази) знижують межу втоми деталей. Також значно знижують циклічну міцність металу пар тертя оксидні плівки на їх поверхні у відсутності мастильного матеріалу. Особливо сильний вплив на втомну міцність має термін експлуатації колісних пар тертя. Основною причиною зниження витривалості внаслідок процесів захоплювання на робочих поверхнях вузлів тертя є велика концентрація напружень, спричинена глибинними виривами, надрізами, мікротріщинами. Процес руйнування гальмових колодок від втоми починається з поверхні деталі. У зв'язку з цим якість поверхні, її структурно-фазовий склад, фізико-механічні властивості поверхневого шару у більшості випадків є визначальним для інтенсивності розвитку процесів зношування деталей від втоми трибосистеми (колісних пар тертя), які експлуатуються в умовах циклічних навантажень. Особливість впливу процесів тертя та зношування на втомну міцність металу полягає в тому, що в момент припрацювання відбувається зміна шорсткості поверхні, структури і властивостей поверхневих шарів. Як показав аналіз літературних джерел, ефективність впливу процесів тертя і зношування на характеристики опору втоми в разі повторно-змінних (циклічних) навантажень мають істотне значення, а тому ігнорувати цим ефектом під час традиційного оцінювання надійності деталей за окремими критеріями, наприклад, зносостійкості приводить часто до невірної оцінки експлуатаційної довговічності елементів трибологічної системи автомобільного чи залізничного транспорту. Тривалу (циклічну) міцність гальмових колодок визначали на спеціалізованій установці моделі 1251 фірми "Інстрон" (Великобританія). Основою для напилювання і наплавлення різних типів покриттів слугувала нормалізована сталь 35. На лабораторній установці досліджували деформації розтягування – стискання при нульовому середньому напруженні і частоті циклів 20Гц. Більшість випробувань проводили в розчинах солі (використовували NaCl промислової чистоти). Процес руйнування гальмових колодок від втоми починається з поверхні деталі. У зв'язку з цим якість поверхні, її структурно-фазовий склад, фізико-механічні властивості поверхневого шару у більшості випадків є визначальним для інтенсивності розвитку процесів зношування деталей від втоми трибосистеми (колісних пар тертя), які експлуатуються в умовах циклічних навантажень. Межі витривалості в разі одночасного впливу сил тертя і циклічних навантажень будуть залежати від швидкості ковзання дотичних поверхонь нормального контактного навантаження, яке визначає силу тертя, і складу навколишнього середовища.

Ключові слова: фрактограми, тертя, руйнування, зношування, структурно-фазовий склад, фізико-механічні властивості, колісна пара, трибологія, циклічна міцність, мікротріщини.



Wear resistance of structural steels nitrided in a cyclically switched discharge with dry friction

M.S. Stechishyn, M.Ye. Skyba, A.V. Martynyuk*, D.V. Zdorenko

¹*Khmelnytskyi National University, Ukraine*

**E-mail: avmart@khmnu.edu.ua*

Received: 20 December 2022; Revised: 25 January 2023; Accept: 20 February 2023

Abstract

The paper examines the method of conducting tribological studies in the dry mode of friction of nitrided and unhardened structural steels 20 and 45 in order to achieve comparable results of laboratory tests with operational characteristics. Preliminary studies of anodized steels of the same steels indicate that under conditions of extreme friction it is extremely difficult, and in some cases impossible, to use such values of specific pressure on the friction surface, at which it would be realistic to compare the results obtained for different samples made of different brands materials and processed using various technological processes. Since during the tests, constant lubrication of the friction zone was ensured, a layer of lubricant was present on the friction surface up to a certain pressure value, which led to extremely small indicators of linear wear. However, depending on the characteristics of the modified surface, there was a critical value of pressure at which the layer of lubricant was squeezed out of the friction zone, which led to instant adhesion of the surfaces. Thus, the study of wear resistance in the dry mode of friction ensures a significantly higher productivity of experiments.

Unlike experiments with limit friction, dry friction can be used for different steels at the same pressure value, which eliminates the problem of comparability of results and contributes to the objectivity of conclusions regarding the effectiveness of various modification processes.

According to the results of previous experiments, such a compromise pressure value can be 16 MPa.

Another important phenomenon for the analysis of the influence of the modification results on the wear resistance characteristics of the surface is established - the effect of relaxation processes in the near-surface layers, which have already acquired structural transformations under the influence of pressure in the friction zone.

For all steels, there is some slowing down of the intensity of wear after a break with a gradual return to the intensity characteristic of a certain brand of steel. The reason for such a phenomenon can only be the relaxation of stresses and the equalization of the characteristics of the structure in the near-surface layers. At the same time, the result is the strengthening of the surface, which explains the decrease in the intensity of the wear process. Over time, as the strengthened layer breaks down, the indicators of the surface condition become equal to those before the break and the intensity of wear is restored.

Key words: nitriding, dry friction, limit friction, wear.

Statement of the problem and analysis of the latest research

The metal surface should be considered as a special variety of defects that destroys the periodicity of the solid body. This thesis is confirmed by the fact of significant acceleration of chemical reactions in the presence of solid catalysts on the surface. The boundary layer, the structure of which differs from the base of the solid body, can interact more actively with external factors that stimulate surface modification. At the same time, it is the presence of a real surface that is the stimulus due to which most of the physical or chemical processes of the interaction of a solid body with the environment take place.

The near-surface layer should be considered as a three-dimensional structure, which differs from the solid body itself, since within several atomic layers it may include atomic nodes different from the atomic nodes of the main volume. However, one should not forget that the near-surface layer is a crystalline structure for which two-dimensional periodicity is preserved. Thus, violation of the indicated natural periodicity of near-surface layers



inevitably affects all characteristics of the surface as a whole, including its ability to resist wear. This circumstance was noted to a greater or lesser extent in classic works on tribology, but there is no coverage of the research results, on the basis of which it would be possible to form practical methods of experiments to find the tribological characteristics of the wear resistance of metals.

It is known that during the adsorption of gases, a monomolecular adsorption layer is formed - a monolayer, and the degree of integrity of the monolayer at low pressure values is proportional to the adsorbate pressure in the gas medium. If gas molecules, in the presence of a strong chemical or physical bond, do not have the opportunity to move on the surface, then we get localized adsorption with the formation of an adsorption complex.

Chemisorbed and physically sorbed gas particles on the surface differ in the type of electronic bond between the adsorbate and the base. If the electronic state of the adsorbed molecule undergoes significant changes up to the formation of chemical bonds with the surface, then we are talking about chemisorption. If the molecule is held on the surface by van der Waals forces, then this type of adsorption refers to physical adsorption. The upper limit for physical adsorption is only 0.6 eV. The chemisorption energy is usually within 1...8 eV [1]. If the energy of a molecule of the external environment is several electron volts, then it will already be able to overcome the potential barrier of the near-surface layer and the conditions for chemical sorption or chemical reaction appear [2]. It is obvious that the mechanical impact on the surface changes the parameters of adsorption phenomena, which also affects the wear processes.

From the above follows the conclusion about the importance of taking into account the parameters of the wear process on the objectivity of the results of the conducted research. This especially applies to their analysis and formation of practical recommendations.

The work [3] analyzed the results of research on wear resistance, which were obtained under conditions of extreme friction. The main conclusion from the analysis was that any wear process is a combination of successive compaction of near-surface layers and their removal. At the same time, the test parameters are of decisive importance, which must be selected taking into account the material and the preliminary treatment of the surface. The results of the experiments show that, under conditions of extreme friction, it is extremely difficult, and in some cases impossible, to use such values of the specific pressure on the friction surface, at which it would be realistic to compare the results obtained for different samples, made of different grades of materials and processed with various technological processes. Since during the tests, constant lubrication of the friction zone was ensured, a layer of lubricant was present on the friction surface up to a certain pressure value, which led to extremely small indicators of linear wear. However, depending on the characteristics of the modified surface, there was a critical value of pressure at which the layer of lubricant was squeezed out of the friction zone, which led to instant adhesion of the surfaces. The presence of compaction and structural transformations of the surface is evidenced by the fact that with a gradual increase in pressure, it was possible to reach relatively high values of the critical pressure. An attempt to immediately conduct tests on new samples at a pressure close to these critical values inevitably caused seizure of the surfaces. The reason for such a phenomenon could only be the gradual compaction of the surface and its strengthening associated with a change in the structure of the near-surface layer. The above and the impossibility of an objective comparison of test results obtained at different pressures explain the need to switch to the scheme of experiments with dry friction.

The purpose of the work is to develop the methodology and criteria for the evaluation of experimental studies of the wear resistance of samples after nitriding in the cyclically switched discharge (CSD) in order to achieve the results of laboratory tests that correspond to the real conditions of operation of the parts.

Methods of conducting experimental research

In order to ensure the independence of the energy parameters of the regime without hydrogen nitriding in the glow discharge (HNGD), the installation was modernized: a block of heating elements was installed in the gas discharge chamber, and a power supply unit from an independent source and also a switching and control unit of the cyclically switched discharge were added to the electrical circuit.

Experimental studies of samples for wear resistance were carried out on a universal machine for testing materials for friction, model 2168VMT. The friction scheme is "disc - finger"; contact type - plane-on-plane sliding (the end of the cylindrical sample slides on a flat metal disk; the material of the counterbody is steel 100Cr6 with a base hardness of HRC61; pressure in the contact zone $p = 16$ MPa; sliding speed $v = 0.1$ m/s [4].

To check the possibility of further comparison of wear processes, objects with significantly different surface characteristics were selected: soft surfaces are represented by samples from steel C22 without modification, modified - from steel C45 after nitriding in a glow discharge. The latter before nitriding had a surface hardness of HV0.1 215, after modification HV0.1 700...730 [5].

The controlled parameter is linear wear h , which was determined as a change in the linear size of the sample, measured normal to the friction surface, as a result of passing a section of length l .

BATR was carried out on an industrial unit of VATP, which corresponds to the diode-type model. A power supply unit from an independent source, as well as a switching and control unit for a cyclically switched discharge, have been added to the scheme. In addition, the installation is additionally equipped with heating elements placed in the gas discharge chamber, which made it possible to arbitrarily change the energy parameters - the voltage U ,

and the value of the current density j (the ratio of the current to the total area of the cage and suspension) [6].

Metallographic studies of nitrided samples were performed after etching in a 3% alcoholic solution of nitric acid. The thickness of the nitride zone was measured on an RX50M microscope. Microhardness was determined on a DuraScan-20 microhardness tester under a load of 1.0 N, with fixation of microhardness values both on the surface and at a distance from it of 0; 25; 50; 100; 200; 300; 500 microns.

The thickness of the nitride zone was measured using a MIM-10 microscope, which allows quantitative analysis of the phase and structural composition of nitrided surfaces.

X-ray phase analysis of nitrided samples was performed on a ДРОН-3 diffractometer in filtered radiation of an iron anode in the range of q angles from 20° to 100° with a scan step of 0.1° and an exposure time of 10 s. X-ray imaging was carried out from the surface to the depth of the nitrided layer.

Presentation of the main material and received scientific research

The results of preliminary tests are shown in Figure 1. It follows from Figure 1 that in the dry friction mode, the intensity of the wear process increases significantly, which means a significant increase in the productivity of experimental studies. Thus, one experiment in the mode of extreme friction lasted for weeks, and in the dry mode it was possible to perform it in several shifts. In addition, the thesis regarding the decisive influence of pressure on the intensity of wear on the friction surface was confirmed: the same indicators of linear wear d were achieved with an increase in pressure with a significantly smaller friction path L . The brand of the material and the initial values of its physical and mechanical indicators in combination with the available modification surfaces also significantly influenced the intensity of wear. Thus, for steel 41CrAlMo7 nitrided in the glow discharge, the intensity of wear is almost an order of magnitude lower compared to steel C22. Similar data were obtained in [7].

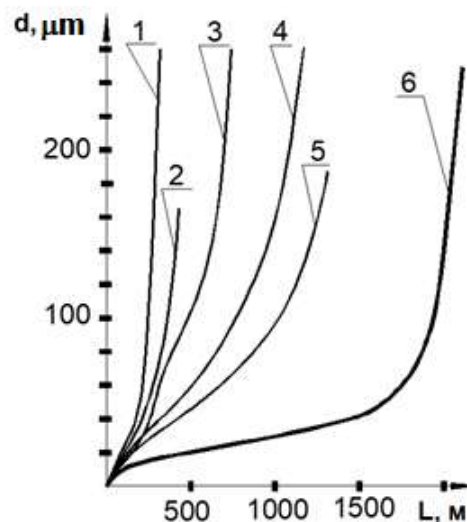


Fig. 1. Dependence of linear wear on the path of friction and pressure: 1 – steel C22, $p=16$ MPa; 2 – steel C45, $p=16$ MPa; 3 - steel C22, $p=10$ MPa; 4 – steel 41Cr4, $p=16$ MPa; 5 – steel C45, $p=10$ MPa; 6 – steel 41CrAlMo7, $p=16$ MPa

In contrast to the methodology of experimental research with extreme friction, in the dry friction mode, results can be achieved at the same pressure values for almost all steels, which excludes the issue of comparability when analyzing the results of research. The importance of this provision is evidenced by the comparison of wear curves for the same steels at different pressure values (Figure 1). Since the same value of linear wear for the same material, but at different pressures, is achieved with significantly different values of the friction path, establishing the relationship between the listed factors would pose a certain problem.

Curves in fig. 1 also confirm the effect on the wear intensity of the physical and mechanical parameters of the surface and its modification. Thus, steels with higher physico-chemical characteristics (41Cr4 and 41CrAlMo7), as well as steels that have undergone a certain modification treatment, wear out under the same conditions (pressure and speed of relative movement) with a lower intensity of wear, which in the graphs corresponds to the angle of their inclination.

The effect of structural transformations of the surface is confirmed by Figure 2, which shows the results of fixation of linear wear with a small interval of the friction path. The wear schedule in this case is a stepped curve of periods of formation of strengthened structures on the surface, when wear is practically absent, and periods of destruction of these surface structures.

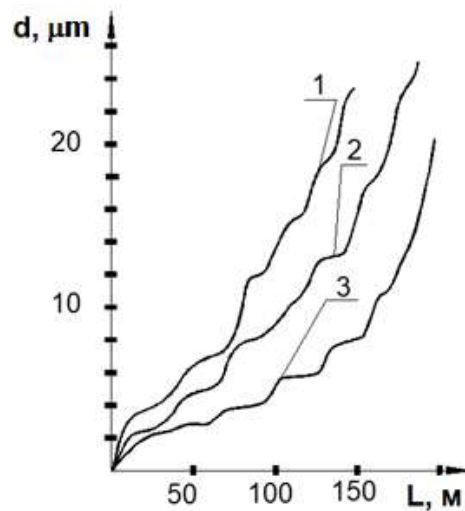


Fig. 2. Character of surface wear in the initial period: 1 - steel C22, 2 - steel 41Cr4, 3 - steel 41CrAlMo7

For modified surfaces, this phenomenon is especially characteristic in the initial period, when the nitride and internal nitriding zone wears out.

Another important phenomenon for the analysis of the influence of the modification results on the wear resistance characteristics of the surface is established - the effect of relaxation processes in the near-surface layers, which have already acquired structural transformations under the influence of pressure in the friction zone.

Black dots on curves 2, 4, 6 show the points when wear resistance tests were suspended and resumed the next day (Figure 3). For all steels, a certain slowdown in wear intensity is noted after a break with a gradual return to the intensity characteristic of a certain brand of steel (Figure 3). The reason for such a phenomenon can only be the relaxation of stresses and the equalization of the characteristics of the structure in the near-surface layers. At the same time, the result is the strengthening of the surface, which explains the decrease in the intensity of the wear process. Over time, as the strengthened layer breaks down, the indicators of the surface condition become equal to those before the break and the intensity of wear is restored.

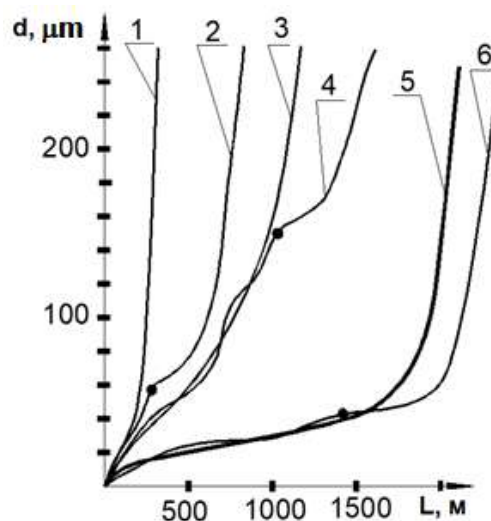


Fig. 3. Effect of relaxation structural transformations of the surface: 1, 2 – steel C22; 3, 4 – steel 41Cr4; 5, 6 – steel 41CrAlMo7 (points for stopping the tests are marked with dots)

Conclusions

Thus, the study of wear resistance in the dry mode of friction ensures a significantly higher productivity of experiments. Unlike experiments with limit friction, dry friction can be used for different steels at the same pressure value, which eliminates the problem of comparability of results and contributes to the objectivity of conclusions regarding the effectiveness of various modification processes. According to the results of previous experiments, such a compromise pressure value can be 16 MPa. The effect of relaxation transformations of surface structures has been established, on the basis of which it is recommended to carry out research on wear resistance

during one continuous session.

References

1. Woodruff D. Modern methods of surface research; ed. V. I. Rakhnovsky / D. Woodruff, T. Delchar. - M. : Mir, 1989. - 564 p.
2. Pleshivtsev N.V. Cathode sputtering / N.V. Pleshivtsev - M. : Atomizdat, 1998. - 343 p.
3. M.S. Stechyshyn, V.V. Lyukhovets, N.M. Stechyshyna, M.I. Tsepenyuk. Wear resistance of structural steels nitroded in cyclic-commuted discharge at limit modes of friction. // Problems of Tribology. – Khmelnytskyi: KHNU, 2022. – V. 27. - №3/105. – P.27-33.
4. Stechishina N.M. Influence of the parameters of hydrogen nitrogen nitrogen in a glow discharge on tribological and physico-chemical properties of steel 40X / N.M. Stechishina, M.S. Stechyshyn, A.V. Martynyuk, N.V. Lukianyuk, V.V. Lyukhovets, Yu.M. Bilyk // Problems of Tribology. – Khmelnytskyi: KHNU, 2021. – V. 26 - №3/101. – P.31-41.
5. Stechyshyn N.M., Stechyshyn M.S., Mashovets N.S. Corrosion-mechanical wear resistance of food production equipment parts: monograph / N.M., Stechyshina, M.S. Stechyshyn, N.S. Mashovets – Khmelnytskyi: KhNU, 2022.-181 p.
6. M. S. Stechyshyn, M. Ye. Skyba, N. M. Stechyshyna, and A. V. Martynyuk. STRESS-CORROSION WEAR OF NITRIDED STEELS IN ACID MEDIA. Mater. Sci., Vol. 58, No. 2, September, 2022. P.121-126.
7. Skyba M. Physico-chemical and tribological properties of nitrogened layers of structural steel / M. Skyba, M. Stechyshyn, N. Stechyshyna, A. Martynyuk, V. Lyukhovets // Actual problems of modern science. Monograph: Bydgoszcz, Poland– 2021. – P.488-499.

Стечишин М.С., Скиба М.Є., Мартинюк А.В., Здоренко Д.В. Зносостійкість конструкційних сталей, азотованих в циклічно-комутованому розряді при сухому терті.

У роботі розглянута методика проведення трибологічних досліджень при сухому режимі тертя азотованих і незміцнених конструкційних сталей 20 і 45 з метою досягнення порівнюваних результатів лабораторних випробувань з експлуатаційними характеристиками. Попередньо проведені дослідження азотованих цих же сталей свідчать про те, що в умовах граничного тертя надзвичайно важко, а в деяких випадках неможливо використовувати такі значення питомого тиску на поверхню тертя, при яких реальним було б співставлення результатів, одержаних для різних зразків, виготовлених з різних марок матеріалів та оброблених за допомогою різних технологічних процесів. Оскільки в ході випробувань забезпечувалось постійне змащування зони тертя, то до певного значення тиску на поверхні тертя був присутній шар мастила, що призводило до надзвичайно малих показників лінійного зношування. Проте в залежності від характеристик модифікованої поверхні існувало критичне значення тиску, при якому шар мастила витискувався із зони тертя, що приводило до миттєвого схоплювання поверхонь. Таким чином, дослідження зносостійкості при сухому режимі тертя забезпечує суттєво більшу продуктивність експериментів. На відміну від експериментів при граничному терті сухе тертя може застосовуватись для різних сталей при однаковому значенні тиску, що виключає проблему порівнянності результатів та сприяє об'єктивності висновків стосовно ефективності різних процесів модифікації. За результатами попередніх експериментів таким компромісним значенням тиску може бути 16 МПа. Встановлене ще одне важливе явище для аналізу впливу результатів модифікації на характеристики зносостійкості поверхні - ефект релаксаційних процесів в приповерхневих шарах, які вже набули структурних перетворень під дією тиску в зоні тертя. Для всіх сталей відмічається деяке сповільнення інтенсивності зношування після перерви з поступовим поверненням до інтенсивності, характерної для певної марки сталі. Причиною такого явища може бути лише релаксація напружень і вирівнювання характеристик структури в приповерхневих шарах. При цьому наслідком є зміцнення поверхні, що і пояснює зниження інтенсивності процесу зношування. з часом, По мірі руйнування зміцненого прошарку, показники стану поверхні стають рівними з тими, що були до перерви і інтенсивність зношування відновлюється.

Ключові слова: азотування, сухе тертя, граничне тертя, знос.



Mathematical model of running-in of tribosystems under conditions of boundary lubrication. Part 1. Development of a mathematical model

A.V. Voitov

State biotechnological university, Kharkiv, Ukraine

E-mail: K1kavoitov@gmail.com

Received: 28 December 2022; Revised: 30 January 2023; Accept: 26 February 2023

Abstract

The paper further developed the methodological approach in obtaining mathematical models that describe the running-in of tribosystems under boundary lubrication conditions.

The structural and parametric identification of the tribosystem as an object of simulation of running-in under conditions of extreme lubrication was carried out. It has been established that the processes of running-in of tribosystems are described by a second-order differential equation and, unlike the known ones, take into account the limit of loss of stability (robustness reserve) of tribosystems. It is shown that the nature of tribosystems running-in conditions of extreme lubrication depends on the gain coefficients and time constants, which are included in the right-hand side of the differential equation.

It is shown that the processes of running-in of tribosystems depend on the type of the magnitude of the input influence on the tribosystem, the first and second derivatives. The input influence is represented as a product of coefficients and a time constant $K_0 \cdot K_2 \cdot T_3$. This allows us to state that the processes of the tribosystem running-in will effectively take place when the input action (load and sliding speed), will change in time and have fluctuations with positive and negative acceleration of these values from the set (program) value. This requirement corresponds to the running-in program "at the border of seizing".

The left part of the equation is the response of the tribosystem to the input signal. Tribosystem time constants T_2 and T_3 have the dimension of time and characterize the inertia of the processes occurring in the tribosystem during running-in. Increasing the time constants makes the process less sensitive to changes in the input signal, the warm-up process increases in time, and the tribosystem becomes insensitive to small changes in load and sliding speed. Conversely, the reduction of time constants makes the tribosystem sensitive to any external changes.

Keywords: tribosystem; running-in; mathematical model of running-in; differential equation; gain; time constant; boundary lubrication; quality factor of the tribosystem; robustness of the tribosystem; volumetric wear rate; coefficient of friction

Introduction

The running-in of tribosystems is the final technological stage in the production process of machines and the initial stage of operation of these machines. In the process of running-in, the tribosystems that make up the machine or unit form bearing surface layers, providing further maximum resource and minimum friction losses. An analysis of the publications of many researchers who are devoted to running in or running-in allows us to state that the completion of the running-in process is reduced not only to the formation of the optimal roughness of the mating friction surfaces. The running-in process includes physical and chemical phenomena, such as thermal, diffusion, deformation, which take place on actual contact spots in the presence of lubricating media and the environment. Therefore, reducing the running-in process, with a simultaneous decrease in wear for running-in and friction losses, will significantly increase the resource of machines and mechanisms, which will provide an economic effect during operation.

An analysis of models of stationary processes and running-in processes in tribosystems shows that there is a large error in modeling the wear rate, up to 18,8%, and the friction coefficient, up to 16,0%. Such a scatter of data in measurements can be explained by the presence of an oscillatory process of wear rate and friction



coefficient during the running-in of the tribosystem, as well as by the ambiguity of the choice of input parameters for modeling. Difficulties that arise in the development of such models are associated with the choice of parameters that affect the process under study. For example, the design of the tribosystem, the lubricating medium, the materials from which the triboelements are made, the roughness of the friction surfaces, the load-speed range of operation, etc. The listed parameters are random functions, which makes it difficult to build mathematical models.

Literature review

An overview work, which is devoted to the processes of running-in, can be considered the work [1]. In this paper, a system analysis and comprehensive studies of the running-in processes are carried out, on the basis of which the definition of the running-in process is formulated. According to the authors, this is a transient process, including a complex interaction between friction surfaces, lubrication, roughness, plastic deformation and wear. The running-in process involves changing key tribological parameters such as surface roughness, surface topography, coefficient of friction and wear rate until a steady state prevails. The paper provides a review of the literature on the running-in processes.

The authors of the works [2-4] analysis of various types of running-in was carried out, where the change in the roughness of the friction surface during running-in is studied. For example, at work [2] developed a model for changing the roughness of friction surfaces as a function of time. The proposed model is non-linear, the optimal values of the model parameters were estimated using the Gauss-Newton algorithm. Experimental results taken from the literature for steel and alloy samples Cu-Zn were used to test the model and confirmed its information content. In works [3, 4], to reduce the running-in time, the initial roughness of the friction surface has been optimized. The authors established a correlation between the initial roughness and deformation processes of surface layers, showed ways to optimize the running-in of tribosystems.

In works [5, 6] the processes of mechanical treatment of friction surfaces with the formation of optimal roughness and its influence on the mechanisms of plastic deformation of surface layers during running-in were studied. On the basis of experimental data, a model of wear during running-in has been developed and the fact of grain refinement of materials of surface layers has been established.

The study of friction surfaces and the formation of films on them during the running-in process was carried out by the authors of the works [7-9]. The authors conclude that the change in friction and wear parameters that occur during running-in are not only the result of changes in surface roughness, but also the microstructure of the surface layers and the formation of a third body. The running-in process is described by piecewise models, which allow modeling not only roughness, but also the formation of a third body as a function of time. Authors of the work [8] claim that the running-in process can be controlled by changing the initial roughness and lubricating medium. For example, at work [9] the evolution of tribofilms on the friction surface during running-in is shown.

Works [10, 11] devoted to the development of models for the running-in of tribosystems. For example, at work [10] the tribosystem is presented as a running-in attractor, which is a stable and time-ordered structure that is formed in the running-in process. The authors carried out a dispersion analysis of the characteristic parameters of the running-in attractors to identify primary and secondary factors that affect the running-in process. According to the authors, the developed models make it possible to predict the running-in process of tribosystems. In work [11] a two-scale model of the formation of the topography of the friction surface during running-in is presented. This model makes it possible to determine the stresses on the actual contact spots and optimize the running-in processes.

The authors of the work [12] the analysis of the influence of the spectral load during the running-in of tribosystems was carried out. The results of experimental studies are discussed and a conclusion is made about the prospects of changing the load, along a given spectrum, during running-in. This approach improves the efficiency of running-in processes.

A similar approach is presented in the work [13]. The authors developed and substantiated the structure of the tribosystems running-in program, which consists of two modes. In the first mode, the maximum load is set, below the "sticking" load at the minimum sliding speed. This mode allows, due to the intense deformation of microprotrusions, to form an equilibrium roughness of friction surfaces and change the structure of thin surface layers. The first mode is called the adaptation of the tribosystem to external conditions. The second mode sets the minimum load and maximum sliding speed. This mode allows to reduce the time of restructuring of the material structure of the surface layers and to complete the formation of secondary structures and oxide films. The second mode is called the trainability and trainability of the tribosystem. The paper presents the transient characteristics of the running-in of tribosystems, which make it possible to establish the relationship between the design of the tribosystem, rational loading modes, running-in time and wear for running-in. The practical significance of the work is to minimize the run-in time and wear during the run-in period.

Summing up the analysis of works devoted to the running-in processes, we can conclude that the novelty of this study is the development of a mathematical model of the running-in process of tribosystems, which will allow modeling the change in wear rate and friction coefficient over time. The study of such processes will make it possible to substantiate the running-in regimes and reduce running-in wear and running-in time, as well as develop a program for effective running-in of various designs of tribosystems. Such models should determine the boundary of the stable operation of the tribosystem, i.e. the boundary of the tribosystem exit to the scoring or the

boundary, when the accelerated wear of the materials of the triboelements begins [14]. Accounting for such regimes will improve the efficiency of modeling the running-in processes of tribosystems.

Purpose

The purpose of this study is to develop a mathematical model of running-in processes in tribosystems in the form of a differential equation and its solutions, which will allow modeling the wear rate and friction coefficient over time, taking into account the robustness range.

Methods

The structural identification of the mathematical model of tribosystems running in conditions of extreme lubrication will be performed according to the following structural and dynamic scheme, which is shown in fig. 1.

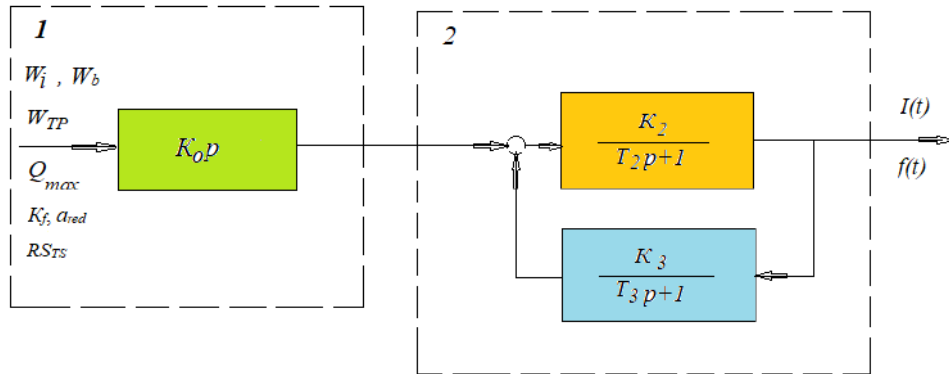


Fig. 1. Structural and dynamic scheme of simulation of tribosystems running-in processes

The structural dynamic scheme is built on the principle of two blocks connected in series.

The first block simulates the change of the following values:

- input impact on the tribosystem W_i , (the power supplied to the tribosystem) is determined by the formula given in the work [15];
- the maximum value of the input impact, when there is accelerated wear of tribosystem materials, or burr of friction surfaces, W_b , is determined by the formula given in the work [14];
- speed of dissipation in the tribosystem W_{TP} , is determined by the formula given in the work [15];
- the maximum value of the quality factor (Q-factor) of the tribosystem Q_{max} during the running-in time, is determined by the formula given in the work [16];
- the design parameters of the tribosystem are taken into account by the form factor K_f , is determined by the formula given in the work [16];
- given value of the coefficient of thermal conductivity of triboelement materials a_{red} , is determined by the formula given in the work [16];
- rheological properties of the structure of composite materials in the tribosystem RS_{TS} , is determined by the formula given in the work [16].

The second block of the structural-dynamic scheme, fig. 1, simulates the reaction of the tribosystem to a change in the input external influence, with a subsequent change and stabilization of the volumetric wear rate $I(t)$ and coefficient of friction $f(t)$ after completion of the running-in. Such processes are accompanied by a change in the roughness and structure of the surface layers of triboelement materials.

The transfer functions of the second modeling block, fig. 1, are similar to the transfer functions of the second block of the structural-dynamic scheme, which is presented in the work [15]. Transfer functions are inertial links and characterize the sensitivity of the tribosystem to input external influences and the ability of the tribosystem to rearrange the surface layers of the materials from which the triboelements are made during running-in. Such a reconstruction is associated with a change in the load, sliding speed, and Q-factor of the tribosystem [16]. Such processes are a function of time.

Applying the methods of the theory of identification of dynamic objects, it is possible, for the structural-dynamic scheme in fig. 1, to obtain an equivalent transfer function for simulating the running-in of the tribosystem:

$$G_{eq} = \frac{K_0 p \cdot K_2 (T_3 p + 1)}{(T_2 T_3) p^2 + (T_2 + T_3) p + K_2 K_3 + 1} \quad (1)$$

We will write the corresponding equation of the tribosystem running-in dynamics in the following form:

$$(T_2 T_3) p^2 + (T_2 + T_3) p + K_2 K_3 + 1 = (K_0 K_2 T_3) p^2 + K_0 K_2 p \quad (2)$$

The differential equation of the second order is written in operator form, where the symbol p , is the differentiation operator, d/dt .

The right-hand side of the differential equation (2), which characterizes the input effect on the tribosystem, contains the first and second derivatives. The input influence is represented as a product of coefficients and a time constant $K_0 \cdot K_2 \cdot T_3$. This allows us to state that the running-in processes of the tribosystem will effectively take place when the input action (load and sliding speed) will change in time and have fluctuations with positive and negative acceleration of these values from the set (program) value. This requirement corresponds to the running-in program "at the border of seizing".

The left part of the equation is the response of the tribosystem to the input signal. Tribosystem time constants T_2 and T_3 have the dimension of time and characterize the inertia of the processes occurring in the tribosystem during running-in.

Increasing time constants T_2 and T_3 , makes the process less susceptible to changes in the input influence, the running-in process increases in time, and the tribosystem becomes insensitive to minor changes in load and sliding speed. Conversely, the reduction of time constants makes the tribosystem sensitive to any external changes.

The procedure of parametric identification or finding expressions for calculating gain coefficients and time constants that characterize the dynamics of the tribosystem run-in process is an experimental material that allows you to select the most significant factors that affect the running-in process.

Gain factor K_0 , which is included in the first block of the structural-dynamic diagram, fig. 1 and in the differential equation, formula (2) takes into account the degree of influence of the input signal (load, sliding speed, tribological characteristics of the lubricating medium) on the value of the output signal (Q-factor of the tribosystem). Based on this physical concept and using the dimensional methods of similarity theory and modeling, we will get an expression:

$$K_0 = \frac{W_i}{W_b} \quad (3)$$

where W_i - the input effect, or the power supplied to the tribosystem, is calculated as the product of the load and the sliding speed, the formula for the calculation is given in works [14, 15];

W_b - input impact, or power, when loss of stability, burr or accelerated wear occurs, the formula for calculation is given in the work [14].

As follows from the expression (3) of the ratio of the active input influence W_i , selected for the tribosystem running-in mode, to the maximum value W_b , when there is a loss of stability, burr or accelerated wear, characterizes the maximum value W_i , which can be used when running in tribosystems. Relation W_i/W_b should not exceed units. Size W_b is determined by modeling according to the method given in the work [14].

The physical meaning of the coefficient K_2 – it is the sensitivity of the tribosystem to changes in external influences (load, sliding speed, Q-factor of the tribosystem). The value of the coefficient K_2 is calculated according to the formula given in the work [14] and has a similar physical meaning.

Coefficient K_3 – characterizes the ability of the tribosystem to self-organize when the values of the input parameters (load, sliding speed, Q-factor of the tribosystem) change. The value of the coefficient K_3 is calculated according to the formula given in the work [14] and has a similar physical meaning.

Time constant T_2 , which is included in the left part of the differential equation (2), characterizes the time during which the temperature gradient stabilizes by the volumes of the triboelements, taking into account the thermal conductivity of materials when the external conditions change, the dimension is a second. Value T_2 is calculated according to the formula given in the work [14] and has a similar physical meaning.

Time constant T_3 , which is included in both the right and left parts of the differential equation (2), characterizes the time during which the tribosystem returns to a stable mode of operation after the cessation of the action of the disturbing force, or the time until the parameters stabilize in the new mode of operation. Value T_3 is calculated according to the formulas given in the work [14] and have a similar physical meaning.

Results

The solution to the above differential equation (2) when simulating the volume rate of wear is the following expression:

$$I(t) = I_{st} \left[1 + (K_0 \cdot K_2)^\lambda(t) \cdot e^{\left(\frac{d_t}{0,3 T_3} t \right)} \cdot (\cos \nu_t t + A_t \sin \nu_t t) \right], \quad (4)$$

where I_{st} – the value of the wear rate of the tribosystem after running-in (stationary mode) is determined by the expression given in the work [18];

λ – exponent, which takes into account the change in the constant T_3 , as a function of running-in time, a dimensionless quantity;

t – running-in time, which varies from zero to completion of the running-in process, dimension second.
 The decrement of damping of oscillations during running-in is represented by the following formula:

$$d_I = \frac{(T_2 + T_{3(I)})}{2 \cdot T_I} \tag{5}$$

The time constant of the tribosystem for simulating the volumetric rate of wear during running-in is represented by the following formula:

$$T_I = \sqrt{T_2 \cdot T_{3(I)}} \tag{6}$$

The frequency of wear rate fluctuations ν_I during running-in:

$$\nu_I = \frac{\sqrt{1 - d_I^2}}{T_I} \tag{7}$$

The amount of deviation of the volume rate of wear from the current value during the oscillating process:

$$A_I = \frac{d_I}{\sqrt{1 - d_I^2}} \tag{8}$$

The solution to the above differential equation (2) when modeling the friction coefficient is the following expression:

$$f(t) = f_{st} \left[1 - (K_0 \cdot K_2)^\lambda(t) \cdot e^{\left(\frac{d_f}{0.3T_f}t\right)} \cdot (\cos \nu_f t + A_f \sin \nu_f t) \right], \tag{9}$$

where f_{st} – the value of the friction coefficient of the tribosystem after running-in (stationary mode) is determined by the expression given in the work [18].

The decrement of damping of oscillations during running-in is represented by the following formula:

$$d_f = \frac{(T_2 + T_{3(f)})}{2 \cdot T_f} \tag{10}$$

The time constant of the tribosystem for simulating the friction coefficient during running-in is represented by the following formula:

$$T_f = \sqrt{T_2 \cdot T_{3(f)}} \tag{11}$$

Frequency of friction coefficient fluctuations ν_f during running-in:

$$\nu_f = \frac{\sqrt{1 - d_f^2}}{T_f} \tag{12}$$

The amount of deviation of the friction coefficient from the current value during the oscillating process:

$$A_f = \frac{d_f}{\sqrt{1 - d_f^2}} \tag{13}$$

When modeling the running-in processes of tribosystems, especially according to the program "at the boundary of seizing", it is necessary to take into account the limiting values of the load and sliding speed when accelerated wear or scuffing occurs. Such parameters are not constant for tribosystems, but depend on the design (shape factor), rheological properties of triboelement materials and their thermal diffusivity, roughness of friction surfaces and sliding speed. A change in the sliding speed leads to a change in the strain rate on the actual contact

patches, which affects the quality factor of the tribosystem and its change during running-in, which is presented in the work [16].

On fig. 2 shows the dependences of the change in the magnitude of the input impact on the tribosystem when scoring or accelerated wear occurs – W_b , when changing the sliding speed and tribological properties of the lubricating medium. The dependencies are built according to the method for assessing the robustness of tribosystems, presented in the works [14, 19] and verified experimentally with an assessment of the reproducibility of the results and the adequacy of the simulation results to the experimental data.

The dependencies are built for the tribosystem «steel 40H + Br.AZh.9-4», $K_f = 12,5 \text{ m}^{-1}$, $Ra = 0,2 \text{ micron}$, $Sm = 0,4 \text{ mm}$.

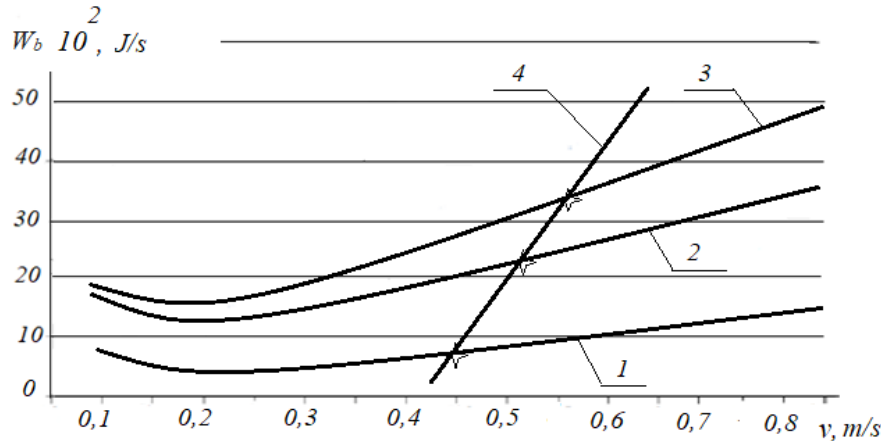


Fig. 2. Dependencies of the value of the input impact, when the loss of stability occurs (accelerated wear or burr), for different values of the sliding speed and tribological properties of the lubricating medium: 1 - MG-15B hydraulic oil; 2 - engine oil M-10G2K; 3 - transmission oil TS-P-15K; 4 – the resulting curve for points that have the same loss of stability value

Analysis of the presented dependencies allows us to draw the following conclusions. The figure field can be divided by curve 4 into two parts. To the left of curve 4 - the loss of stability of tribosystems occurs due to the occurrence of accelerated wear. To the right of curve 4 - due to tearing of friction surfaces. Points on curves 1, 2, 3, marked with "stars" have the physical meaning of the points of transition of buckling from accelerated wear of friction surfaces to scuffing of surfaces.

As follows from the dependencies, curves 1, 2, 3 have a minimum, where the occurrence of accelerated wear occurs at the minimum values of the input action, which is supplied to the tribosystem. This minimum can be explained by the absence of protective structures on the friction surfaces, since activation energy is not enough for their formation. There is an adsorbed viscous lubricating film on the friction surface. With an increase in the power supplied to the tribosystem, the activation energy becomes sufficient to form, first, viscoelastic structures, and then, solid elastic structures (right side of line 4).

These dependencies formed the basis for obtaining the exponent λ , which is presented in formulas (4) and (9) and which can be expressed by the following relationship:

$$\lambda = \frac{T_3(v = v_{red})}{T_3(W_b = \min)} \quad (14)$$

where $T_3(v = v_{red})$ – the value of the time constant at the sliding speed, which corresponds to the tribosystem running-in mode, dimension s;

$T_3(W_b = \min)$ – the value of the time constant at the sliding speed, which corresponds to the minimum value of the input influence, when the tribosystem loses stability, dimensionality s. This is the minimum on the curves, fig. 2.

When modeling the change in the volumetric wear rate during running-in, it is necessary to substitute the value in formula (14) $T_{3(v)}$, the formula for calculation is presented in the work [14]. When modeling the friction coefficient, in formula (14) it is necessary to substitute the value $T_{3(f)}$, the formula for calculation is presented in the work [14].

Exponent λ with the coefficients K_0, K_2 in the solutions of differential equations (4) and (9), takes into account the margin for stable operation of the tribosystem during running-in. Or, according to work [14] – tribosystem robustness margin. The method for determining the robustness of a tribosystem is described in the work [14].

Applying formulas (4) – (14), it is possible to simulate the processes of running-in of tribosystems over time when the following input factors are changed:

- load, N;

- sliding speed, m/s;
- geometric dimensions of the tribosystem, which are taken into account by the form factor K_a , 1/m;
- coefficients of thermal conductivity of materials of moving and fixed triboelements a_{red} , m²/s;
- rheological properties of the structure of combined materials in the tribosystem RS_{TS} , 1/m;
- tribological properties of the lubricating medium E_u , J/m³;
- roughness of friction surfaces Ra and Sm , m.

Conclusions

The structural and parametric identification of the tribosystem as an object of simulation of running-in under conditions of extreme lubrication was carried out. It has been established that the processes of running-in of tribosystems are described by a second-order differential equation and, unlike the known ones, take into account the limit of loss of stability (robustness reserve) of tribosystems. It is shown that the nature of tribosystems running-in conditions of extreme lubrication depends on the gain coefficients and time constants, which are included in the right-hand side of the differential equation.

It is shown that the processes of running-in of tribosystems depend on the type of the magnitude of the input influence on the tribosystem, the first and second derivatives. The input influence is represented as a product of coefficients and a time constant $K_0 \cdot K_2 \cdot T_3$. This allows us to state that the running-in processes of the tribosystem will effectively take place when the input action (load and sliding speed) will change in time and have fluctuations with positive and negative acceleration of these values from the set (program) value. This requirement corresponds to the running-in program "at the border of seizing".

The left part of the equation is the response of the tribosystem to the input signal. Tribosystem time constants T_2 and T_3 have the dimension of time and characterize the inertia of the processes occurring in the tribosystem during running-in. Increasing the time constants makes the process less sensitive to changes in the input signal, the warm-up process increases in time, and the tribosystem becomes insensitive to small changes in load and sliding speed. Conversely, the reduction of time constants makes the tribosystem sensitive to any external changes.

References

1. Khonsari M.M., Ghatrehsamani Sahar, Akbarzadeh Saleh. On the running-in nature of metallic tribo-components: A review. *Wear*, 2021, *Volumes 474–475*, 203871 <https://doi.org/10.1016/j.wear.2021.203871> [English]
2. Hanief M., Wani M.F. Modeling and prediction of surface roughness for running-in wear using Gauss-Newton algorithm and ANN. *Applied Surface Science*, 2015, *Volume 357*, Pages 1573-1577 <https://doi.org/10.1016/j.apsusc.2015.10.052> [English]
3. Stickel D., Fischer A., Bosman R. Specific dissipated friction power distributions of machined carburized martensitic steel surfaces during running-in. *Wear*, 2015, *Volumes 330–331*, Pages 32-41. <https://doi.org/10.1016/j.wear.2015.01.010> [English]
4. Linsler D., Schröckert F., Scherge M. Influence of subsurface plastic deformation on the running-in behavior of a hypoeutectic AlSi alloy. *Tribology International*. 2016, *Volume 100*, Pages 224-230. <https://doi.org/10.1016/j.triboint.2016.01.033> [English]
5. Cao H.M., Zhou X., Li X.Y., Lu K. Friction mechanism in the running-in stage of copper: From plastic deformation to delamination and oxidation. *Tribology International*. 2017, *Volume 115*, Pages 3-7. <https://doi.org/10.1016/j.triboint.2017.05.027> [English]
6. Mezghani S., Demirci I., Yousfi M., Mansori M.El. Running-in wear modeling of honed surface for combustion engine cylinderliners. *Wear*. 2013, *Volume 302*, Pages 1360-1369. <https://doi.org/10.1016/j.wear.2013.01.026> [English]
7. Blau Peter J. On the nature of running-in. *Tribology International*. 2005, *Volume 38, Issues 11–12*, Pages 1007-1012. <https://doi.org/10.1016/j.triboint.2005.07.020> [English]
8. Matthias Scherge. The Running-in of Lubricated Metal-Metal Contacts - A Review on Ultra-Low Wear Systems. *Lubricants*, 2018, 6(2), 54; <https://doi.org/10.3390/lubricants6020054> [English]
9. Alexander D.Jenson, Sougata Roy, Sriram Sundararajan. The evolution of hardness and tribofilm growth during running-in of case carburized steel under boundary lubrication. *Tribology International*. 2018, *Volume 118*, Pages 1-10. <https://doi.org/10.1016/j.triboint.2017.09.019> [English]
10. Yuankai Zhou, Xue Zuo. Hua Zhu, Tang Wei. Development of prediction models of running-in attractor. *Tribology International*. 2018, *Volume 117*, Pages 98-106. <https://doi.org/10.1016/j.triboint.2017.08.018> [English]
11. Furustig J., Almqvist A., Bates C.A., Ennemark P., Larsson R. A two scale mixed lubrication wearing-in model, applied to hydraulic motors. *Tribology International*. 2015. *Volume 90*, Pages 248-256. <https://doi.org/10.1016/j.triboint.2015.04.033> [English]

12. Blau P.J., Cooley K.M., Bansal D., Smid I., Eden T.J., Neshastehriz M., Potter J.K., Segall A.E. Spectrum loading effects on the running-in of lubricated bronze and surface-treated titanium against alloy steel. *Wear*. 2013, Volume 302, Pages 1064-1072. <https://doi.org/10.1016/j.wear.2012.11.071> [English]
13. Vojtov V. A., Biekurov A. Sh., Voitov A. V., Tsymbal B. M. Running-in procedures and performance tests for tribosystems // *Journal of Friction and Wear*, 2019, Vol. 40, No. 5, pp. 376–383. DOI: 10.3103/S1068366619050192 [English]
14. Vojtov V., Voitov A. Modelyuvannya mezh funktsionuvannya trybosystem v umovakh hranychnoho mashchennya // *Problems of Friction and Wear*. – 2021, – №. 4 (93). – S. 58-69. [https://doi.org/10.18372/0370-2197.4\(93\).16262](https://doi.org/10.18372/0370-2197.4(93).16262) [Ukraine]
15. Voitov, A. Structural identification of the mathematical model of the functioning of tribosystems under conditions of boundary lubrication. *Problems of Tribology*, 2021, V. 26, No 2/100, P. 26-33. <https://doi.org/10.31891/2079-1372-2021-100-2-26-33> [English]
16. Vojtov V.A., Voitov A.V. Assessment of the quality factor of tribosystems and it's relationship with tribological characteristics. *Problems of Tribology*, 2020, V. 25, No 4/97, P. 45-49. DOI: 10.31891/2079-1372-2020-97-3-45-49 [English]
17. Voitov, A. Parametric identification of the mathematical model of the functioning of tribosystems in the conditions of boundary lubrication. *Problems of Tribology*, 2021, V. 27, No 3/101, P. 6-14. <https://doi.org/https://doi.org/10.31891/2079-1372-2021-101-3-6-14> [English]
18. Voitov A. V. Razrabotka matematycheskoy modely statsyonarnykh protsessov v trybosystemakh v us-lovyyakh hranychnoy smazky. *Tekhnichnyy servis ahropromyslovoho, lisovoho ta transportnoho kompleksiv*. – Kharkiv: KHNTUS·H, - 2019. – Vyp. 16, s. 16-28. [Russian]
19. Voitov, A.; Fenenko, K.; Fenenko, O. Simulation of change in rheological properties of structure of combined materials in tribosystem. *IOP Conf. Ser. Mater. Sci. Eng.* 2021, 1021, 012052. <https://doi.org/10.1088/1757-899X/1021/1/012052>.

Войтов А.В. Математична модель припрацювання трибосистем в умовах граничного мащення.
Частина 1. Розробка математичної моделі

У роботі отримав розвиток методичний підхід в отриманні математичних моделей, які описують припрацювання трибосистем в умовах граничного мащення.

Виконано структурну та параметричну ідентифікацію трибосистеми, як об'єкта моделювання припрацювання в умовах граничного мащення. Встановлено, що процеси припрацювання трибосистем описується диференціальним рівнянням другого порядку та на відміну від відомих враховує межу втрати стійкості (запас робастності) трибосистем. Показано, що характер припрацювання трибосистем в умовах граничного мащення залежить від коефіцієнтів підсилення і постійних часу, які входять в праву частину диференціального рівняння.

Показано, що процеси припрацювання трибосистем залежать від величини вхідного впливу на трибосистему, перша та друга похідні. Вхідний вплив представлено у вигляді добутку коефіцієнтів та постійної часу $K_0 \cdot K_2 \cdot T_3$. Це дозволяє стверджувати, що процеси припрацювання трибосистеми ефективно проходитимуть, коли вхідний вплив (навантаження і швидкість ковзання), змінюватимуться в часі і мати коливання з позитивним і негативним прискоренням цих величин від встановленого (програмного) значення. Такій вимозі відповідає програма припрацювання «на межі заїдання».

Ліва частина рівняння - це реакція трибосистеми на вхідний сигнал. Постійні часу трибосистеми T_2 та T_3 мають розмірність часу і характеризують інерційність процесів, що протікають в трибосистемі, під час припрацювання. Збільшення постійних часу робить процес менш сприйнятливим до зміни вхідного сигналу, процес припрацювання збільшується в часі, а трибосистема стає нечутливою до незначних змін навантаження та швидкості ковзання. І навпаки, зменшення постійних часу, робить трибосистему чутливою до будь яких зовнішніх змін.

Ключові слова: трибосистема; припрацювання; математична модель припрацювання; диференціальне рівняння; коефіцієнт підсилення; постійна часу; граничне мащення; добротність трибосистеми; робастність трибосистеми; швидкість об'ємного зношування; коефіцієнт тертя



Tribomonitoring of the quality of aviation hydraulic oils according to lubricity and rheological indicators

O.A. Ilina, O.O. Mikosianchyk*, O. P. Yashchuk, R.H. Mnatsakanov, N.M. Berezhivskiy

National Aviation University, Ukraine

**E-mail: oksana.mikos@ukr.net*

Received: 10 January 2023; Revised: 08 February 2023; Accept: 28 February 2023

Abstract

The study proposes a diagnostic control method for assessing the quality of commercial batches of hydraulic oils based on the kinetics of changes in the thickness of lubricating layers, shear stresses of the lubricating material, and effective viscosity in tribotechnical contact. Timely and high-quality tribomonitoring of lubricants provides a perspective on their rational use and reduced wear of equipment parts. The developed methodology simulates the operation of gears in rolling conditions with a slip of 30% using a roller analogy. Samples of AMG-10 oil from two manufacturers were analyzed. For "Bora B" AMG-10 oil (sample 1) with gradients of the sliding speed of the lubricating layer in contact from $5.63 \cdot 10^3$ to $5.73 \cdot 10^5$ c^{-1} , the effective viscosity is set at the level of 4249 and 5039 Pa·s at a bulk oil temperature of 20 and 100 °C, respectively, which indicates the resistance of oil components to destruction under conditions of increasing shear rate gradient. For AMG-10 oil (sample 2), the effective contact viscosity decreases by 1.53 times both at an oil temperature of 20 °C and at 100 °C and is 2764 Pa·s (at 20 °C) and 3309 Pa·s (at 100 °C), which indicates the destruction of the components of the lubricant. For "Bora B" AMG-10 oil, effective lubricating properties have been established both during the start-up period and at maximum revolutions in conditions of rolling with slipping. It was shown that at start-up, regardless of the temperature of the lubricant, the mixed lubrication mode dominates. At the maximum revolutions of the tested samples, the hydrodynamic lubrication mode dominates, which indicates the effective lubricating properties of the Bora B AMG-10 oil. According to the kinetics of changes in the rheological parameters of oils, it was established that the resistance of the lubricant's components to mechano-thermal destruction under non-stationary lubrication conditions contributes to the effective formation of a lubricating layer in contact with a high bearing capacity.

Key words: aviation oils, rheological properties, lubrication mode, effective viscosity, shear rate gradient.

Introduction

The reliability of tribotechnical systems is established at the design stage, ensured during production, and confirmed during the operation of machines and mechanisms. Lubricating material significantly affects reliability indicators. Modern requirements for the reliability of tribomechanical systems are related to the qualitative improvement of lubricating materials and their components. In general, they are due to an in-depth analysis of the lubricating medium's state and the metal's contact surface in the friction process. The production technology of lubricating materials and their components is intensively developing and improving. New lubricating materials on mineral and synthetic bases are being created. Serious developments are underway to optimize the component composition of oils and lubricants, improving their physical, chemical, and operational properties.

The correct selection of lubricants and triboelement materials often determines the reliability of machines and mechanisms with highly loaded friction units. Therefore, studying patterns that determine the interaction of friction surfaces and lubricants requires comprehensive laboratory research. The analysis of expert practice allows for revealing the connection between the properties (physical, chemical, consumer) and the intended purpose of specific categories of lubricants. Currently, there are two approaches to the analysis of lubricants: the analysis of lubricants during production (incoming control of basic components, additives, and commercial batches of finished products) and the analysis of operational oil (diagnostic control).



These two directions are different from each other. Thus, during production and incoming control, the quality indicators must fall within the specified, previously known limits determined by standards and technical conditions. During diagnostic control, monitoring not so much the absolute values of specific quality indicators as the change of these values over time is necessary. For each indicated area of quality control of commercial or operational lubricants, it is essential to correctly choose the most convenient methods of analyzing the indicators of interest. These indicators include viscosity, flash point, additive content, total acid/alkaline number, water content, soot, total content of ferromagnetic and other wear particles, nitration, sulfonation, and many other indicators. The correct choice of lubricants and their timely and high-quality diagnostics are among the main conditions that increase durability and efficiency and preserve the technical accuracy of machines and mechanisms for an extended period. In addition, timely and high-quality tribomonitoring of lubricants provides a perspective on their rational use, reducing the wear of equipment parts. These measures aim to reduce the cost of repairing machines and mechanisms, reduce their downtime, and reduce the cost of manufactured products.

Literature review

Due to the complexity of physicochemical processes in the zone of frictional contact, the properties of contact surfaces and lubricating material during friction are challenging to describe from the point of view of classical mechanics. Therefore, to establish regularities of tribological and rheological indicators of friction systems in the limit mode of lubrication: studies of the mechano-thermal stability of the limit film [1], the influence of the shear rate gradient on the change in the effective viscosity and shear stresses in the lubricant [2] are actively being conducted to predict the effectiveness of the formation of the thickness of the lubricating film in contact.

The resistance of the lubricating film to mechanical destruction due to an increase in the shear rate gradient is a determining factor that ensures the normal performance of friction pairs in critical conditions. The destruction of the lubricating film during friction is one of the leading factors determining the intensification of energy processes occurring in the contact zone. It manifests in violating the structural suitability of the contact surfaces and lubricant under critical friction conditions, destroying previously formed metastable structures. [3].

In structural adaptation, lubricating boundary layers of varied nature are formed on activated metal surfaces during friction. The initially created lubricating layer has a solid structure, is characterized by non-Newtonian properties, and binds to both surfaces. When stress is applied, the layer will deform in shear until the applied shear stress is large enough to overcome adhesion to the surface. According to [4], outside of this condition, the sliding lubricant layer can behave according to two schemes. According to the first scheme, the lubricant in contact behaves as a liquid or remains attached to both surfaces but "melts" in the center. According to the second scheme, the lubricating layer retains its solid structure, and interlayer sliding occurs between areas of the lubricating material. When the action of the external shear force stops, the lubricant reorganizes its structure to its original state but with a constant shift between its two surfaces (Fig. 1).

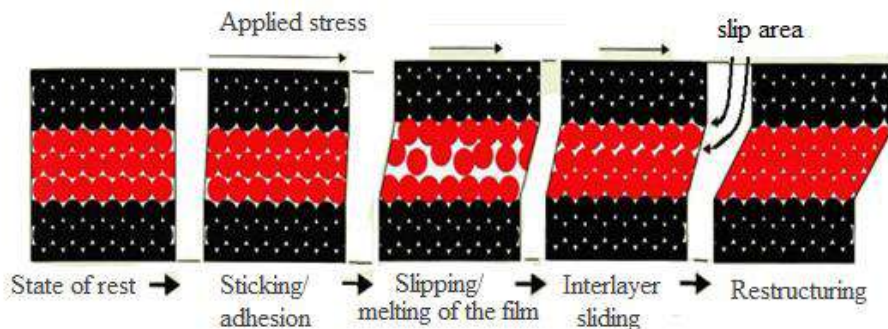


Fig. 1. The influence of shear stress on the lubricating film's deformation and its structure's reorganization [4].

According to [5], the lubricant is characterized by heterogeneity of rheological properties along the thickness of the film in frictional contact: a surface boundary layer with rheological properties different from the properties of the main part of the material in the center is formed near the wall. The lubricant flows right next to the wall as pressure is created during the system's operation. At the same time, the flow rate is zero, and the lubricant's viscosity is maximum [6]. Therefore, the material of the contact surfaces can significantly influence the rheological properties of the lubricant. The research paper [7] presents the results of studies on the formation of boundary layers in industrial lithium (LT4-C3) and calcium (STP) lubricants near the walls of six different materials: two elastomeric materials (nitrile-butadiene rubber (NBR), silicone rubber (MVQ/ VMQ)), two thermoplastic materials (polyoxymethylene (POM), polyethylene (PE)) and two metal alloys (copper C11000 and steel 304). Tests have shown that metal alloys have the most significant ability to adsorb lubricant particles on their surface. Elastomeric materials have a minor influence on the change in structural viscosity near the wall, which indicates their low capacity to form a surface layer in the tested commercial lubricants.

An experimental method for determining the interfacial shear strength based on the measured friction force and contact area during linear contact loading on coated metals has been developed [8]. It was found that the shear strength at the interface affects the overall sliding friction force under the test conditions.

In [9], the mechanism of adhesion of the boundary layer of lubricant to the surfaces forming a hydrodynamic wedge is considered. If molecules of the lubricant are in close proximity to a solid body, then their behavior is primarily determined by the influence of forces from this body. A particular rheology intermediate between the rheology of solids and liquids is characteristic of an oil film in such "boundary" conditions. With distance from the surface of the solid body, the influence of the force field created by it weakens, and its volumetric properties return to the lubricant. At the same time, boundary films have a thickness of $0.01\div 0.05\ \mu\text{m}$ and less.

In the mathematical modeling of the behavior of Newtonian/non-Newtonian fluids, rheological models of pseudoplastic and viscoplastic fluids and their parameters are used. For example, when building models of non-Newtonian fluids, the principle of mechanical modeling proposed by Rayner [10] is used. According to this principle, the behavior of various substances is defined as a parallel or sequential combination of elements with viscous, elastic, or plastic deformation. In [11], a general thermodynamic model of the melting of an ultrathin film of lubricant was proposed, and the value of the critical shear rate at which the lubricant melts by the shear melting mechanism was determined. It was established that the action of shear stresses leads to an increase in the volume of the lubricant, and, as a result, to an increase in the thickness of the lubricating layer in contact. The mathematical relationship between the volume and the thickness of the lubricating layer can be represented as:

$$\frac{\delta V}{V_0} = \frac{A\delta h}{Ah} = \frac{\delta h}{h}, \quad (1)$$

where δV – volume change, V_0 – initial volume, h – oil layer volume, A – contact area.

In this way, the importance of the established patterns of change of rheological indications in oily material in tribotechnical contact gives feasibility to predict the effectiveness of the formation of a boundary layer on active contact surfaces. It is especially essential in the case of boundary conditions, as the resistance of boundary melting to mechanical destruction ensures the movement of antifriction and anti-wear indicators in contact. Therefore, the actual direct assessment of the viscosity of the oily material is the analysis of its rheological characteristics under the dominance of different operating modes.

Purpose

To analyze the influence of the gradient of the shear rate, the shear stresses of the lubricating layer, and the effective viscosity in contact on the lubrication mode of commercial batches of aviation hydraulic oils.

Objects of research and experimental conditions

Oils to be studied:

- Sample 1 is oil "Bora B" AMG-10 according to TU U 19.2-38474081-010: 2016 with change 1 (produced by the LLC "Bora B", Ukraine);
- Sample 2 is oil AMG-10 according to GOST 6794-75 with changes 1 - 5 (produced by the LLC "NPP Kvalitet").

Sample 1 was developed to organize work on avoiding oil import and overcome the critical dependence of the defense industry of Ukraine on import supplies of AMG-10 oil.

The study of the samples was carried out on a software-hardware complex to evaluate the tribological characteristics of triboelements, for which a special software had been developed for stepper motor control and online visual evaluation of the kinetics of changes in the main tribological parameters of tribocontact [12]. Work of gears in the conditions of rolling with sliding was modeled using the software-hardware complex by means of a roller analogy (fig. 1).

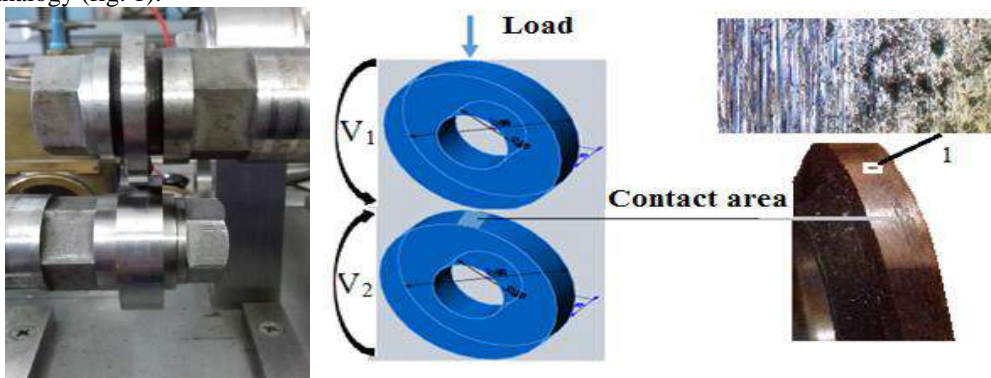


Fig. 2. The diagram of the loading node of the test samples with rotation at speeds V_1 and V_2 and the appearance of the friction tracks of the 30ChGSA steel sample; 1 – section of the contact surface of the sample.

Lubrication properties (hydrodynamic and non-hydrodynamic components of the lubricating film thickness) were determined by the method of voltage drop in the mode of normal glow discharge. Rheological characteristics of the lubricant (shear rate gradient, shear stress of lubricating layers, effective viscosity in contact) were evaluated by the kinetics of changes in the lubricating layer thickness, rotation speed of the leading and lagging surfaces and temperature of the lubricating layer.

Rollers (steel 30ChGSA, HRC 48...52, Ra 0.34 μm) were used as the material of contact surfaces. Lubrication of the contact surfaces was performed through immersing the lower roller in a bath of oil.

Testing was conducted in nonstationary conditions, which provide for the cyclicity of repetition in the start-up – stationary operation – braking – stop mode. The total duration of the cycle was 80 s.

Maximum rotation speed: 700 rpm for the leading surface and 500 rpm for the lagging surface. Sliding: 30%. Maximum contact load by Hertz: 200 MPa. Total number of cycles: 100. Temperature of oil: 20 $^{\circ}\text{C}$ (cycles 1-45), rise to 100 $^{\circ}\text{C}$ (cycles 46-50), 100 $^{\circ}\text{C}$ (cycles 51-100).

Analysis of the main results

Table 1 presents the averaged results of experimental studies of the rheological and lubricating properties of the investigated aviation hydraulic oils.

Table 1

Rheological and lubricating characteristics of aviation hydraulic oils

Parameter	Lubricant			
	Sample 1		Sample 2	
	Temperature of lubricant, $^{\circ}\text{C}$			
	20	100	20	100
Oil layer shear stress, МПа	7,68 – 16,53	5,585 – 14,7	7,913 – 15,36	7,145 – 14,98
Effective contact viscosity, Pa·c	1836 – 8065	104,9 – 9182	1130 - 6789	78,67 - 7544
Thickness of boundary adsorption layers, μm	0,34 – 1,985	0,118– 1,992	0,118 – 1,38	0,104 – 1,57
Lubrication mode at startup	0,71 - 4,13	0,25 – 4,14	0,25 – 2,87	0,22 – 3,27
Thickness of the lubricating layer in contact, μm	3,95 – 8,768	4,65 – 9,698	3,055 – 7,8	3,454 – 7,93
Lubrication mode at maximum revolutions	8,22 – 18,24	9,67 – 20,1	6,35 – 16,22	7,18 – 16,49

Characteristics of sample 1. "Bora B" AMG-10 oil is characterized by effective rheological properties. Ensuring the hydrodynamic lubrication regime at the maximum revolutions of the cycle duration, in rolling conditions with 30% slip occurs due to the high bearing capacity of the lubricant, the formation in contact of hydro- and non-hydrodynamic components of the thickness of the lubricating layer, which are characterized by low shear stresses, on average, 9.4 MPa regardless of oil temperature (Fig. 3).

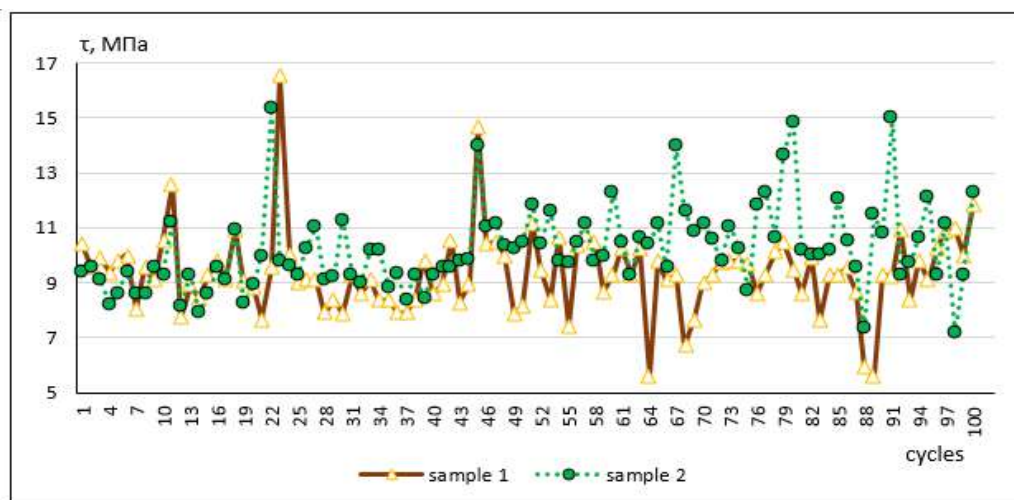


Fig. 3. Kinetics of changes in shear stress of the lubricating layer in contact (τ).

Despite the high gradients of the sliding speed of the lubricating layer in contact, from $5.63 \cdot 10^3$ to $5.73 \cdot 10^5$ c^{-1} , which occur at the maximum sliding speed of 0.71 m/s in conditions of rolling from sliding, the lubricant is characterized by effective with a viscosity at the level, on average, of 4249 and 5039 Pa·s at the volume temperature of the oil of 20 and 100 °C, respectively (Fig. 4). This testifies to the resistance of oil components to destruction under conditions of increasing shear rate gradient. The most significant decrease in the effective viscosity in contact with 105 - 250 Pa·s occurs in the conditions of the initial increase in oil temperature (45 - 49 test cycles). This is due to a change in the nature of the boundary adsorption layers, which are characterized by effective adaptation in a wide range of temperatures.

Characteristics of sample 2 AMG-10 oil, similar to sample 1, are characterized by effective rheological properties. The shear stress of the lubricating layers is set at the level, on average, of 9.4 MPa at an oil temperature of 20 °C, which is similar to the indicator for sample No. 1. When the oil temperature rises to 100 °C, this parameter increases to 10.82 MPa, which is slight, 1.15 times more, compared to sample 1 (Fig. 3).

Compared to sample 1, the effective contact viscosity decreases, on average, by 1.53 times at an oil temperature of 20 °C and 100 °C and is 2764 Pa·s (at 20 °C) and 3309 Pa·s (at 100 °C). However, with an increase in temperature during 45-50 cycles, a sharp decrease of this parameter was established to 78-240 Pa·s, which is due to the adaptation of the boundary layers of the lubricant to the change in the temperature regime in the frictional contact. The range of change in the gradient of the sliding speed of the lubricating layer (γ) in contact at the maximum sliding speed of 0.71 m/s in the conditions of rolling from sliding for samples 1 and 2 is from $4.51 \cdot 10^3$ to $5.73 \cdot 10^5$ c^{-1} .

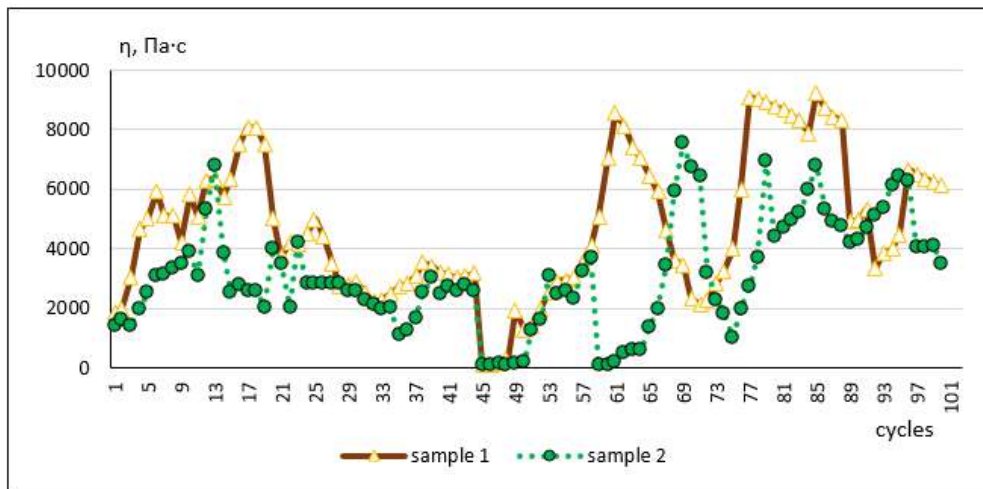


Fig. 4. Kinetics of changes in the effective oil viscosity (η) in contact.

Depending on the thickness of the lubricating layer, the lubrication mode in the frictional contact is determined according to the λ criterion:

$$\lambda = \sqrt{\frac{h}{R_{a1}^2 + R_{a2}^2}}, \quad (2)$$

where h is the thickness of the lubricating layer; R_a is the average arithmetic deviation of the profile of the contacting surfaces.

An informative indicator of the transition conditions from dry to hydrodynamic lubrication is the Hertz-Striebeck diagram. Fig.5 and Table 1 present the calculated values of the lubrication mode for the studied lubricants.

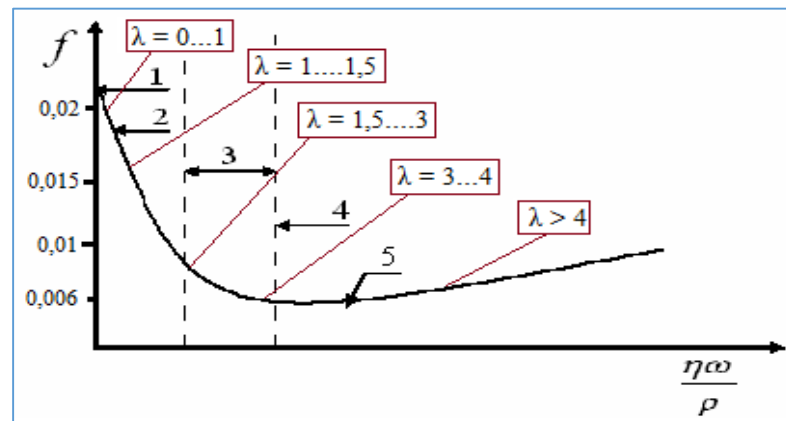


Fig. 5. Friction coefficient (f) and lubrication mode (λ) according to the Hersey-Striebeck diagram: 1 - dry, 2 - marginal, 3 - mixed; 4 - elastohydrodynamic; 5 - hydrodynamic lubrication modes.

The studied oil "Bora B" AMG-10 is characterized by effective lubricating properties during the start-up period and at the maximum studied revolutions. Breakdown of the lubricating layer at start-up and direct metal contact of the friction surfaces was not established. A semi-dry lubrication mode was set only for a short time during running-in and initial temperature rise. At start-up, regardless of the temperature of the lubricant, the mixed mode of lubrication dominates. At the maximum revolutions of the tested samples, the lubrication hydrodynamic mode dominates, indicating the effective lubricating properties of the oil "Bora B" AMG-10. For the tested AMG-10 oil at a bulk oil temperature of 20 and 100 °C, the thickness of the marginal adsorption layers is 1.44 times smaller, which leads to a deterioration of the lubrication regime in contact at start-up and the dominance of the marginal lubrication regime in 25% of the working cycles. As the temperature of the lubricant increases, long-term restoration of the protective boundary films of the oil takes place, and the period of their formation increases by 2.5 times, causing the implementation of a semi-dry lubrication mode at start-up. The total thickness of the lubricating layer is 1.27 times smaller compared to "Bora B" AMG-10 oil, regardless of the temperature of the lubricant. Thus, the resistance of the components of the studied sample 1 to mechano-thermal destruction under non-stationary lubrication conditions contributes to the effective formation of a lubricating layer in contact with a high bearing capacity, which ensures the dominance of the mixed or hydrodynamic mode of lubrication. Consequently, during the operation of the tribosystem in such conditions, optimal antifriction and antiwear characteristics of lubricants will be manifested, which is the basis for developing recommendations for the selection of commercial batches of oils for operation in conditions of rolling with slipping based on the proposed methodology for evaluating the rheological and lubricating properties of lubricants.

Conclusions

1. The conducted research on the software-hardware complex simulated gears' operation in rolling conditions with sliding using a roller analogy. Commercial AMG-10 oils from different manufacturers were studied. The errors of the obtained experimental values of the studied parameters are within 7-10%.

2. "Bora B" AMG-10 oil (sample 1) is characterized by low shear stresses, on average, 9.4 MPa, regardless of the oil temperature. For AMG-10 oil (sample 2), the shear stress of the lubricating layers is set at 9.4 MPa at an oil temperature of 20 °C, similar to the indicator for "Bora B" AMG-10 oil. When the oil temperature rises to 100 °C, this parameter increases by 1.15 times.

3. For "Bora B" AMG-10 oil (sample 1), the effective formation of the thickness of the lubricating layer in contact, resistance to the gradient of the shear rate, and effective viscosity is 4249 and 5039 Pa·s at the bulk oil temperature of 20 and 100 °C respectively. For AMG-10 oil (sample 2), the effective contact viscosity decreases by 1.53 times both at an oil temperature of 20 °C and at 100 °C and is 2764 Pa·s (at 20 °C) and 3309 Pa·s (at 100 °C), which indicates the destruction of the components of the lubricant.

References

1. Zaskoka A. N., Ljashenko Ja. A. Uchet temperaturnoj zavisimosti vjazkosti nen'jutonovskih smazok v modeli granichnogo trenija pri fazovom perehode vtorigo roda / A. N. Zaskoka, Ja. A. Ljashenko // Fizicheskaja mezomehanika. – 2014. – T. 17. – №. 2. – C. 93-100.
2. Development of methods of monitoring and diagnostics of operational properties of lubricants according to tribotechnical parameters / O. O. Mikosianchyk, R. G. Mnatsakanov, O. Ye. Yakobchuk et al. // Problems of friction and wear. – 2021. – 1 (90). – C.11-18.
3. Forecasting of the maximum linear wear of contact surfaces in extreme friction conditions / R. Mnatsakanov, O. Mikosianchyk, O. Yakobchuk et al. // Problems of friction and wear. – 2018. - 4 (81). - C. 4-12.
4. Hähner G., Spencer N. Rubbing and Scrubbing / G. Hähner, N. Spencer // Physics Today. – 1998. - 51(9). – P. 22-27.
5. Czarny R. The Influence of Surface Material and Topography on the Wall Effect of Grease / R. Czarny // Lubrication Science. – 2002. - 14(2). - P. 255–274.
6. Rozpodil lokal'nih shvidkosteij v kruglij trubi za rozginnogo ruhu ridini / O. M. Jahno, R. M. Gnativ, I. R. Gnativ, S. F. Razavi // Journal of Mechanics and Advanced Technologies NTUU "Kyiv Polytechnic Institute". Serija mashinobuduvannja. – 2018. - Vol. 84, № 3. - P. 86 – 90.
7. Czarny R., Paszkowski M., Knop P. The Wall Effect in the Flow of Commercial Lubricating Greases / R. Czarny, M. Paszkowski, P. Knop // Journal of Tribology. – 2016. - Vol. 138. - P. 031803.
8. Characterization of interfacial shear strength and its effect on ploughing behaviour in single-asperity sliding / T. Mishra, M. de Rooij, M. Shisode et al. // Wear. – 2019. Vol. 436-437. – P. 203042.
9. Maksimenko O.P., Peremit'ko V.V., Samohval V.M. Teorija i praktika z mashhuvannja metalurgijnih mashin. Navch. posibnik. – Dnipropetrovs'k: «Sistemi tehnologij», 2006r. – 172 s.
10. Kaminer A.A., Jahno O.M. Gidromehanika v inzhenernoj praktike. – K.: Tehnika, 1987. – 175 s.
11. Non-Equilibrium Evolutional Thermodynamics of Boundary Friction / L.S. Metlov, A.V. Khomenko, I.A. Lyashenko, S.N. Chepul'skyi // J. Nano- Electron. Phys. – 2010. - T.2, No2. – P.79-93.
12. Development of methods for evaluation of lubrication properties of hydraulic aviation oils / O. Ilina, O. Mikosianchyk, R. Mnatsakanov, O. Yakobchuk // Problems of Tribology. – 2021. - 26(3/101). – P. 42–47.

Ільїна О. А., Мікосянчик О. О., Ящук О. П., Мнацаканов Р.Г., Березівський Н.М. Трибомоніторинг якості авіаційних гідравлічних олиव за змащувальними та реологічними показниками

Запропонована методика діагностичного контролю оцінки якості товарних партій гідравлічних олив за кінетикою зміни товщини мастильних шарів, напружень зсуву мастильного матеріалу та ефективною в'язкістю в триботехнічному контакті. Своєчасний та якісний трибомоніторинг мастильних матеріалів надає перспективу щодо їх раціонального використання та зменшення зносу деталей обладнання. В розробленій методиці за допомогою роликаної аналогії моделюється робота зубчастих передач в умовах кочення з проковзуванням 30%. Проаналізовано зразки оливи АМГ-10 двох виробників. Для оливи «Бора Б» АМГ-10 (зразок №1) при градієнтах швидкості зсуву мастильного шару в контакті від $5,63 \cdot 10^3$ до $5,73 \cdot 10^5 \text{ c}^{-1}$ встановлена ефективна в'язкість на рівні 4249 та 5039 Па·с при об'ємній температурі оливи 20 та 100 °С відповідно, що свідчить про стійкість компонентів оливи до деструкції в умовах зростання градієнту швидкості зсуву. Для оливи АМГ-10 (зразок 2) ефективна в'язкість в контакті знижується в 1,53 раз як при температурі оливи 20 °С, так і при 100 °С та становить 2764 Па·с (при 20 °С) та 3309 Па·с (при 100 °С), що свідчить про деструкцію компонентів мастильного матеріалу. Для оливи «Бора Б» АМГ-10 встановлені ефективні змащувальні властивості як в період пуску, так і при максимальних обертах в умовах кочення з проковзуванням. Встановлено, що при пуску, незалежно від температури мастильного матеріалу, домінує змішаний режим мащення, при максимальних обертах досліджуваних зразків домінує гідродинамічний режим мащення, що свідчить про ефективні змащувальні властивості оливи «Бора Б» АМГ-10. За кінетикою зміни реологічних показників олив встановлено, що стійкість компонентів мастильного матеріалу до механо-термічної деструкції при нестационарних умовах мащення сприяє ефективному формуванню мастильного шару в контакті з високою несучою здатністю.

Ключові слова: авіаційні оливи, реологічні властивості, режим мащення, ефективна в'язкість, градієнт швидкості зсуву.



Thermal and stress-strain state of friction pairs in ventilated disc brakes of lightweight vehicles

K. Holenko¹, O. Dykha^{1*}, J. Padgurskas², O. Babak¹

¹*Khmelnytskyi National University, Ukraine,*

²*Vytautas Magnus University, Lithuania*

**E-mail: tribosenator@gmail.com*

Received: 11 December 2022; Revised: 20 January 2023; Accept: 11 February 2023

Abstract

The work is dedicated to the thermal behavior and stress-strain state of ventilated disc brakes installed in the lightweight vehicles (scooters, electric bikes, ATVs, etc.) using ANSYS environment in various experiment modes. Modeling of the temperature distribution in the rotor (disc) and the corresponding brake pads is determined taking into account a number of factors and input parameters during the braking operation: the amount of rotation speed, the gap between the pads and the disc, the speed of load application, thermal expansion, etc. Numerical modeling of the transient thermal and the stress fields in the area of contact between the pads and the rotor is carried out by the method of sequential thermostructural connection of the intermediate calculation states of the brake model in the ANSYS Coupled Field Transient environment. For a comprehensive assessment of brake behavior, our research considers two load approaches: constant long-term (20 s) with an influence factor in the form of thermal expansion as a result of contact pair friction; linear load from the pads on the disc with a corresponding increase in pressure up to the moment when the rotation of the system is blocked. Our research presents an assessment of the rotor ventilation channels influence on the nature of the contact spot with the brake pads (open far-field contact, sliding contact, sticking contact, etc.). In addition, it is demonstrated that despite the linear increase in pads pressure on the rotor, the graphs of temperatures, volume (thermal expansion) and stresses are of parabolic character with a disproportionate increase in indicators. Such a result forces us to come to the conclusion that it is not possible to predict the behavior of the brakes based on the analysis during a short period of time of the experiment - conducting long-term analytical studies is extremely important in the case of brakes.

Key words: friction, brake disc, brake pads, thermal load, stress-strain state, heat flow, von Mises stress, contact pressure, thermal expansion

Introduction

Scientific and technological progress has provided the industry with significant theoretical developments in the field of heat and mass transfer, for example, in spheres such as tribology or thermodynamics, which have developed over several decades with progress in many sectors: nuclear energy, aerospace and aviation, automotive, etc. Modeling of problems related to the phenomenon of heat or mechanical energy transfer in general and through friction pair contacts in particular, is of primary importance in the design of relevant units, for example, disc brakes of vehicles. Many authors raised such topics in their publications as: design and thermal analysis of disc brake for minimizing temperature [1]; effect of cross-drilled hole shape on crack of disc brake rotor [2]; thermal analysis of disc brakes using FEA [3-4]. In fact, it is not only about the development of new models of brakes, but also about the selection of optimal options for systems for existing vehicles, taking into account their class, type and operating conditions. As you know, brakes are a device that creates frictional resistance to move a system element (rotor) to stop further movement, so we can get acquainted with the modeling and analysis of FSAE car disc brake using FEM in [5] and discover the enhancement in design and thermal analysis of disc brake rotor in [6]. Brakes are a mechanism used to reduce the speed or stop the cycle of movement of a vehicle. Long-term use of the brake in a lightweight vehicle (bicycle and motorcycle) causes heating during the braking process [7-9], so that the rotor is deformed (jammed between the pads or breaks) due to high temperature and thermal expansion. Actually, the



thermal analysis of disc brake is the topic of publication [7], which could be effectively supplemented by the study on crack initiation at small holes of one-piece brake discs in [9]. In the research [10] authors present the velocity and relative contact size effect on the thermal constriction resistance in sliding solids. The influence of the braking time on the soundness of ventilated disc brake systems is reflected in [11-12]. Topic of investigation of temperature and thermal stress in ventilated disc brake based on 3D thermomechanical coupling model raised in [13] is similar to our work and makes sense to be researched. Our goal is to proceed the analysis of the behavior of the system under conditions of long-term friction at constant pressure with a corresponding increase in temperature and volume of the model, as well as with a variable load in the system (from the hydraulic cylinder), which leads to blocking of the brakes with plastic disc deformations (determination of stresses according to Mises).

The purpose of the work

Formation of a methodology for analytical studies of thermal modes of the lightweight vehicles disc brakes operation as a result of friction pairs contact with variable and constant pressure in the ANSYS Coupled Field Transient software environment. Analysis of the influence on heat dissipation and stress distribution of such factors as: duration of braking, convection in the environment, geometry of the brake disc and pads, system actuation time.

Results of studies under constant load

A disc brake is a system consisting of a brake disc (rotor), brake pads and calipers actuated by a hydraulic cylinder. The brake disc rotates with the wheel and the pads mounted on the brake calipers clamp it to stop or slow the wheel (Fig. 1). Brake pads generate heat through friction, converting kinetic energy into heat to reduce the total kinetic energy of the vehicle. Thus, due to the thermal energy generated during the braking process, the temperature of the disc on the contact part increases and generates fatigue stresses accumulation, causing cracks or plastic deformations that reduce the service life of the disc. Usually, ventilated discs are used to improve the efficiency of heat dissipation, because they have channels for air circulation: the higher the rotational speed of the disc, the higher the centrifugal force, which contributes to the dissipation of heat.

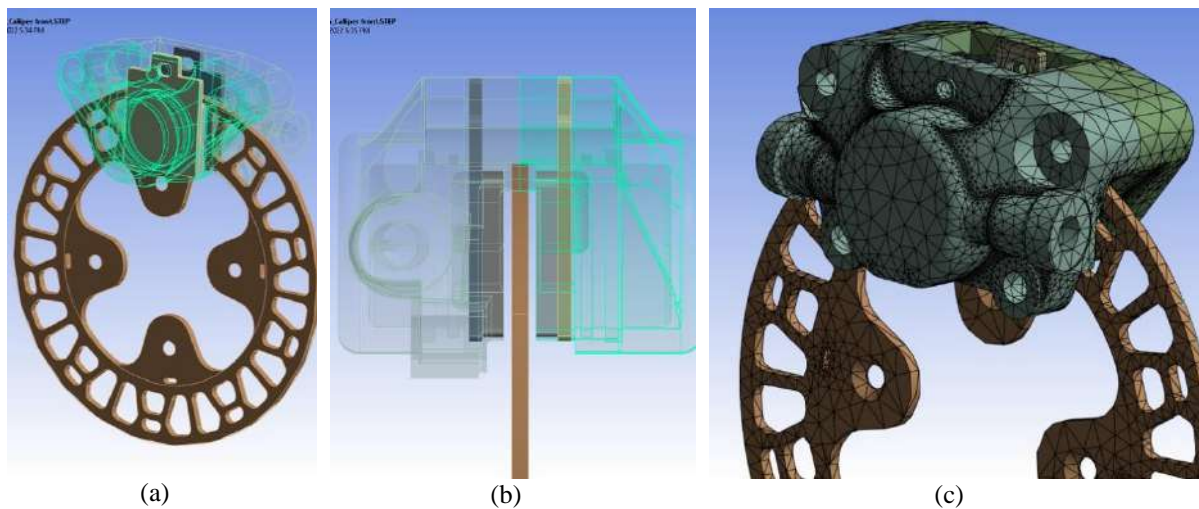


Fig. 1. Solid disc brakes model: a) isometry; b) the gap between the disc and the pads in the initial state (1.5 mm); c) FE grid of the model

To select the optimal brake system according to the target vehicle, it is advisable to determine the required pressure [10-12] from the brake pads:

$$P = F_d / S\mu, \quad (1)$$

where: P - pressure between the disc and the pad; F_d - force acting on the disc; S - surface of the pad in contact with the disc; μ - coefficient of friction.

The actual value of the pressing force F_d can be found as follows:

$$F_d = k \cdot \left(M \frac{v^2}{2} \right) / \left[2 \frac{r}{R} \left(vt - \frac{1}{2} \left(\frac{v}{t} \right) t^2 \right) \right], \quad (2)$$

where: k – load factor – 0.3 (corresponding to 30%); M – mass of the vehicle; r – brake disc radius; R – wheel radius; v – vehicle speed.

We apply the following values to the boundary conditions of the calculation: time of the experiment $t = 20$ s; coefficient of friction $\mu = 0.2$ c; angular velocity $w = 3.5$ rad/s, which corresponds to a wheel speed of $200^\circ/s$. Wheel is rotated due to the hub with the 4 holes for mounting bolts (Fig. 1a), where are observed the highest meanings of stress (Fig. 2b); the movement of pad Δ is symmetrical and presented in steps (Table 1). The initial gap between pads and disc is 1.5 mm. Starting from 0.3 s and until the end of the experiment $\Delta = 1.501$ mm – thus, the full contact between friction pairs is simulated.

Table 1

Brake pads travel during the experiment (20 s)

Time moment	0 s	0.1 s	0.2 s	0.3 s	20 s
Δ	0 mm	0.75 mm	1.5 mm	1.501 mm	1.501 mm

The FEM model consists of 101529 elements; applied material is Structural Steel (typical characteristics are embedded in Ansys); the number of time steps is 200 (duration of a step is 0.1 s); the total calculation time on the equipment (2 Intel Xeon processors 24 cores, RAM 48 Gb, NVIDIA GeForce 4Gb video) was 10 hours 42 min.

Let's analyze the stress maps of the brake pads and the ventilated disc (Fig. 2) - as we can see, there is a stress increase tendency while the experiment continues:

- the pad is pressed to the disc in 0.2 s and its stress increases from 8.3 MPa (caused by reactions from the rotational movement in the holes for mounting bolts attaching the disc to the hub) to 223 MPa (when Δ reaches 1.501 mm). Further, as the experiment progresses, the stress increases to a maximum of 647 MPa at a time of 18.2 s. The intermediate state of stress at the moment of time 17.4 s is presented in Fig. 2b (the curve is "max, MPa"). The curves "min, MPa" and "average, MPa" correspond to the minimally loaded locations of the body and the average value of loads for all its locations, respectively.

- the pad stress increases to 22 MPa in the first 0.2 s (the period of pressing against the disc) and then reaches up to 138 MPa at the time of 19.5 s (Fig. 2a).

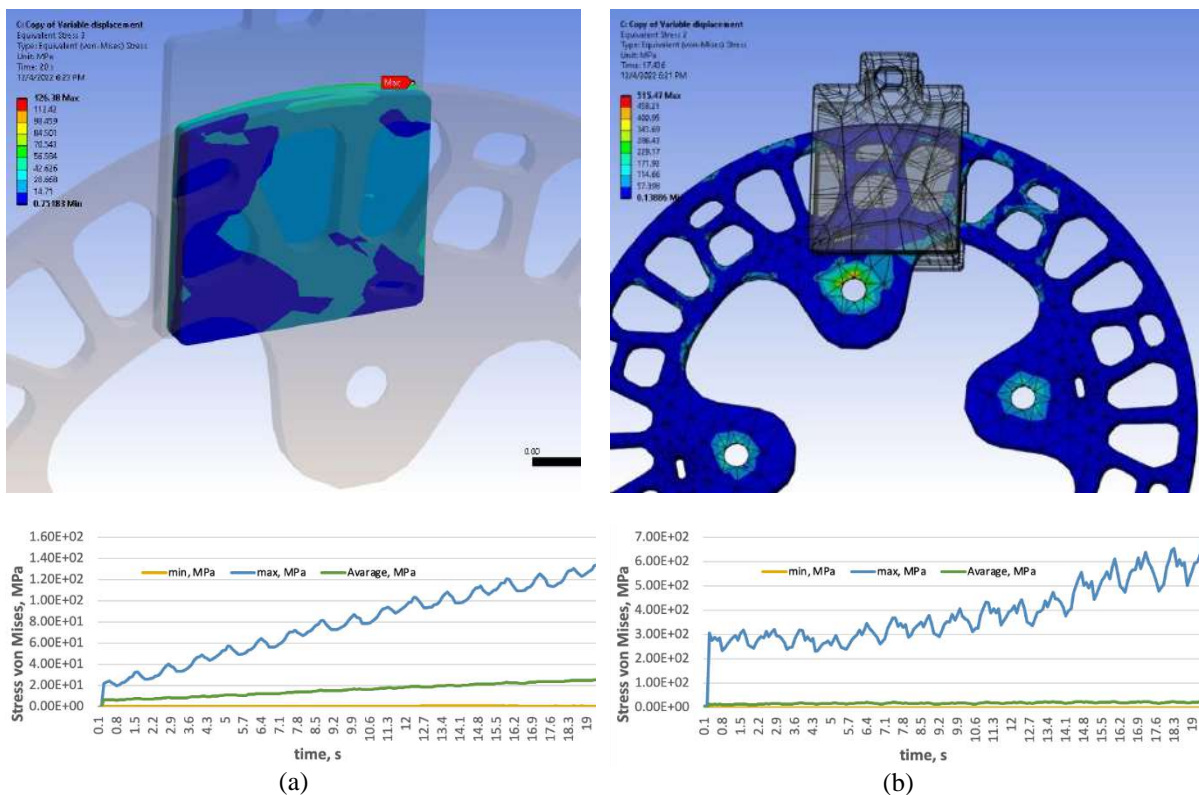


Fig.2. Stress in the braking system at a constant load: a) brake pad and stress graph over time; b) ventilated disc and stress graph over time

What should be paid attention to: despite the constant value of the displacement of the pads (it is stable and equal 1.501 mm during the entire experiment lasting 20 s), the stress values fluctuate and increase. Why do we observe such processes? Let's consider the answers to both questions sequentially.

1) Stress fluctuations are explained by the uneven structure of the disc itself (holes in the structure for ventilation): as it rotates, the area of contact with the pad is constantly changing, and thus the pressure and stress change as well. Let's visually check the nature of the pad contact with the disc at different moments of time (Fig. 3) - the unevenness of the distribution is dictated by the channels in the disc that affect the contact spot: the position and movement of the contact element determines its condition relative to the target surface associated with it.

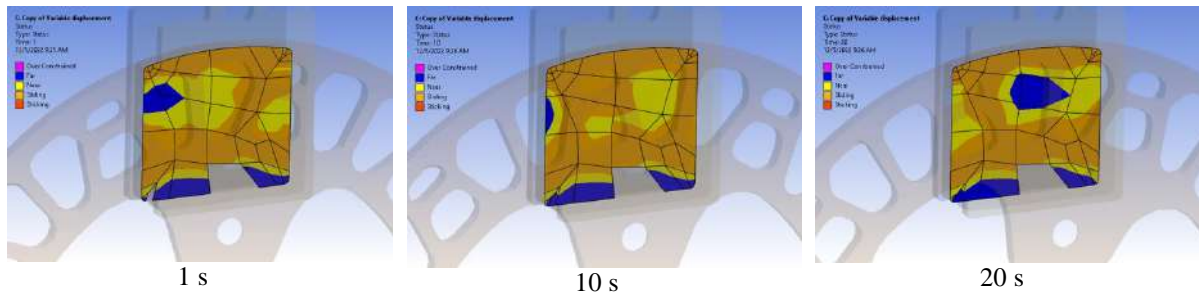


Fig.3. Analysis of brake pad contact area at different moments of time

ANSYS monitors each contact element and assigns a status:

- STAT = 0 Open far-field contact (open remote contact) – blue color;
- STAT = 1 Open near-field contact (open near field contact) – yellow color;
- STAT = 2 Sliding contact (sliding contact) – orange color;
- STAT = 3 Sticking contact (sticking contact) – red color.

An element is considered to be in close contact if its integration points (Gauss points or nodal points) are within the code-calculated (or user-defined) distance to the corresponding target surface. This distance is called the pinball area. A pinball domain is a circle (in 2-D) or a sphere (in 3-D) centered around a Gauss point.

The friction coefficient may depend on the relative speed of the contacting surfaces. As a rule, the static coefficient of friction is higher than the dynamic one. ANSYS provides the following exponential friction damping model:

$$\mu = MU \cdot (1 + (FACT - 1) \exp(-DC \cdot v_{rel})), \quad (3)$$

where: μ – friction coefficient; MU - dynamic coefficient of friction (using the MP command in Ansys); $FACT$ - the ratio of static to dynamic friction coefficients (the minimum value is set by default 1.0); DC - damping coefficient (by default it is equal to 0 and has the unit of dimension time/length), so time has a certain value in static analysis); v_{rel} - slip velocity calculated by ANSYS. "Friction Decay" shows an exponential decay curve (Fig. 4a), where the static coefficient of friction is defined as:

$$\mu_s = MU \cdot FACT \quad (4)$$

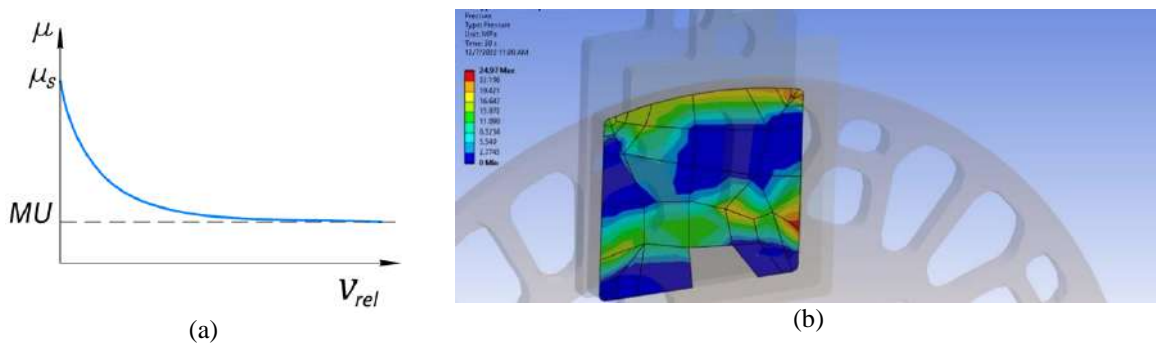


Fig.4. Research of friction: a) exponential curve of friction damping; b) pressure map on the pad surface at the time of 20 s

The damping coefficient can be determined if the static and dynamic coefficients of friction and at least one data point are known ($\mu_1; v_{rel1}$). The equation to describe friction damping can be written as follows:

$$DC = -\frac{1}{v_{rel1}} \cdot \ln\left(\frac{\mu_1 - MU}{MU(FACT - 1)}\right) \quad (5)$$

If no damping factor is specified in the simulation process, and $FACT$ is greater than 1.0, then the friction coefficient will suddenly change from static to dynamic value as soon as the contact reaches the sliding state. It should be noted that such behavior is strongly not recommended, since the gap can lead to convergence difficulties when solving the problem [7-8].

2) Why does the value of stresses in the disc and brake pads increase, if they remain stationary and do not increase the external load from the hydraulic cylinder? By the way, what is the maximum pressure value recorded during the experiment (Fig. 5)?

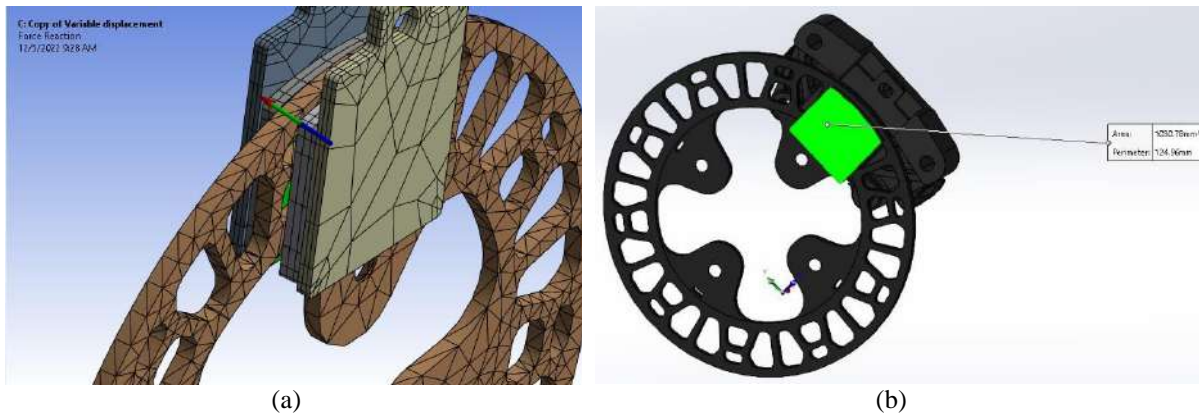


Fig. 5. Determination of pressure in the disc brake system: a) FEM model with load vector; b) determination of the brake pad area (SolidWorks environment)

We have measured the maximum value of the load (Fig. 5a) during the experiment in the Ansys environment: 7968.5 N at the time of 18.2 s. The pad area is 1030.78 mm² (Fig. 5b), which corresponds to a pressure of 7.73 MPa. It's possible to observe a similar value on the graph (Fig. 6d - orange color), which shows the average pressure value over the pad area. However, taking into account that the contact area varies, as shown in Fig. 3, and can occupy up to 35-40% of the pad area due to the ventilation holes at certain moments of time, the pressure value increases up to 20 MPa. This is a typical value for disc brakes in automotive and two-wheeled vehicles. Therefore, our experiments with the applied boundary conditions are approaching to the natural tests.

The reason of the stress increase is the thermal expansion of the disc and pads (increase in volume) as a result of heating (Fig. 6a, b) and internal energy growth (Fig. 6c), which leads to a decrease in the gaps between disc and pads with the appropriate pressure rise (Fig. 6d). It should be noted that the increase in the volume of the pad is relatively linear over time, but the disc expands according to a geometric progression - in fact, this already prompts the idea of the feasibility of scientific research on ventilation holes in the structure of the disc, the selection of their optimal configuration, etc.

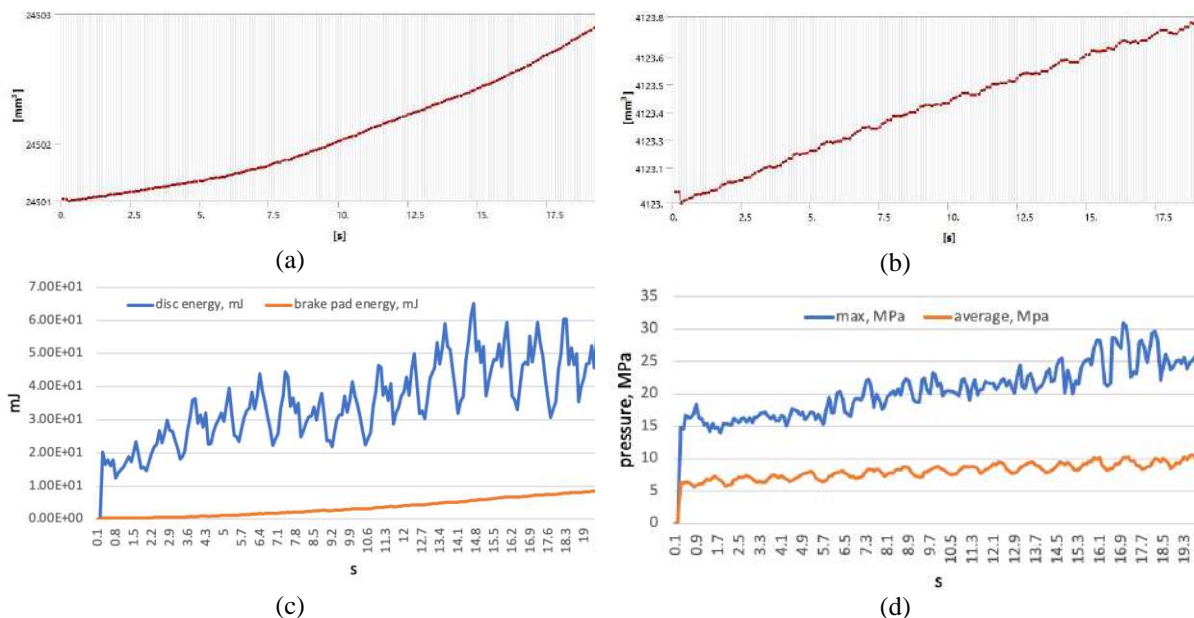


Fig.6. Thermal state analysis of disc brakes: a) volume of the disc; b) volume of pads; c) growth of energy over the friction; d) pressure on the pad surface (average in area and maximum in locations)

Fig. 7 shows temperature maps of the disc at certain moments of time. Thus, the value of the disc temperature during the experiment lasting 20 seconds reached 34.87°C. It should be understood that the following boundary conditions were applied as a part of our research: temperature $T(x,y,z) = 22^{\circ}\text{C}$ at time $t = 0$ s and zero value of convection (please note that the simulation of moving air masses assumes 5 W/m²C in a static position and around 25 W/m²C - in dynamics) to obtain clean results of body heating and heat flux (fig. 8a,c). The value of the pad's temperature reached - 35.04°C, which is shown on the graph of both elements heating (disc and pads) -

Fig. 8b. It's quite exciting to observe how close are both graphs (Fig.8b) – heat transfer from pads to rotors could be visually observed by the temperature equalizing between both units at any time moment.

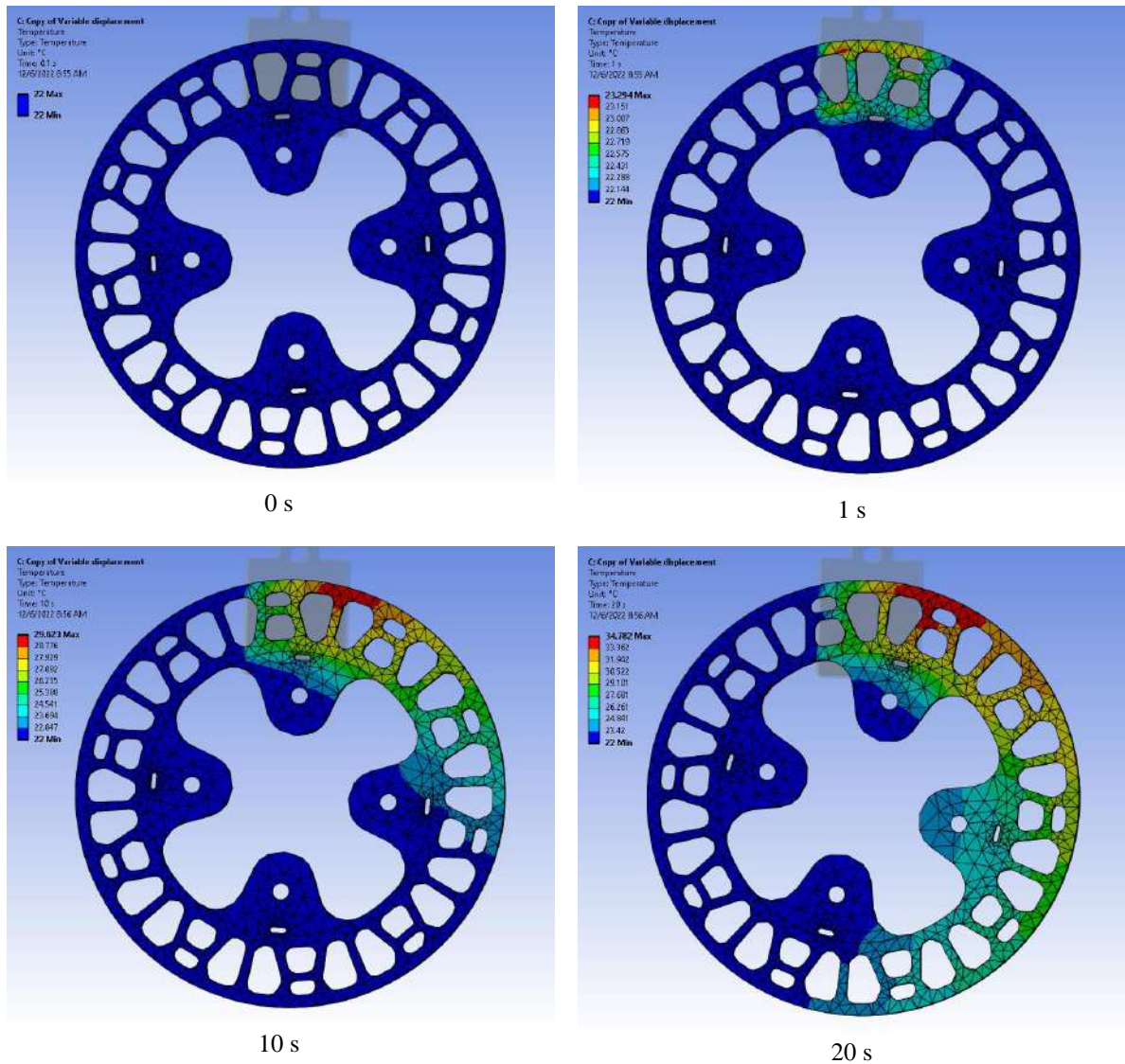


Fig. 7. Temperature maps of the brake disc at different times of the experiment

Let's turn to the theory of the thermal state description of the body - the first law of thermodynamics, which shows on the thermal energy saving [13]:

$$C_p \left(\frac{\partial T}{\partial t} + \{v\}^T \{L\} T \right) + \{L\}^T \{Q\} = p \quad (6)$$

In our calculated case, there is no internal pressure source ($p = 0$), and therefore equation (6) will be written as follows:

$$\rho C_p \left(\frac{\partial T}{\partial t} + \{v\}^T \{L\} T \right) + \{L\}^T \{Q\} = 0, \quad (7)$$

where:

$$\{L\} = \left\{ \begin{array}{c} \frac{\partial}{\partial x} \\ \frac{\partial}{\partial y} \\ \frac{\partial}{\partial z} \end{array} \right\}, \quad \{v\} = \left\{ \begin{array}{c} v_x \\ v_y \\ v_z \end{array} \right\}, \quad (8)$$

where: $\{L\}$ – vector operator, $\{v\}$ – vector speed of the vehicle.
Let's write Fourier's law (7) in matrix form:

$$\{Q\} = -[K]\{L\}T, \quad (9)$$

where: $[K]$ – matrix with the corresponding coefficients K_{xx}, K_{yy}, K_{zz} by axes X, Y, Z, which are equal in all directions for isotropic materials: $K_{xx} = K_{yy} = K_{zz}$ [13]:

$$[K] = \begin{bmatrix} K_{xx} & 0 & 0 \\ 0 & K_{yy} & 0 \\ 0 & 0 & K_{zz} \end{bmatrix} \quad (10)$$

When combining equations (7) and (9), we get the following expression:

$$\rho C_p \left(\frac{\partial T}{\partial t} + \{v\}^T \{L\} T \right) + \{L\}^T ([K] \{L\} T) \quad (11)$$

Let's rewrite (11) in the following form:

$$\rho C_p \left(\frac{\partial T}{\partial t} + v_x \frac{\partial T}{\partial t} + v_y \frac{\partial T}{\partial t} + v_z \frac{\partial T}{\partial t} \right) = \frac{\partial}{\partial x} \left(k_x \frac{\partial T}{\partial x} \right) + \frac{\partial}{\partial y} \left(k_y \frac{\partial T}{\partial y} \right) + \frac{\partial}{\partial z} \left(k_z \frac{\partial T}{\partial z} \right) \quad (12)$$

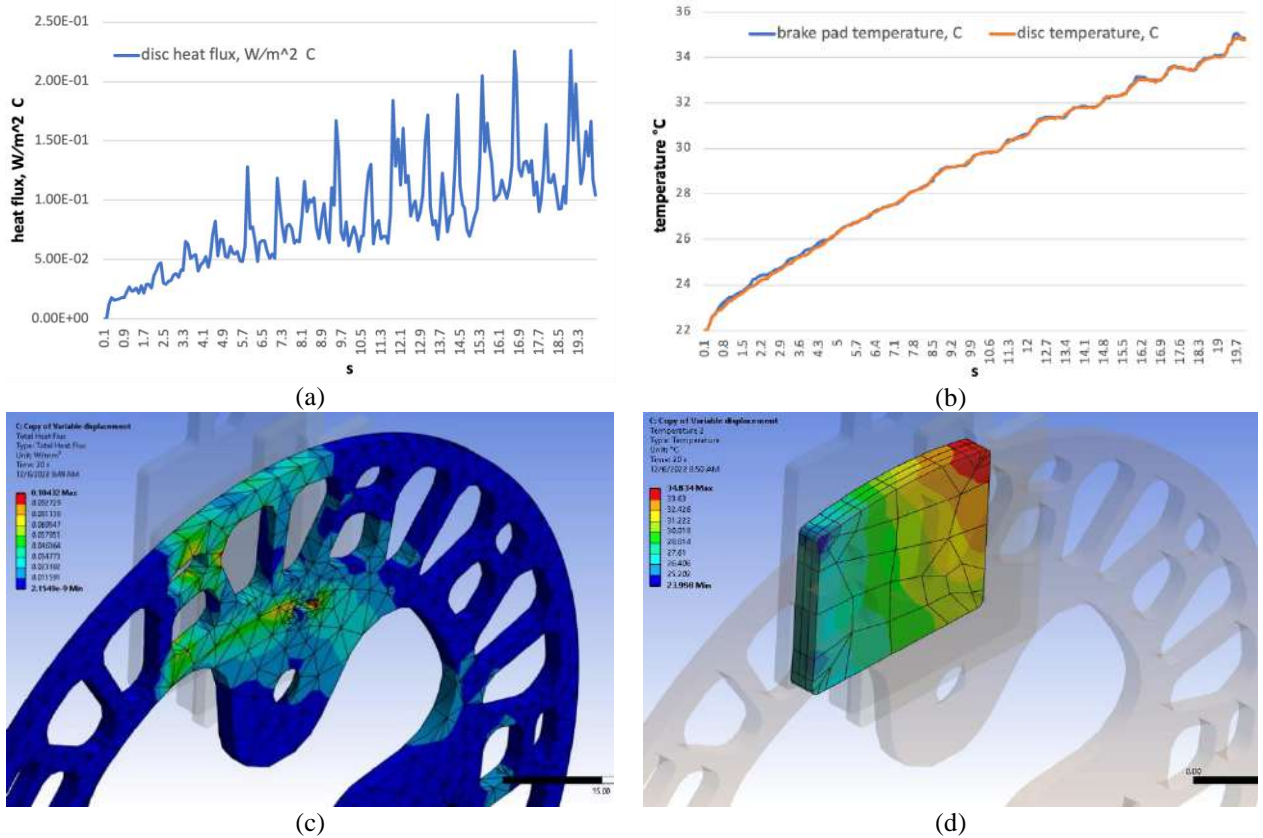


Fig. 8. Heat load of brakes: a) heat flow of the disc; b) temperature of the disc and pad; c) heat flow of the disc at 20 s; d) temperature of the pad at 20 s

In general, the typical boundary conditions of thermal calculation can be attributed to [13]:

- surface temperature: $SURF_T: T = T^*$;
- thermal dissipation on the surface: $SURF_Q: \{Q\}^T \{n\} = -Q^*$;
- convection on the surface: $SURF_C: \{Q\}^T \{n\} = h(T_p - T_f)$,

where: $SURF_T$, $SURF_Q$, $SURF_C$ – surface temperature, flow and convection; T^* - the temperature given at the surface; Q^* - the heat flux given at the surface; T_p – surface body temperature; T_f - environment temperature; h - coefficient of convective heat transfer.

In turn, the thermal expansion presented in the graph (Fig. 6a) can be described by the following conditions, which are relevant for the behavior of solid bodies:

- thermal coefficient of volumetric expansion (measured in inverse degrees Kelvin, K^{-1}):

$$\alpha = \frac{1}{V} \left(\frac{\partial V}{\partial t} \right) \quad (13)$$

If the volume expansion coefficient changes significantly with temperature, then the equations must be integrated:

$$\frac{\Delta V}{V} = \int_{T_0}^{T_0+50} \alpha(T) dT \tag{14}$$

- thermal expansion of the area of a solid body:

$$\Delta S = 2\alpha S_1 \Delta t, \tag{15}$$

where: T_0 - initial temperature; ΔS – area change (for example, brake pads or disc); S_1 – starting area; Δt – temperature change.

Results of studies under variable load

We have previously considered the behavior of the brake system consisting of a disc and pads under a constant external load (pressure) from hydraulic cylinder on them: the static position of the pads during the entire experiment lasting 20 s and constant travel ($\Delta=1.501$ mm). How will the system show itself if we increase the pressure in the hydraulic cylinder and set the pads movement according to the linear law (Table 2)?

Table 2

Dynamics of brake pads movement during the experiment (20 s)

Moment of time	0 s	0.1 s	0.2 s	0.3 s	1 s	5 s	10 s
Δ	0 mm	0.75 mm	1.5 mm	1.501 mm	1.508 mm	1.548 mm	1.598 mm

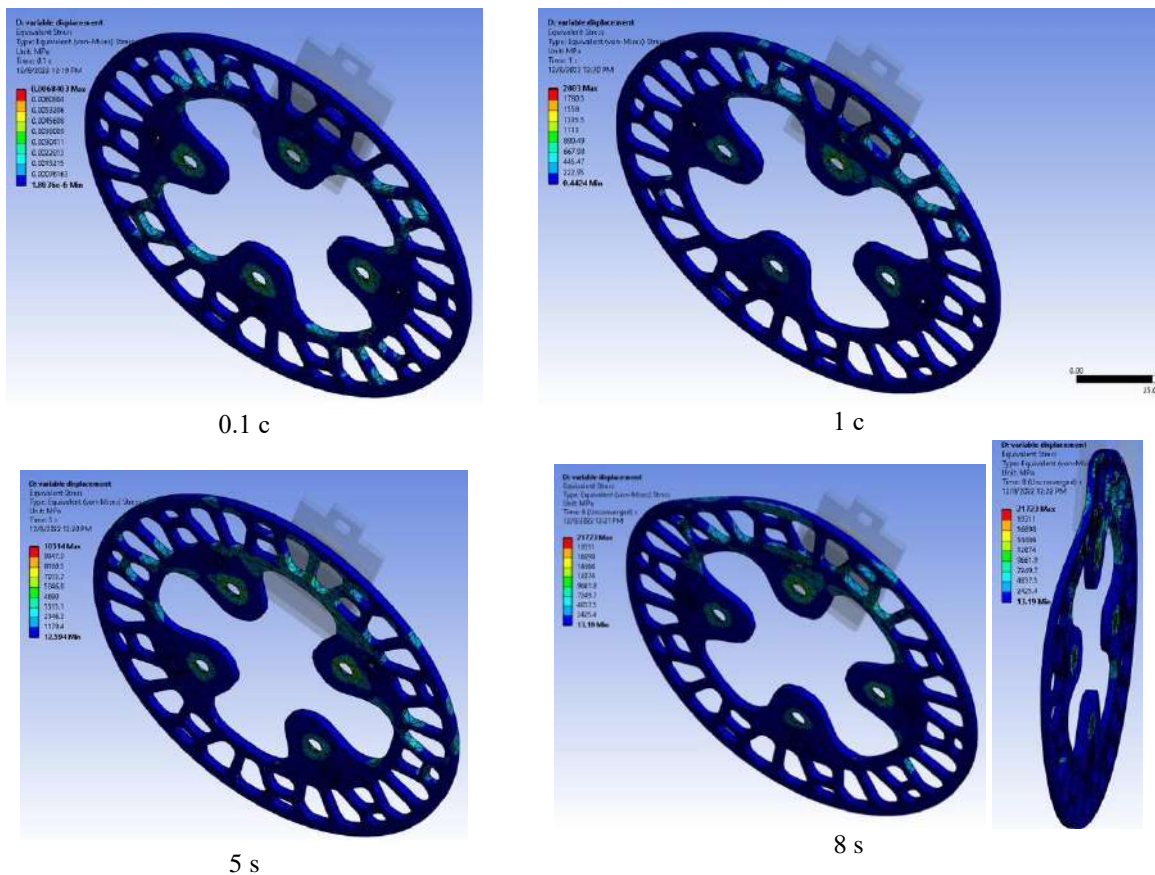


Fig. 9. Stress-deformable state of the brake rotor

This setting of boundary conditions leads to jamming of the brakes, because two factors come into play: the increase in pressure from the side of the pads; the thermal expansion of pads together with the disc. The stress map at the critical moment is presented in Fig. 9 - the plastic deformation of the disc is visually observed as a result of an attempt at inertial scrolling. As you can see, the experiment stopped at the 8th second - the further process is a static state of the system and does not require an assessment of its behavior (the disc cools down to the initial 22°C). Rotor and pad stress trends are demonstrated on Fig.10 – fluctuations on the graph mean the

ventilation channels influence on the stress meaning. Additional plasticity of the material during the long-term friction is provided by an increase in temperature as a result of pressure growth - the disc model received 32-37% higher temperature values compared to the previous experiment (unchanged travel of pads $\Delta=1.501$ mm). Such results lead to the opinion of the necessity to arrange not only the structural optimization of the disc (ventilation channels), but also force to think about the relevance of using heat-resistant materials for the production of brakes: ceramics, which is a standard point in the premium segment of cars, sports cars, etc.

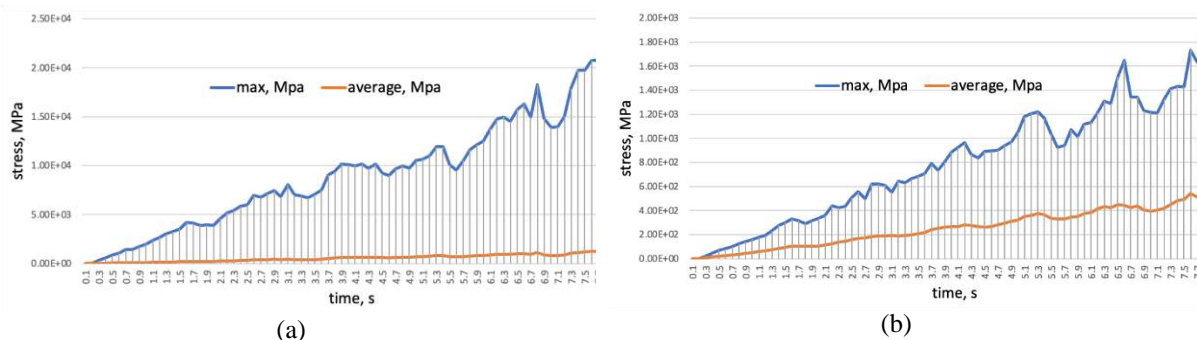


Fig. 10. Brake stress under the variable load: a) disc stress graph; b) pads stress graph

Conclusions

1. The results of thermal behavior and stress-strain state of ventilated disc brakes presented in the work using the ANSYS Coupled Field Transient calculation environment are of a practical nature not only from the point of view of designing new vehicles with the appropriate selection of the optimal brake configuration for them, but also the optimization of existing structures. The research provides such valuable data as: temperature distribution along the rotor and pads during the friction process; heat dissipation, cooling and ventilation activities; selection of suitable materials for the production of friction pairs; creating an optimal configuration of the disc ventilation holes; determination of the required pressure in the hydraulic cylinders, taking into account the mass of the vehicle and the conditions of its operation (speed, convection of the medium, etc.).

2. The results obtained in the conditions of a pads static position during the entire experiment lasting 20 s with their constant travel ($\Delta=1.501$ mm) allow us to quantitatively assess the influence of thermal expansion on the key performance indicators of the brakes as a result of friction (heating from 22°C to 35.04°C). This approach provides an understanding of the necessity to remove heat and ventilate the brakes, because the trends presented in the graphs indicate an exponential rather than a non-linear increase of the disc volume during heating, and suggest the inevitability of jamming / burning of the brakes (depending on the degree of vehicle movement inertia) with prolonged contact of friction pairs.

3. The use of the ANSYS Coupled Field environment in conjunction with the boundary conditions proposed in the work allows you to form your own effective brake modeling methods, which is especially useful in the conditions of small design studios and workshops, which, in fact, are often involved in the production and design of lightweight vehicles: motorcycles, e-bikes, ATVs, scooters, buggies, etc.

References

1. Deepak S. Hugar, U. B. Kadabadi, "Design and Thermal Analysis of Disc Brake for Minimizing Temperature", International Research Journal of Engineering and Technology (IRJET), Volume: 04, Issue: 07, July -2017
2. Kang, H.; Jung, T.; Hong, Y.; Park, S. Effect of Cross-drilled Hole Shape on Crack of Disc Brake Rotor. J. Korean Soc. Automot. Eng. 2018, 26, 67–76.
3. Lee, H.-H. Finite Element Simulations with ANSYS Workbench 2021: Theory, Applications, Case Studies; SDC Publications: Gunpo-si, Korea, 2021.
4. Jaenudin, J. Jamari, M. Tauviquirrahman, "Thermal Analysis of Disc Brakes using Finite Element Method", American Institute of Physics, 1788, 030028 (2017); doi: 10.1063/1.4968281.
5. Reddy, V.C.; Reddy, M.G.; Gowd, G.H. Modeling and analysis of FSAE car disc brake using FEM. Int. J. Emerg. Technol. Adv. Eng. 2013, 3, 383–389.
6. Santosh Kumar Kallepalli, Harish Musti, DR.K.Sudhakar Reddy, "Enhancement in Design and Thermal Analysis Of Disc Brake Rotor", International Journal Of Engineering Sciences & Research Technology, February, 2017.
7. Mr. Sumeet Satope, Akshaykumar Bote, Swapneel D. Rawool, "Thermal Analysis of Disc Brake", International Journal for Innovative Research in Science & Technology, Volume 3, Issue 12, May 2017.
8. Swapnil Umale, Dheeraj Varma, "Disc Brake Rotor Selection through Finite Element Analysis", International journal of recent trends in engineering & research, Volume 02, Issue 4; April - 2016.

9. Nakatsuji T, Okubo K, Fujii T, Sasada M, Noguchi Y. Study on crack initiation at small holes of one-piece brake discs. SAE, Inc.; 2002. p. 01–0926.
10. Laraqi N. Velocity and relative contact size effect on the thermal constriction resistance in sliding solids. ASME J Heat Transfer 1997;119:173–7.
11. Gwak, W.-G.; Hong, C.-K.; Kim, Y.-J. Influence of the Braking Time on the Soundness of Ventilated Disc Brake Systems. J. Auto-Veh. Saf. Assoc. 2016, 8, 7–12.
12. Belghazi H, El Ganaoui M, Labbe JC. Analytical solution of unsteady heat conduction in a two-layered material in imperfect contact subjected to a moving heat source. Int J Therm Sci 2010;49(2):311–8.
13. Ali Belhocine, Mostefa Bouchetara. Investigation of temperature and thermal stress in ventilated disc brake based on 3D thermomechanical coupling model. Department of Mechanical Engineering, USTO Oran University, L.P 1505 El-Mnaouer, USTO, 31000 Oran, Algeria.

Голенко К.Е., Диха О.В., Падгурскас Ю., Бабак О.П. Термічний та напружено-деформований стан пар тертя вентиляованих дискових гальм легких транспортних засобів

Робота представляє собою дослідження теплової поведінки та напружено-деформованого стану вентиляованих дискових гальм легких транспортних засобів (скутерів, електробайків, квадроциклів, тощо) за допомогою розрахункового середовища ANSYS в різних режимах випробувань. Моделювання розподілу температури в роторі (диску) і відповідних гальмівних колодках визначається з урахуванням ряду факторів і вхідних параметрів під час операції гальмування: величини швидкості обертання, зазору між колодками і диском, швидкості прикладення навантаження, теплового розширення та ін. Чисельне моделювання перехідного теплового поля та поля напружень в області контакту колодок та диску здійснюється методом послідовного термоструктурного зв'язку проміжних розрахункових станів моделі гальм у середовищі ANSYS Coupled Field Transient. Для комплексної оцінки поведінки гальм в публікації розглядаються два підходи навантажень: сталі (тривалістю 20 с) з фактором впливу у вигляді температурного розширення в результаті тертя контактних пар; лінійне навантаження з боку колодок на диск з відповідним зростанням тиску аж до моменту блокування обертання системи. Також дослідження включає в себе оцінку впливу вентиляційних каналів ротора на характер плями контакту з гальмівними колодками (відкритий дальній контакт, контакт ковзання, залипання тощо). Крім того, показано, що незважаючи на лінійне зростання тиску колодок на ротор, графіки температур, об'єму (теплового розширення) і напружень мають параболічний характер із непропорційним зростанням показників. Такий результат змушує прийти до висновку, що неможливо передбачити поведінку гальм на основі аналізу короткого проміжку часу експерименту - проведення довгострокових аналітичних досліджень є надзвичайно важливим у випадку гальм.

Ключові слова: тертя, гальмівний диск, гальмівні колодки, теплове навантаження, напружено-деформований стан, тепловий потік, напруження фон Мізеса, контактний тиск, теплове розширення.



Optimization of the technology for applying discrete coatings in restoration of bronze parts by electrospark alloying

E.K. Solovykh, I.V. Shepelenko*, M.I. Chernovol, S.O. Mahopets, A.E. Solovuch, S.E. Katerynych

**Central Ukrainian National Technical University, Kropyvnytsky, Ukraine*

E-mail: kntucpfzk@gmail.com

Received: 18 December 2022; Revised: 25 January 2023; Accept: 18 February 2023

Abstract

In this work, a multicriteria optimization of the technology for applying discrete coatings by electrospark alloying in the restoration of bronze parts is carried out. As criteria for optimizing the process of electrospark alloying, tribotechnical characteristics were chosen – the wear intensity and friction coefficient of the coating. As adjustable parameters, those design, technological and operational factors that have the greatest influence on the value of optimization criteria are used: coating material; lubricant; operating current; amplitude of electrode oscillations; sliding speed; specific load. As a result of experimental studies, experimental dependences of wear intensity and friction coefficient for various coating materials, sliding speeds and lubrication conditions were obtained. The use of multicriteria optimization of the electrospark alloying technology made it possible to obtain various alternative coating options and technological parameters of their application for various operating conditions. Of the studied coatings, the most effective is a two-layer coating with the first layer SP-2 and an outer layer of the base material bronze BrAZhMts 10-3-1.5, which is explained by the formation of wear-resistant areas based on Mn and Ni. Multiparametric optimization of the electrospark alloying technology made it possible to reveal a combination of structural and technological factors that ensure the formation of discrete coatings with high operational properties in the restoration of bronze parts.

Key words: electrospark alloying, discrete coatings, bronze parts, multicriteria optimization, tribotechnical characteristics, design and technological factors.

Introduction

Parts made of bronze are one of the most common elements of plain bearings, which limit the resource of the entire unit. Taking into account the high cost of such material, its scarcity, rapid wear, as well as the fact that such parts are usually replaced with new ones during repairs, makes the problem of restoring bronze parts relevant [1-3].

The data of bronze parts fault detection results during the modern aircraft overhaul indicate that about 82% of the parts are rejected due to increased wear [4]. This is due to high specific loads at low sliding speeds, contamination of the contacting friction surfaces with abrasive, dust, condensate, as well as the non-additivity of the lubricant. Such units, in addition to plain bearings, include swivel-bolt joints, hinges with ball supports, etc.

The search for progressive coating application technologies for the restoration of worn parts operating under extreme friction and wear conditions showed that the coating application methods that are traditionally used in the aircraft repair industry do not allow effective restoration of triboconjugations parts "steel – bronze".

It was shown in [5-7] that one of the most effective and economical ways to eliminate wear of parts, including bronze ones, is the method of electrospark alloying (ESA).

Literature review

A number of works [8, 9, etc.] are devoted to the study of bronze parts restoration technology.

The work [8] presents a classification of existing methods applicable to the restoration of bronze plain bearings. According to this classification, all methods can be divided into two main groups:



- restoration of parts by applying coatings on worn surfaces;
- restoration of parts dimensions by plastic deformation.

At the same time, the author [8] concluded that the presented recovery methods require the final machining operation (boring, grinding, etc.) in order to obtain dimensional accuracy and surface roughness. Therefore, to restore the internal surfaces of bronze bushings, it is advisable to use combined processing methods.

In works [5, 6], the effectiveness of bronze parts restoration by ESA was declared. The predominant area of ESA application is the restoration and hardening of worn parts. This method is based on the use of a concentrated energy flow – a spark discharge. ESA differs from a number of other methods of applying wear-resistant coatings by the low energy intensity of the process, environmental friendliness, and simplicity of the technological operation. The use of ESA technology does not require highly qualified service personnel, as well as the previous preparation of the hardened surface. ESA is characterized by small equipment dimensions, the possibility of local coating application on any conductive materials, and is implemented both in a mechanized version (with process automation) and in a manual vibrator version [10]. A comparison of the ESA method with gas-thermal spraying and laser processing shows the advantages of ESA in power consumption, equipment dimensions, material utilization rate, equipment cost and the need for surface preparation. In contrast to such mass technologies as gas-thermal spraying and PVD, much less research has been devoted to the ESA method. This refers the ESA technology to developing and promising technologies.

The ESA method is increasingly used in industry to improve the wear resistance and hardness of machine parts surface, including those operating at elevated temperatures and aggressive environments, to increase heat and corrosion resistance, as well as to restore worn surfaces of machine parts during repairs. Despite the fact that ESA has a positive effect on the wear resistance of the surface layer, its disadvantages often limit the implementation of this method for a wide range of machine parts. Such disadvantages include a change in surface roughness after ESA, uneven surface hardening, a negative effect of an electric discharge on the fatigue properties of products, and the appearance in some cases of a sublayer with reduced hardness in hardened products [5].

The undoubted advantage of the ESA method is the possibility of applying coatings of a discrete structure, which were studied by the scientific school of Professor B.A. Lyashenko. They found that a feature of most worn parts is the local nature and uneven wear. Taking into account this feature, the authors [5-7] developed a technology for restoring parts by applying discrete coatings of variable thickness in accordance with the diagram of uneven wear.

The efficiency of applying discrete coatings is confirmed by a number of studies [6, 7, etc.]. In particular, it was shown in work [10] that the minimum wear of the coating is observed at continuity $\psi = 55...65\%$ (Fig. 1).

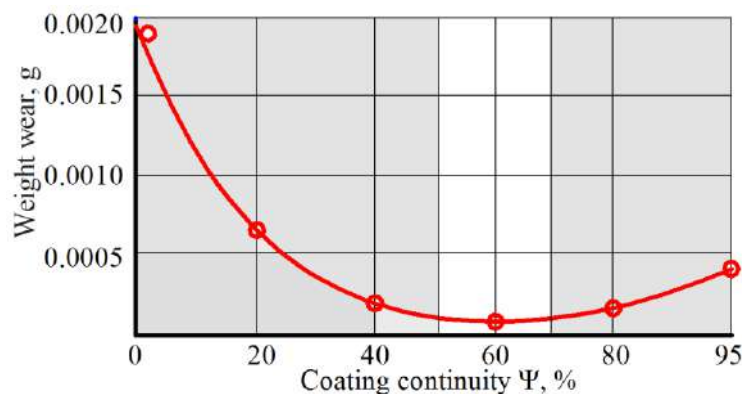


Fig. 1. Dependence of wear on coating continuity [10]

When applying discrete coatings, the ESA method has a number of advantages:

- a single electric discharge makes it possible to ensure the stability of the dimensions and properties of a separate discrete section of the coating;
- by changing the electrical parameters of each individual discharge, it is possible to apply discrete sections of various sizes and, above all, of various thicknesses;
- by changing the pulse frequency or the speed of the electrode and the part relative movement, it is possible to control the number of discrete sections on the working surface of the part, as well as the continuity of the coating;
- there is no need for additional heat treatment, since the discrete section is in a hardened state when the discharge heat is removed to the mass of the part;
- the ability to restore large parts.

In order to develop a technology for the restoration of bronze parts by ESA, it is very important to establish a connection between the tribotechnical characteristics of the studied surface and with design, technological, and operational factors. This will allow choosing coating options and technological parameters of their application for various conditions, providing the formation of coatings with high operational properties.

Purpose

The aim of the work is to find optimal solutions and establish connections between tribotechnical characteristics – wear rate and friction coefficient with design, technological and operational factors when applying discrete coatings by the ESA method.

Research Methodology

Bronze BrAZhMts 10-3-1.5, which works in triboconjugations of aviation equipment in contact with steel 30HGSN2A, was chosen as the base material for coating application. The chemical composition of the studied materials is presented in Tables 1-2.

Table 1

Chemical composition of bronze BrAZhMts 10-3-1.5, % [11]

Fe	Si	Mn	P	Al	Cu	Pb	Zn	Sn	Impurities
2 - 4	≥ 0.1	1 - 2	≥ 0.01	9 - 11	82.3 - 88	≥ 0.03	≥ 0.5	≥ 0.1	0.7

Table 2

Chemical composition of steel 30HGSN2A, % [11]

C	Si	Mn	Ni	S	P	Cr	Cu	Fe
0.27 - 0.34	0.9 - 1.2	1.0 - 1.3	1.4 - 1.8	≥ 0.025	≥ 0.025	0.9 - 1.2	≥ 0.3	~94

To apply coatings by the ESA method, a serial installation "Elitron-22" was used. The electrode materials were SP-1 and SP-2 alloys, the compositions of which are given in Table 3.

Table 3

Chemical composition of electrodes, % [6]

Name of electrode material	Composition of elements, %					
	Al	Si	Mn	Fe	Ni	Cu
SP-1	3 - 5	1	38 - 40	1 - 2	34 - 35	16 - 17
SP-2	-	8 - 9	36 - 37	1 - 2	33 - 34	1

When choosing an antifriction wear-resistant material for ESA electrodes, Mn and Ni were taken as the basis. Manganese increases strength, plasticity and corrosion resistance. Nickel improves mechanical properties, increases heat resistance and corrosion resistance. A further increase in the tribotechnical characteristics of the electrode material was carried out by introducing alloying additives Al, Si, Fe and Cu [6].

Studies on friction and wear of experimental coatings were carried out on a universal friction machine SMT-1 according to the "disk – block" scheme. In this case, the lubrication conditions were provided by a special hermetic chamber. CIATIM-201, AMG-10, and Svintsol-01 were used as a lubricating environment [6].

For a rational choice of the discrete coating structure parameters, preliminary experiments were carried out to establish the dependence of wear resistance on the continuity characteristic ψ . The coefficient ψ is determined by the ratio of discrete coatings area to the total area.

The size of the coating area was determined based on the results of metallographic analysis of the surface using digital image processing methods on a PC (Fig. 2). For this purpose, a program was written in C++ using the Qt framework and OpenCV image processing libraries [12].

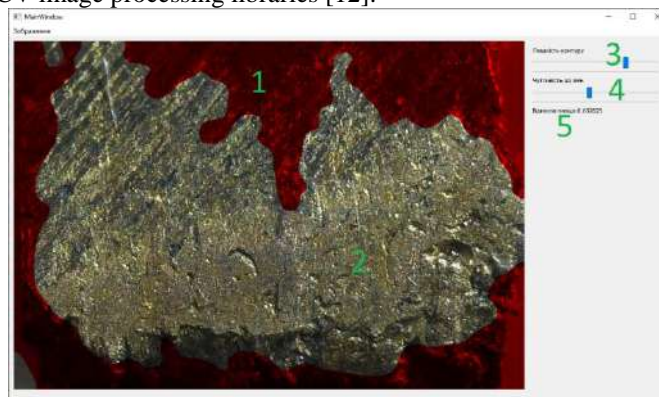


Fig. 2. The interface of the program for determining the coating area: 1 – a selected area without an applied coating; 2 – not selected area with an applied coating; 3, 4 – controls that allow you to adapt the selection algorithm to the capabilities of the chamber; 5 – the ratio of not selected area to the total area of the photograph [12]

Since the minimum wear of the coating is observed at continuity $\psi = 55...65\%$ (Fig. 1), in all further studies, continuity $\psi = 0.6$ was used.

Three types of coatings were tested:

1) coating by electrode SP-1;

2) coating by electrode SP-2;

3) two-layer coating SP-2 + AP with the first layer SP-2 and the outer layer of the base material – bronze BrAZhMts 10-3-1.5.

The composition of the coating SP-2 + AP is justified by the fact that for high anti-scratch resistance it is advisable to apply a thin layer of a softer material on a hard surface, which plays the role of a solid lubricant. In this case, defects in the form of scratches will not appear on the surface, which, in practice, always puts out of action the triboconjugation. The SPD method was used as the finishing treatment of the coatings. Hardening of the coating surface layers by the SPD method ensures the achievement of the required surface roughness and dimensions of parts without machining, as well as an increasing its hardness and wear resistance [13]. As criteria for optimizing the ESA process, the main tribotechnical characteristics are chosen – the wear rate and the friction coefficient of the coating.

Results

The use of expert evaluation methods and a series of screening experiments [14] made it possible to obtain an average a priori ranking of the input factors influencing the ESA process (Fig. 3).

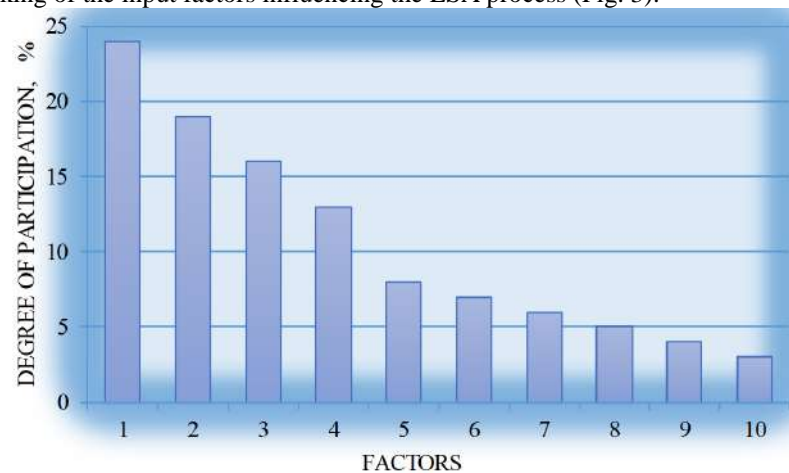


Fig. 3. Ranked number of factors: 1 – coating material; 2 – operating current of the ESA; 3 – amplitude of the ESA electrode oscillations; 4 – sliding speed; 5 – specific load; 6 – lubricant; 7 – coating thickness; 8 – electrode diameter; 9 – discreteness parameter ψ ; 10 – application time

Modeling the coating application process based on the analysis of the conducted ranking made it possible to determine the group of parameters that have the greatest influence on the value of the optimization criteria, and therefore, the following factors were included in the planning matrix as adjustable factors: coating material; lubricant; operating current of the ESA; amplitude of electrode oscillations; sliding speed; specific load. Controlled factors and levels of their variation are presented in Table 4.

Table 4

Controlled factors and levels of their variation

Factors	Levels of variation		
	Coating material	SP-1	SP-2
Lubricant	AMG-10	Svintsol-01	CIATIM-201
Operating current, A	1 - 4		
Electrode oscillation amplitude, mm	0,2 - 0,5		
Sliding speed, m/s	0,1 - 0,5		
Specific load, MPa	0 - 20		

Taking into account the data (Table 4), an experiment plan was generated. As a result of experimental studies, the tribotechnical characteristics of the studied coatings of a discrete structure were obtained when changing structural, technological and operational factors according to the plan of the experiment. Based on the results obtained, the dependences of the wear intensity and friction coefficient were constructed in accordance with the working matrix of experiment planning. Dependences of wear intensity and friction coefficient for various coating materials, sliding speeds and lubrication conditions are shown in Fig. 4-6.

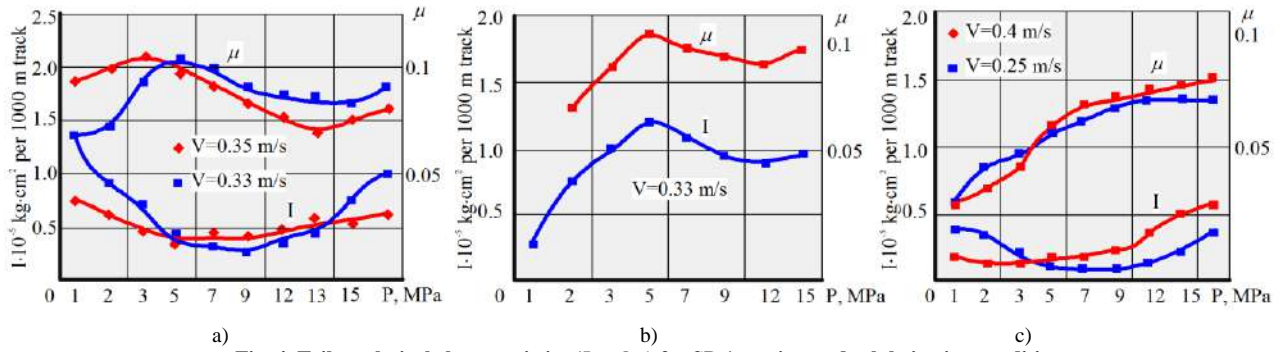


Fig. 4. Tribotechnical characteristics (I and μ) for SP-1 coating under lubrication conditions:
 a – AMG-10 lubricant; b – CIATIM-201 lubricant; c – Svintsol-01 lubricant

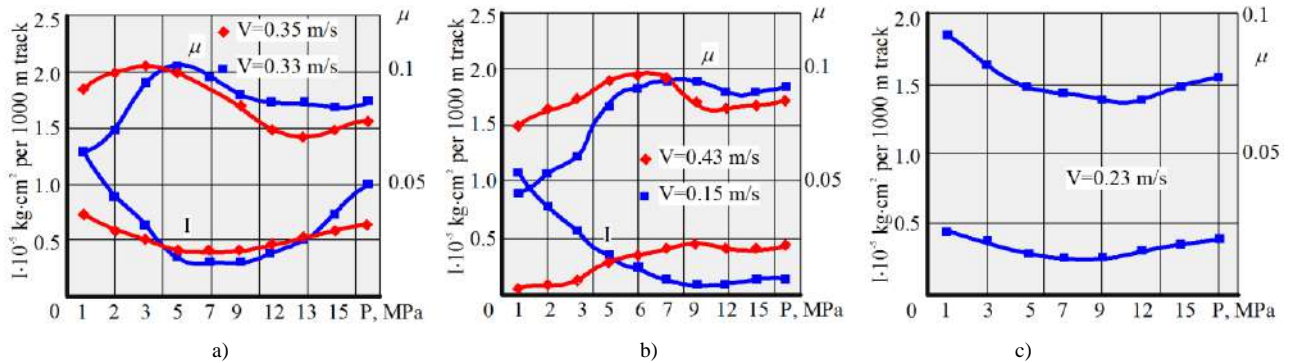


Fig. 5. Tribotechnical characteristics (I and μ) for SP-2 coating under lubrication conditions:
 a – AMG-10 lubricant; b – CIATIM-201 lubricant; c – Svintsol-01 lubricant

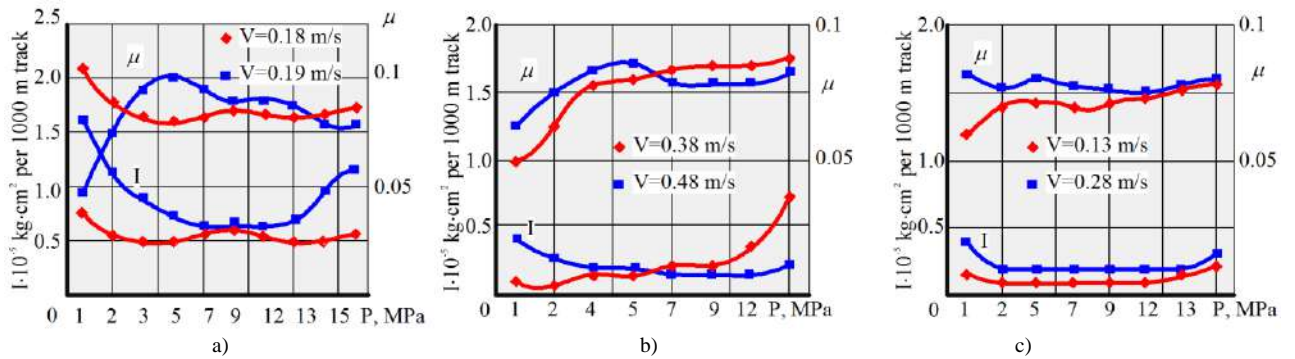


Fig. 6. Tribotechnical characteristics (I and μ) for SP-2 + AP coating under lubrication conditions:
 a – AMG-10 lubricant; b – CIATIM-201 lubricant; c – Svintsol-01 lubricant

According to X-ray structural analysis, the surface structure during friction represents a stable secondary structure, the quantitative characteristics of which sharply change at $P_{cr} \geq 3.5 \text{ MPa}$. The results of the conducted experiment made it possible to reveal the tribotechnical characteristics of the coatings under the conditions of using various lubricants, at various sliding speeds and specific loads.

Of the studied coatings, the best results were shown by the SP-2 + AP coating. There are no scratches, cracks, or wear marks on the friction surface of this coating, which, in our opinion, is the result of wear-resistant areas formation based on Mn and Ni and is confirmed by micro-X-ray structural analysis data (Fig. 7).

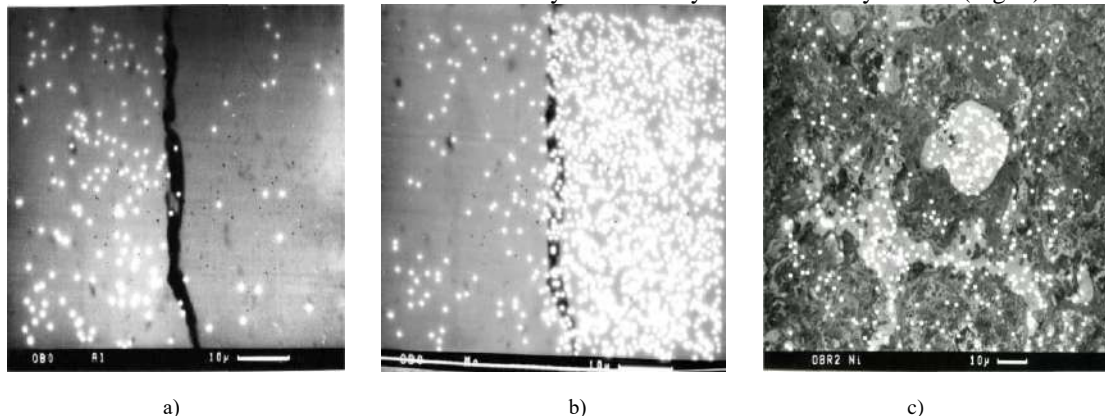


Fig. 7. Depth of penetration and distribution of alloying elements from the SP-2 coating into the base: a – aluminum distribution; b – manganese distribution; c – nickel distribution

The influence of the lubricant type on the friction surface is shown in Fig. 8.

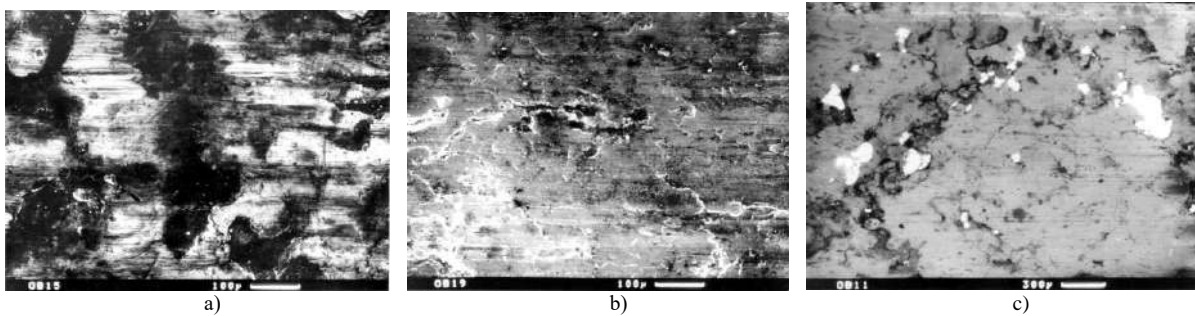


Fig. 8. Microstructure of the friction surface of electrospark coatings in a lubricating environment: a – AMG-10; b – CIATIM-201; c – Svintsol-01

It should be noted that the CIATIM-201 anti-friction consistent lubricant is currently used to reduce friction and wear in the control units of aircraft and their engines, landing gear attachment points and mechanisms for closing it, wheel bearings and various electrical units, weapons mechanisms, special equipment and devices. When operating aviation equipment for hydraulic systems, in which sealing parts and hoses are made of oil-resistant rubber, AMG-10 oil is currently used as a working fluid. Svintsol-01 lubricant is characterized by a high antiwear effect and is a product of the combination of CIATIM-201 consistent lubricant and 10% lead powder, and is used in the operation of aviation equipment in units where the high specific pressure takes place, as it has a high stability of the boundary lubricating skin due to the presence of lead powder, which plays the role of a solid lubricant and protects the contact surfaces from scratching [15].

A more complete and accurate assessment of the connection between tribotechnical characteristics and design, technological and operational factors is provided by regression analysis of experimental results.

A graphical study of response surfaces shows a significant influence of factors on dependent variables (Fig. 9).

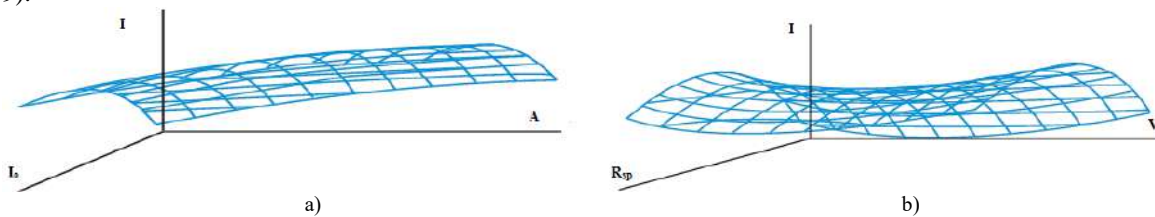


Fig. 9. Wear intensity response function I from:

a – operating current I_0 and amplitude of the electrode A oscillations; b – sliding speed V and specific load R_{sp}

The thickness of the coating plays a significant role in optimizing the ESA technology. Therefore, a separate experiment was carried out to establish the dependence of the wear intensity I on the coating thickness h_c while fixing the remaining ranked factors. The results are shown in Fig. 10.

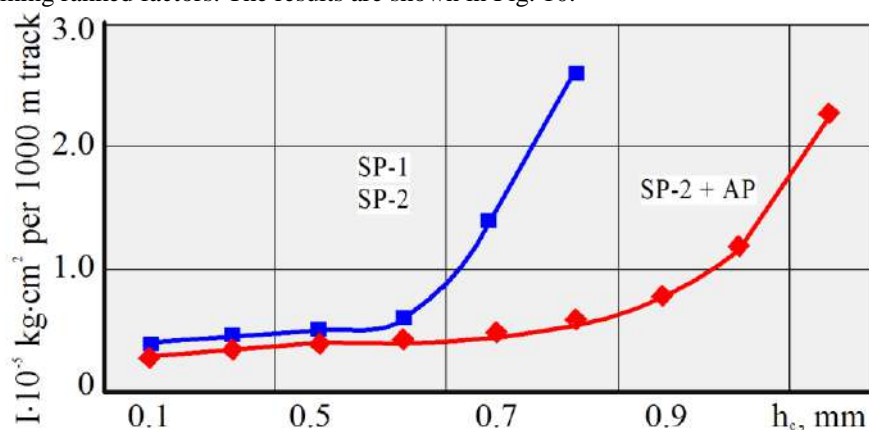


Fig. 10. Dependence of wear intensity I on coating thickness h_c ($V = 0.2$ m/s, $R_{sp} = 15$ MPa, under conditions of Svintsol-01 lubrication)

For normal operation of coatings SP-1 and SP-2, their thickness should not exceed 0.6 mm. Coating SP-2 + AP has a high anti-scratch resistance due to the plastic outer layer. This makes it possible to apply SP-2 + AP coating up to 0.8 mm thick without decreasing of operational characteristics.

Thus, with the help of mathematical models, through multicriteria optimization, it is possible to obtain several alternative coating options and technological parameters of their application for various operating conditions.

Conclusions

Multicriteria optimization of applying discrete coatings technology in the restoration of bronze parts by electrospark alloying led to the following conclusions:

1. Alternative variants of coatings and technological parameters of their application for various operating conditions have been obtained.
2. Of the studied coatings, the most effective is the two-layer coating SP-2 + AP with the first layer SP-2 and the outer layer of the base material bronze BrAZhMts 10-3-1.5. This is explained by the formation of wear-resistant sections based on Mn and Ni.
3. Multiparametric optimization of the ESA technology made it possible to reveal a combination of structural and technological factors that ensure the formation of coatings with high operational properties.

References

1. Kelemesh, A., Gorbenko, O., Dudnikov, A., Dudnikov, I. (2017). Research of wear resistance of bronze bushings during plastic vibration deformation. Eastern-European Journal of Enterprise Technologies. Vol. 2, No. 11 (86). pp. 16-21. [doi:10.15587/1729-4061.2017.97534](https://doi.org/10.15587/1729-4061.2017.97534).
2. Shepelenko I. Restoration of bronze bushes by the method of surface plastic deformation/ I. Shepelenko, Warouma Arifa, V. Sherkun// International Journal of Engineering & Technology, 5 (2016), pp.29–32. <https://doi.org/10.14419/ijet.v5i1.5651>
3. Kropivnyj V.N., Shepelenko I.V., Cigankova L.I. (2005). Perspektivi vikoristannya difuzijnoyi metalizaciyi dlya vidnovlennya bronzovih vtulok [Zbirnik naukovih prac «Tehnika v silskogospodarskomu virobniectvi, galuzeve mashinobuduvannya, avtomatizaciya» Vip.16] S. 196-198.
4. Lyashenko B.A., Ermolaev V.V., Mirnenko V.I. (1997). Elektroiskrovoe legirovanie, kak perspektivnyj metod vosstanovleniya detalej aviacionnoj tehniki [Materialy seminaru «Tehnologiya i instrument iz STM v avtomobilnoj i aviacionnoj promyshlennosti»] S.30-31.
5. Lyashenko B.A., Novikov N.V., Klimenko S.A. (2017). Diskretnoe modifitsirovanie poverhnostnogo sloya detaley mashin i instrumentov. Kiev, ISM im. V.N.Bakulya, 264 s.
6. Lyashenko B.A., Solovyih E.K., Mirnenko V.I. i dr. (2010). Optimizatsiya tehnologii naneseniya pokrytity po kriteriyam prochnosti i iznosostoykosti. Kiev, NAN Ukrainyi, IPP im. G.S. Pisarenko, 193 s.
7. Solovyih E.K. (2012). Tendentsii razvitiya tehnologiy poverhnostnogo uprochneniya v mashinostroenii. Kirovograd, KOD, 92 s.
8. Shepelenko I.V. (2003). Udoskonalennya procesu obrobki shatunnih vtulok poverhnevimi plastichnim deformuvannam pri yih vidnovlenni [Avtoreferat disertaciyi kandidata tehnicnih nauk] 17 s.
9. Kropivnyj V.M., Shepelenko I.V., Kulyeshkov Yu.V. (2005). Doslidzhennya mehanichnih vlastivostej bronzi pislya vibrorozkochuvannya i deformuyuchogo protyaguvannya [Zbirnik naukovih prac «Tehnika v silskogospodarskomu virobniectvi, galuzeve mashinobuduvannya, avtomatizaciya» Vip. 16] –S. 96-99.
10. Solovyih E.K. (2013). Naukovo-metodologichni osnovi pidvishennya nesuchoyi zdatnosti funkcionalnih pokrytity konstruktivnimi i tehnologichnimi metodami [Avtoreferat dysertatsii doktora tehnicnykh nauk] 36 s.
11. Sushko O.V., Posvyatenko E.K., Kyurchev S.V. i dr. (2019). Prikladne materialoznavstvo. Melitopol, TOV «Forward press», 352 s.
12. Shepelenko I.V., Dryeyev O.M., Budar Mohamed R.F. (2020). Vznachennya yakosti metalevih pokrytity [Materiali Mizhnarodnoyi naukovo-praktichnoyi konferenciyi «Molod i tehnicnij progres v APK». Innovacijni rozrobki v agrarnij sferi. Tom 2. Harkiv] S.298-299.
13. Solovyih E.K. (2010). Vybory alternativnyh tehnologij naneseniya iznosostojkikh pokrytity diskretnoj struktury [Zbirnik naukovih prac «Tehnika v silskogospodarskomu virobniectvi, galuzeve mashinobuduvannya, avtomatizaciya» Vip.23] S.236-239.
14. Solovyih E.K., Kapishon L.S. (2012). Alternativnye tehnologii diskretnykh pokrytity [Materialy nauchno-tehnicheskogo seminaru «Sovremennye problemy proizvodstva i remonta v promyshlennosti i na transporte». Svalyavy] S.239-240.
15. Lyashenko B.A., Mirnenko V.I., Solovyih E.K. (2007). O zamene bronzy v oporah skolzheniya na alyuminievye splavy s diskretnymi pokrytityami [Naukovo-tehnicnij zbirnik «Problemi tertya ta znoshuvannya». T.48] S. 149-159.

Солових Е.К., Шепеленко І.В., Черновол М.І., Магопець С.О., Солових А.Е., Катеринич С.Е.
Оптимізація технології нанесення дискретних покриттів при відновленні бронзових деталей електроіскровим легуванням

В роботі виконано багатокритеріальна оптимізація технології нанесення дискретних покриттів електроіскровим легуванням при відновленні бронзових деталей. В якості критеріїв оптимізації процесу обрано триботехнічні характеристики: інтенсивність зношування та коефіцієнт тертя покриття. Як регульовані параметри використано саме ті конструкційні, технологічні та експлуатаційні фактори, які найбільшою мірою впливають на вихідну величину: матеріал покриття; мастило; робочий струм; амплітуда коливань електроду; швидкість ковзання; питоме навантаження. В результаті проведення експериментальних досліджень отримано експериментальні залежності інтенсивності зношування та коефіцієнта тертя від питомого навантаження для різних матеріалів покриттів, швидкостей ковзання та умов змащення. Застосування багатокритеріальної оптимізації технології електроіскрового легування надало змогу отримати різні альтернативні варіанти покриттів та технологічних параметрів їх нанесення для різних умов експлуатації. Із досліджених покриттів найбільш ефективне – двошарове покриття з першим шаром СП-2 та зовнішнім шаром із матеріалу основи – бронзи БраЖМц 10-3-1,5, що пояснюється утворенням зносостійких ділянок на основі Mn та Ni. Багатопараметрична оптимізація технології електроіскрового легування дозволила виявити поєднання конструкційних та технологічних факторів, які забезпечують формування дискретних покриттів з високими експлуатаційними властивостями при відновленні бронзових деталей.

Ключові слова: електроіскрове легування, дискретні покриття, бронзові деталі, багатокритеріальна оптимізація, триботехнічні характеристики, конструкційні та технологічні фактори



Establishing the peculiarities of tire wear of garbage trucks during the transportation of municipal solid waste

O.V. Berezyuk¹, V.I. Savulyak¹, V.O. Kharzhevskiy²

¹*Vinnytsia National Technical University, Ukraine*

²*Khmelnytskyi National University, Ukraine*

E-mail: berezyukoleg@i.ua

Received: 25 December 2022; Revised: 30 January 2023; Accept: 25 February 2023

Abstract

The article is dedicated to the establishment of peculiarities of tire wear of garbage trucks during the transportation of solid waste. Using the planning of the first-order experiment with the first-order interaction effects using the Box-Wilson method, adequate dependencies of wear of garbage truck tires on the front and rear axles due to the transported mass of municipal solid waste and the mileage of the garbage truck were determined. It was established that, according to the Student's criterion, among the investigated factors of influence, the wear of garbage truck tires on both the front and rear axles is most affected by the transported mass of municipal solid waste, and the least – by the mileage of the garbage truck. The response surfaces of the objective functions – tire wear of the garbage truck on the front and rear axles and their two-dimensional sections in the planes of the impact parameters are shown, which allow to visually illustrate the indicated dependences of the objective function data on individual impact parameters. The dependencies of the number of routes of the garbage truck to the maximum allowable tire wear on the front and rear axles were obtained. The response surfaces of the target functions – the number of routes of the garbage truck to the maximum permissible wear of the tires on the front and rear axles and its two-dimensional sections in the planes of the influence parameters, which allow to visually illustrate the specified dependencies, are obtained. The expediency of conducting further research on the influence of speed, unevenness of the road surface, weather conditions and other factors on the wear of garbage truck tires has been revealed.

Key words: wear, tire, garbage truck, municipal solid waste, dependence, experiment planning.

Introduction

The increase of the wear resistance, reliability and durability of machine parts occupies a prominent place among the important tasks of utility engineering [1, 2]. The collection and transportation of municipal solid waste (MSW) to landfills, processing and disposal sites in Ukraine is mainly carried out by body garbage trucks in the amount of more than 3,800 units, which are able to compact solid waste, reducing transportation costs and the required area of landfills. At the same time, during the technological operation of solid waste transportation by garbage trucks, their tires are subjected to intensive wear. This is due to the significant carrying capacity and length of garbage trucks' routes, since the placement of solid waste landfills takes place outside the sanitary zone, which in Ukraine is 30 km from populated areas. The wear and tear of the fleet of garbage trucks of municipal enterprises of Khmelnytskyi region during 2015-2020, despite the measures taken, almost did not change: it decreased only from 63% to 59% [3, 4]. According to the text of Resolution of the Cabinet of Ministers of Ukraine No. 265 [5], it is particularly important to ensure the use of modern highly efficient garbage trucks in the country's communal economy, as the main link in the structure of machines for collection, transportation and primary processing of solid waste. This allows not only to solve a number of environmental problems, but also to increase the reliability of the work of utility companies as a whole. The planning of renewal, maintenance and repair of garbage trucks is facilitated by the determination of the regression dependencies of wear of garbage truck tires on the front and rear axles from the transported mass of municipal solid waste and the mileage of the garbage truck.



Analysis of recent research and publications

In the materials of the work [6], an improved mathematical model of the operation of the solid waste dehydration drive in the garbage truck was proposed, which takes into account the wear of the auger, made it possible to numerically study the dynamics of this drive during start-up and determine that with an increase in the wear of the auger, the pressure of the working fluid at the inlet of the hydraulic motor of the drive increases, and the angular the speed and frequency of rotation of the auger are significantly reduced with a constant supply of working fluid.

The power-law regularities of changes in the nominal values of the pressures at the hydraulic motor inlet, angular velocity and rotation frequency of the auger depending on the amount of its wear were determined, the last of which describes the deviation from the optimal rotation frequency of the auger during its wear and was used to determine the energy intensity of solid waste dehydration taking into account the wear of the auger. It was found that the wear of the auger by 1000 μm leads to an increase in the energy intensity of solid waste dehydration by 11.6%, and, therefore, to an increase in the cost of their dehydration in the garbage truck and acceleration of the wear process.

In the article [7] it was established that the resource of large-sized tires depends on many factors of the operating conditions, which lead to their premature scrap due to an excess of the thermal state and, as a result, peeling of the tread. Management of the thermal state of the large-sized tire, taking into account the rational loading of the dump truck during operation, allows you to achieve its maximum productivity. To determine the productivity in various conditions of operation of quarry dump trucks, the computer program "Optimal degree of loading" has been developed.

The paper [8] provides an analysis and assessment of factors affecting the wear of large-size tires of quarry dump trucks, and recommendations for increasing their service life.

In the materials of the article [9], the problem of increasing the accuracy of determining the resource of pneumatic tires of trucks is considered. Tire resource calculations were carried out using 5 methods, the results of which were compared with the results of an experimental study, which showed the need to refine the calculation methods to solve the specified problem. It is noted that the more accurately the tire resource is determined, the more qualitative the management of the technological processes of tire maintenance, their replacement, and scrapping will be, which will significantly affect traffic safety and the economic indicators of the operation of the motor vehicle enterprise.

In work [10], a mathematical model of wear of a highly elastic wheel during its rolling on a rigid base was developed. In the proposed model, it is assumed that wear occurs in the sliding region, and the intensity of wear is a power-law function of pressure. A distinctive feature of the model is accounting for changes in contact pressures on the contact area, the size of the contact area, and the extent of the sliding sub-region during wear. An analytical dependence was obtained for calculating the length of the slip zone. The kinetics of the change in the radius of a highly elastic wheel during wear was studied. A theoretical-experimental method of calculating the wear life of a massive highly elastic wheel when rolling on a rigid base is proposed. An analysis of the influence of the relative slip on the durability of a massive highly elastic tire was carried out. The nature of the influence of the parameters of the wear law on the evolution of contact characteristics and the service life of the wheel was studied.

In the article [11], on the basis of measurements of the height of the tire tread pattern in operating conditions, one-factor linear and quadratic models of the dependence of car tire wear on mileage were determined. Factors affecting critical wear of tires were analyzed: accumulation of fatigue stresses and destruction in the tread rubber array; increasing unevenness of wear along the length of the treadmill, which results in variability of the rolling radius; increasing the stiffness of the tire in the tangential and normal directions; reducing the diameter of the tire. Recommendations for reducing the wear of truck tires for the enterprise in real conditions have been developed. Recommendations for improving control over the technical condition of the company's vehicle fleet based on information on the nature and intensity of tire wear are proposed.

The authors of the paper [12] describe the specifics of the work of vehicles for collecting and transporting municipal solid waste to the places of their further handling, show the method of measuring the height of the tire tread pattern, and also give the average arithmetic values of the wear of garbage truck tires installed on the front and rear axles depending on from the transported mass of solid household waste and the mileage of the garbage truck.

In the article [13], a regression analysis was used to determine a regularity that describes the dynamics of wear and tear of garbage trucks in general in the Khmelnytskyi region and allows it to be predicted and planned for the infrastructure of municipal enterprises (warehouse and renewal of garbage trucks, production base for maintenance and repair), which is necessary for solving problems of municipal solid waste management.

However, as a result of the analysis of known publications, the authors did not find specific mathematical dependences describing the tire wear of the garbage truck on the front and rear axles on the transported mass of solid household waste and the mileage of the garbage truck.

Aims of the article

The aims is to study the influence of the transported mass of municipal solid waste and mileage on the wear of garbage truck tires.

Methods

The determination of the dependencies of garbage truck tire wear on the front and rear axles from the transported mass of municipal solid waste and garbage truck mileage was carried out by planning a first-order experiment with first-order interaction effects using the Box-Wilson method [14]. The coefficients of the regression equations were determined using the developed computer program "PlanExp", which is protected by a certificate of copyright registration and is described in the work [15].

Results

Preliminary processing of the results of experimental studies [12] showed that the wear of garbage truck tires on different axles is a function of the following 2 main parameters:

$$u_{FA}, u_{RA} = f(m, L), \quad (1)$$

where u_{FA}, u_{RA} – tire wear of the garbage truck on the front and rear axles, respectively, μm ; m – transported mass of solid household waste, tons; L – mileage of the garbage truck, km.

The study of the influence of the above factors on the wear of garbage truck tires when processing the results of one-factor experiments by the method of regression analysis is associated with significant difficulties. Therefore, in our opinion, it is advisable to conduct a multivariate experiment to obtain a regression equation for the response functions – wear of garbage truck tires on different axles using the planning of a multivariate experiment using the Box-Wilson method [14].

The average arithmetic values of wear of garbage truck tires installed on one axle depending on the transported mass of solid household waste and the mileage of the garbage truck are given in the table 1 [12].

Table 1

Average arithmetic values of wear of garbage truck tires installed on one axle [12]

№	Transported mass m , tons	Mileage L , km	Wear, μm	
			Front axle	Rear axle
1	41,16	1304,63	98,715	136,8
2	46,9	1021,63	114,55	157,5
3	76,72	1597,33	191,5	245,8

Based on the data in table 1, using the planning of the first-order experiment with first-order interaction effects, applying the developed software, which is protected by a certificate, after rejecting insignificant factors and interaction effects according to the Student's criterion, the dependencies of wear of garbage truck tires on different axes depending on the transported mass of solid household waste and garbage truck mileage:

$$u_{FA} = 2,507m - 0,006786L + 8,186 \cdot 10^{-5} mL; \quad (2)$$

$$u_{RA} = 3,539m + 0,003974L - 2,615 \cdot 10^{-4} mL. \quad (3)$$

In the fig. 1 are shown the response surfaces of the target functions – tire wear of the garbage truck on the front u_{FA} and rear u_{RA} axles and their two-dimensional cross-sections in the planes of the influence parameters, constructed with the help of dependencies (2, 3), which allow you to visually illustrate the specified dependencies.

It was established that according to Fisher's test, the hypothesis about the adequacy of regression models (2, 3) can be considered correct with 95% reliability. The coefficient of multiple correlation was $R = 0.99999$, which indicates the high accuracy of the obtained results.

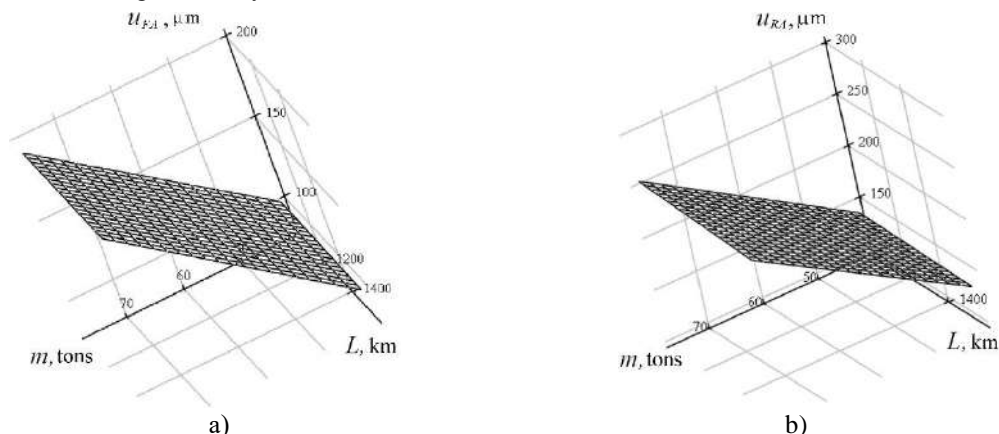


Fig. 1. Response surfaces of the target functions - the wear of the tires of the garbage truck on the front u_{FA} and rear u_{RA} axes and its two-dimensional sections in the planes of influence parameters: (a) – $u_{FA} = f(m, L)$, (b) – $u_{RA} = f(m, L)$

According to the Student's criterion, it was established that among the investigated factors of influence, the weight of municipal solid waste transported has the greatest influence on the wear of garbage truck tires on both the front and rear axles, and the least – the mileage of the garbage truck.

To determine the number of routes of the garbage truck before the maximum allowable tire wear, we will use the following formulas:

$$m = m_1 n; \quad (4)$$

$$L = L_1 n; \quad (5)$$

$$u = h - h_{\min}, \quad (6)$$

where m_1 – the carrying capacity of the garbage truck, tons; L_1 – length of route of the garbage truck, km; n – the number of garbage truck routes; h – tread depth of a new tire, μm ; h_{\min} – minimum allowable tire tread depth, μm (for trucks $h_{\min} = 1 \text{ mm}$).

After substituting formulas (4-5) into dependencies (2, 3), we will obtain dependencies of the number of routes of the garbage truck to the maximum allowable tire wear on the front and rear axles:

$$n_{FA} = \frac{\sqrt{(2,507m_1 - 0,006786L_1)^2 + 3,274 \cdot 10^{-4} m_1 L_1 (h - h_{\min})} - 2,507m_1 + 0,006786L_1}{1,637 \cdot 10^{-4} m_1 L_1}; \quad (7)$$

$$n_{RA} = \frac{\sqrt{(3,539m_1 + 0,003974L_1)^2 - 1,046 \cdot 10^{-3} m_1 L_1 (h - h_{\min})} + 3,539m_1 + 0,003974L_1}{5,23 \cdot 10^{-4} m_1 L_1}. \quad (8)$$

In the fig. 2 are shown the response surfaces of the objective functions – the number of routes of the garbage truck to the maximum allowable wear of tires on the front n_{FA} and rear n_{RA} axles and its two-dimensional sections in the planes of the influence parameters, which are constructed with the help of dependencies (7, 8) and allow to visually illustrate the specified dependencies.

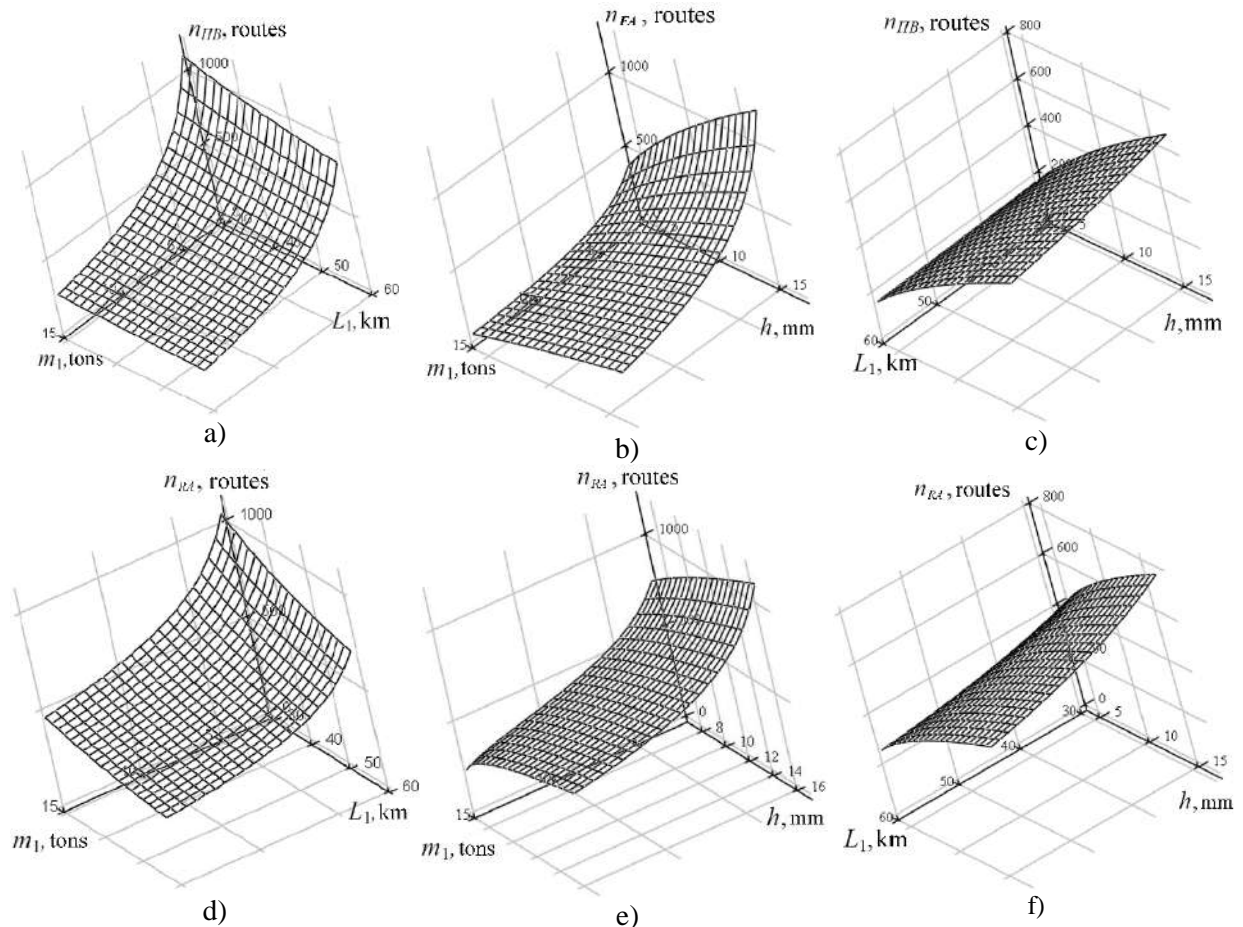


Fig. 2. The response surfaces of the objective functions – the number of trips of the garbage truck to the maximum allowable wear of the tires on the front n_{FA} and rear n_{RA} axes and their two-dimensional sections in the planes of the impact parameters: (a) – $n_{FA} = f(m_1, L_1)$, (b) – $n_{FA} = f(m_1, h)$, (c) – $n_{FA} = f(L_1, h)$, (d) – $n_{RA} = f(m_1, L_1)$, (e) – $n_{RA} = f(m_1, h)$, (f) – $n_{RA} = f(L_1, h)$

The determination the impact of speed, road surface irregularities, weather conditions and other factors on garbage truck tire wear requires further research.

Conclusions

According to Fisher's criterion the adequate dependencies of tire wear of the garbage truck on the front and rear axles due to the transported mass of municipal solid waste and mileage of the garbage truck were determined. It was established that, according to the Student's criterion, among the investigated factors of influence, the wear of garbage truck tires on both the front and rear axles is most affected by the transported mass of municipal solid waste, and the least – by the mileage of the garbage truck. The response surfaces of the objective functions – tire wear of the garbage truck on the front and rear axles and their two-dimensional sections in the planes of the impact parameters are shown, which allow you to visually illustrate the indicated dependences of the objective function data on individual impact parameters. The dependencies of the number of routes of the garbage truck to the maximum allowable tire wear on the front and rear axles were obtained. The response surfaces of the target functions – the number of routes of the garbage truck to the maximum permissible wear of the tires on the front and rear axles and its two-dimensional sections in the planes of the influence parameters, which allow to visually illustrate the specified dependencies, are constructed. The determination of the impact of speed, road surface irregularities, weather conditions and other factors on garbage truck tire wear requires further research.

References

1. Khomenko I.M., Kindrachuk M.V., Kobrynets' A.K. (2010) Hranychnodopustymyy znos mashyn [Maximum permissible wear of machines]. *Problems of friction and wear*, 52, 28-37
2. Dykha O.V.(2018) Rozrahunkovo-eksperymental'ni metody keruvannja procesamy granychnogo zmashhuvannja tehnychnyh trybosystem [Computational and experimental methods of controlling processes of boundary lubrication of technical tribosystems]: monograph. Khmelnytskyi: KhNU.
3. Ministry of Regions. (2016) Stan sfery povodzhennja z pobutovymy vidhodamy v Ukraini za 2015 rik [State of the field of household waste management in Ukraine in 2015]. URL: <https://www.minregion.gov.ua/wp-content/uploads/2016/04/Zbortpv4-oblasti1.pdf>
4. Ministry of Regions. (2021) Stan sfery povodzhennja z pobutovymy vidhodamy v Ukraini za 2020 rik [State of the field of household waste management in Ukraine in 2020]. URL: https://www.minregion.gov.ua/wp-content/uploads/2021/06/rozdil-4-2020_oblasti.pdf
5. Cabinet of Ministers of Ukraine(2004). Postanova № 265 “Pro zatverdzhennja Programy povodzhennja z tverdymy pobutovymy vidhodamy” [Resolution No. 265 "On Approval of the Solid Household Waste Management Program"] . URL: <http://zakon1.rada.gov.ua/laws/show/265-2004-%D0%BF>
6. Bereziuk O.V., Savulyak V.I., Kharzhevskiy V.O. (2021) The influence of auger wear on the parameters of the dehydration process of solid waste in the garbage truck. *Problems of Tribology*, 26(2/100), 79-86.
7. Kulpin A.G., Stenin D.V., Kultayev E.E., Kulpina E.E., Borovtsov V.A. (2016) Influence of service conditions of quarry dump trucks on the thermal state large-size tires. *Proceedings of Symposium: Coal in the 21st Century: Mining, Processing and Safety*, 116-119. Atlantis Press.
8. Boltayevich Y.U., Anvarovich M.A., Sobirovich T.S., Quvondiq Ulug'bek o'g U. (2022) Influence of Ambient Temperature on the Intensity of Tread Wear of Large Tires. *Eurasian Journal of Engineering and Technology*, 13, 100-105.
9. Kravchenko O.P., Sakno O.P., Lukichov O.V., Vynokurov V.D. (2011) Analiz modelei rozrakhunku pokaznykiv dovhovichnosti, znosu i resursu pnevmatychnykh shyn vantazhnykh avtomobiliv [Analysis of models for calculating durability, wear and service life of pneumatic truck tires]. *Zbirnyk naukovykh prats Donets'koho instytutu zaliznychnoho transportu*, 25, 92-95.
10. Morozov A.V., Bukovskiy P.O. (2018) Method of constructing a 3d friction map for a rubber tire tread sliding over a rough surface. *Journal of Friction and Wear*, 39, 129-136.
11. Zakharov S.V., Kravchenko O.P., Lukichov O.V., Sakno O.P. (2011). Modeliuvannia protsesu znosu shyn ta matematychni zalezhnosti yoho vid narobitku v umovakh ekspluatatsii vantazhnykh avtomobiliv [Modeling of the tire wear process and its mathematical dependence on earnings in the conditions of truck operation], *Visnyk Zhytomyrskoho derzhavnogo tekhnichnogo universytetu. Tekhnichni nauky*, 3(58), 27-32.
12. Lobov N.V., Maltsev D.V., Genson E.M. (2019) Improving the process of transport of solid municipal waste by automobile transport. *Proceedings of IOP Conference Series: Materials Science and Engineering*. 1(632), 012033. IOP Publishing.
13. Bereziuk O.V., Savulyak V.I., Kharzhevskiy V.O. (2022) Dynamics of wear and tear of garbage trucks in Khmelnytskyi region. *Problems of Tribology*, 27(3/105), 70-75.
14. Andersson O. (2012) *Experiment: planning, implementing and interpreting*. John Wiley & Sons.
15. Berezyuk O.V. (2018) Modeliuvannia kompresiiinoi kharakterystyky tverdych pobutovykh vidkhodiv u smittievozi na osnovi kompiuternoï prohramy “PlanExp” [Modeling of compression characteristics of solid household waste in a garbage truck based on the computer program “PlanExp”]. *Visnyk Vinnyts'koho politekhnichnogo instytutu*, 6, 23-28.

Березюк О.В., Савуляк В.І., Харжевський В.О. Встановлення закономірностей зносу шин сміттевозів під час транспортування твердих побутових відходів

Стаття присвячена встановленню закономірностей зносу шин сміттевозів під час транспортування твердих побутових відходів. За допомогою використання планування експерименту першого порядку з ефектами взаємодії першого порядку методом Бокса-Уілсона визначено адекватні закономірності зносу шин сміттевоза на передній та задній осях від перевезеної маси твердих побутових відходів та пробігу сміттевоза. Встановлено, що за критерієм Стьюдента серед досліджених факторів впливу найбільше на знос шин сміттевоза як на передній, так і на задній осях впливає перевезена маса твердих побутових відходів, а найменше – пробіг сміттевоза. Показано поверхні відгуків цільових функцій – зносу шин сміттевоза на передній та задній осях та їхні двомірні перерізи в площинах параметрів впливу, які дозволяють наглядно проілюструвати вказані залежності даних цільових функцій від окремих параметрів впливу. Отримано закономірності кількості рейсів сміттевоза до граничнодопустимого зносу шин на передній та задній осях. Побудовано поверхні відгуків цільових функцій – кількості рейсів сміттевоза до граничнодопустимого зносу шин на передній та задній осях та її двомірні перерізи в площинах параметрів впливу, які дозволяють наглядно проілюструвати вказані залежності. Виявлено доцільність проведення подальших досліджень впливу швидкості руху, нерівностей дорожнього покриття, погодних умов та інших факторів на знос шин сміттевоза.

Ключові слова: знос, шина, сміттевоз, тверді побутові відходи, закономірність, планування експерименту.



Increasing the Wear Resistance of Restored Car Parts by Using Electrospark Coatings

D.D. Marchenko*, K.S. Matvyeyeva

**Mykolayiv National Agrarian University, Mykolayiv, Ukraine*

E-mail: marchenkodd@mnau.edu.ua

Received: 15 January 2022; Revised: 16 February 2023; Accept: 05 March 2023

Abstract

The work scientifically substantiates the application of effective technology for the restoration of worn car parts by applying new electrospark coatings based on electroerosion nanomaterials. The developed technology is characterized by technological flexibility, cheapness, simplicity, does not require the use of expensive and scarce materials and equipment, and also meets the requirements of environmental safety. The proposed technology can be used to restore a wide range of parts for cars, tractors and other machines. Experimentally established dependences of the effect of the properties of electroerosive materials on the properties of electrospark coatings of restored car parts. It is shown that the content of nano-sized particles in the electrode material contributes to the improvement of the physical and mechanical properties of electrospark coatings. The dependences of the influence of the properties of electrospark coatings on the resource of restored car parts were experimentally established. It is shown that the resource of the shafts of turbocompressors restored according to the recommended technology is higher than the resource of new shafts by an average of 1.5 times. Experimentally established rational modes of applying wear-resistant coatings to worn shafts of turbocompressors, which provide the necessary complex of physical and mechanical properties of the coating and the given resource of the shafts as a whole (rotation frequency of the part, min - 1 - 50; electrode feed, mm/min - 0.4 ... 0.5). The characteristics of wear resistance of electrospark coatings of turbocompressor shafts, obtained using electroerosion nanomaterials, were studied. It is shown that the average value of the coefficient of friction of the electrospark coating was 0.146 instead of 0.486 without coating, which is 3.3 times lower. According to the results of production tests, it was found that the duration of operation of the turbocharger, with the restored method of electrospark treatment with a nanostructured electrode shaft, increased by 2.1 times compared to a new industrially manufactured shaft. Thus, when abrasive material containing a fraction of 0.1...0.4 mm was introduced, the operating time of the turbocompressor with a restored shaft was 12.8 hours, and the operating time of the turbocompressor with a new shaft without wear of the nominal size was 8.1 hours.

Key words: wear resistance, electrospark coatings, restoration, car parts, nanomaterials

Introduction

Restoration of worn parts of cars ensures saving of metal, fuel, energy and labor resources, as well as rational use of natural resources and protection of the environment. To restore the functionality of worn car parts, 5...8 times less technological operations are required compared to the manufacture of new parts.

Ensuring the necessary nomenclature of spare parts in the warehouses of motor transport enterprises requires large-scale development of the car repair infrastructure and scientifically based methods of organizing and managing the processes of restoring worn car parts. Solving this important scientific and national economic task leads to the objective need to have scientific principles for the organization of effective car repair production, which determined the choice of topic, the relevance of scientific research taking into account its theoretical and practical significance, the formulation of the goal, scientific novelty and tasks of the thesis.

A car is a complex technical system, the elements of which have different characteristics of resistance to loss of operational condition. They are influenced by both internal structural factors, which depend on the purpose and properties of the element, and a set of external factors defined as the operating conditions of the car.



A modern car consists of 15...20 thousand parts, of which 7...9 thousand lose their original properties during operation, and about 3...4 thousand parts have a service life shorter than that of the car as a whole. All this causes the greatest idle time of cars, resource costs of operation [1].

Literature review

A literature review showed that more than 70% of worn parts of automotive equipment could rationally be reused after restoration. This significantly reduces the resource costs of motor vehicle enterprises, and in addition, it is economically justified for repair production. The cost of restoring parts in most cases does not exceed 25-30% of their cost, and with the qualified appointment of the restoration technology, 100% resource is achieved. The different service life of car parts is due to various reasons. The main ones are: performed functional purposes, a diverse range of loads, different types of friction in connected parts and different materials from which they are made, precision and quality of processing in connected parts.

Automotive parts of the "shaft" type make up a large part of the nomenclature of parts that can be restored. In most cases, it is these details that limit the life of machine components and assemblies. The coefficient of their recovery during the overhaul of machines is 0.25 ... 0.95. The length of the restored shafts is 100...4000 mm, but more than 90% of these parts have a length of slightly more than 1000 mm. The diameters of the shafts are equal to 12...210 mm, but the diameter of 98% of the shafts does not exceed 60 mm. The average weight is about 3 kg.

In parts of the "shaft" type, defects most often appear on the landing surfaces under the bearings and threaded surfaces. Surfaces under bearings are restored when worn more than 0.017...0.060 mm; surfaces of fixed joints (places for hubs with key grooves, etc.) due to additional parts - if worn more than 0.04...0.13 mm; surfaces of movable joints - when worn more than 0.4...1.3 mm; for sealing - more than 0.15 ... 0.20 mm. Key grooves are restored when worn with a width of more than 0.065...0.095 mm; slotted surfaces - when worn more than 0.2...0.5 mm [2].

With the entire set of renewable shaft surfaces 46% wear to 0.3 mm; 27% – from 0.3 to 0.6 mm; 19% - from 0.6 to 1.2 mm and 8% - more than 1.2 mm (Fig. 1).

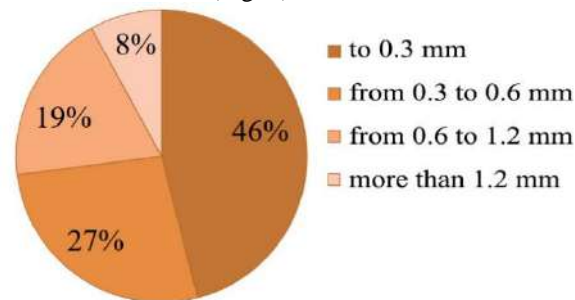


Fig. 1. Analysis of defects of parts of the "shaft" type according to the degree of wear

The main requirement that must be fulfilled during the restoration of shafts is to ensure the size and roughness of the restored surfaces, their hardness, the integrity of the coating, the strength of the adhesion of the applied layers to the base metal, as well as the symmetry, alignment, radial and end runout of the treated surfaces, parallelism of the lateral surfaces of the spline teeth and keyway grooves of the shaft axis.

Shafts of automobile machinery are made mainly of medium-carbon and low-alloy steels. They are subjected to surface hardening with high frequency currents, cementation followed by hardening, normalization.

After analyzing literary sources [1-4], it is customary to divide the defects of "shaft" type car parts into three groups: mechanical damage, chemical-thermal damage, and wear of "shaft" type car parts.

Mechanical damage to parts of the "shaft" type occurs as a result of damage to its surface with cracks, risks and burrs, as well as possible bending of the shaft, its breakage or twisting.

In a number of cases, risks and indentations are formed on the surfaces of parts of the "shaft" type, especially often this happens in shaft - sliding bearing combinations, as a result of contamination of the lubricant or the abrasive effect of particles of foreign origin.

Micron-sized cracks may form on the surface of shaft-type parts due to the influence of excessive local loads, impacts from the ignition of the working mixture or other types, as well as overloading of the shaft. The appearance of this defect occurs in the most loaded places of "shaft" type parts - at the border of the bearing surface. This defect is especially common in crankshafts and camshafts of the internal combustion engine of cars. Shafts made of cast iron are most prone to cracks. In addition to cracks arising as a result of impact forces, fatigue cracks appear in the most stressed places of shaft-type parts as a result of long-term exposure to alternating loads. In some cases, cracks may appear as a result of thermal action. Also, mostly for shafts of small diameter (up to 1 mm), bending and deformation of parts as a result of shock loads is characteristic. Such a defect appears, for example, in the turbocharger rotor shaft. As a result of fatigue of the metal, its breakdowns and breakdowns are observed during strong impacts of collapses, which often occur on cast parts. In a number of cases, due to the

influence of a large torque associated with overcoming temporary significant resistances during operation, "shaft" type parts are prone to twisting [5].

Purpose

The purpose of the article is to improve, on the basis of scientific research, the technology of restoration and surface strengthening of worn car parts through the use of electrospark coatings based on electroerosion nanomaterials that provide a given resource.

Research methodology

The electroerosion dispersion (EED) method was chosen to obtain electrode material for electrospark alloying (ESA). An installation for obtaining nanodispersed powders from conductive materials was used as equipment, which includes a voltage regulator, a pulse generator, and a reactor (Fig. 2) [8].

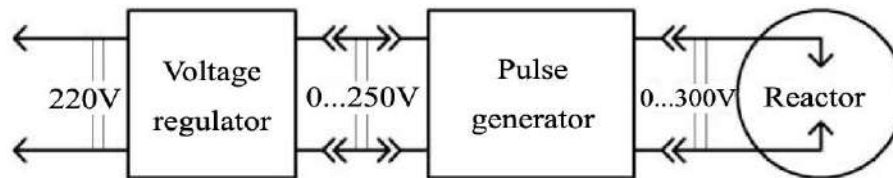


Fig. 2. Structural diagram of the EED installation

The voltage regulator regulates and sets the desired variable voltage in front of the pulse generator. In this installation, a single-phase voltage regulator PHO-260-10 TU 16.-817.298-70 is used, which allows you to adjust the output voltage of 0...260 V, and the current up to 45 A and the maximum power of 12 kW.

A pulse generator (PG) is a device that converts industrial frequency alternating current and generates pulses of a given amplitude, duration and follow-up frequency. GI requirements: high efficiency, maintain the established dispersion mode in the EED process, i.e. stability in work [4-6].

The reactor is a container filled with distilled water as a working fluid and dispersing material loaded into it - scrap high-speed steel of the P6M5 brand. A desiccator 2-240 GOST 25336-82 was used as a reactor vessel. From the pulse generator, electrodes of the same brand as the dispersing object are immersed in the container. Installation parameters: voltage, pulse frequency and capacity of discharge capacitors are selected experimentally based on the dispersion material.

The powder obtained from high-speed steel of the P6M5 grade by the EED method was studied on the equipment discussed below.

To determine the coefficient of friction and the intensity of wear of the surface of the sample with an electrospark coating applied to it and the counterbody, the automated friction machine "Tribometer" of the company "CSM Instruments" (made in Switzerland) was chosen. The used device (Fig. 3) is connected to the computer for control.



Fig. 3. Automated friction machine "Tribometer"

The tests are carried out according to the standard "ball-disc" scheme, which allows the use of the Hertz Model, and comply with the international standards ASTM G99-959 DIN50324, that is, they can serve to evaluate the wear resistance of the sample and the counterbody.

The surface roughness of the samples was examined using the "SURTRONIC 25" profilometer (Fig. 4). It has a multifunction RS-232 port, with which data can be transferred to a computer for further analysis using the optional advanced data processing software with the advanced analysis program "Talyprofile" or to a printer for printing.



Fig. 4. Profilometer "SURTRONIC 25"

The program allows you to calculate parameters, set calculation modes in full accordance with international standards. Special functions allow you to obtain a vertical/horizontal display of the profile, artificially cut the profile, thereby simulating wear of the surface, enlarge individual sections for a more detailed examination, obtain an inverted profile, exclude from the calculation "unwanted" sections of the profile, remove the shape, and also calculate separately waviness and roughness.

The electroerosion dispersion method is based on the melting of metal particles from the surface by a pulse of electric discharge. If a voltage (distance) is applied between the electrodes immersed in a liquid dielectric, when they approach (increase in voltage), the dielectric breaks down - an electric discharge occurs, and a plasma with a high temperature is formed.

Since the time used in this method of processing electric pulses does not exceed 0.01 s, the released heat does not have time to spread deep into the material (metal waste), and even a small amount of energy is enough to heat, melt and vaporize a small amount of metal. In addition, the pressure developed by the plasma particles when they hit the electrode contributes to the emission (erosion) of not only molten, but also simply heated matter. Since electrical breakdown, as a rule, occurs along the shortest path, the most closely spaced parts of the electrodes are destroyed first. When approaching one electrode of a given shape (tool) to another (workpiece), the surface of the latter will take the shape of the surface of the first. The productivity of the process and the quality of the resulting surface are mostly determined by the parameters of the electric pulses (their duration, tracking frequency, pulse energy) [7].

Research results

In order to identify the distribution of elements on the surface of the electroerosion powder, X-ray spectral microanalysis was performed with the help of the scanning electron microscope "QUANTA 600 FEG" and the X-ray radiation analyzer of the company "EDAX" integrated into it and the following results were obtained (Fig. 5).

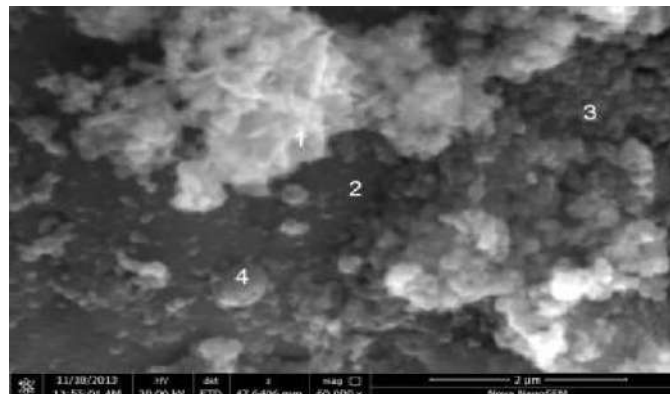


Fig. 5. Points of X-ray spectral microanalysis of powder

In the Table 1 shows the results of X-ray spectral microanalysis of powders.

Table 1

Results of X-ray spectral microanalysis of P6M5 high-speed steel powder

Element	C	O	Al	Mo	V	Cr	Fe	W
Weight, %	7,145	9,5	0,15	1,95	0,64	1,9	73,37	5,17

Thus, X-ray spectral microanalysis made it possible to determine the elemental composition of micro-objects of powder particles obtained by electroerosion dispersion of high-speed steel waste based on the characteristic X-ray radiation excited in them.

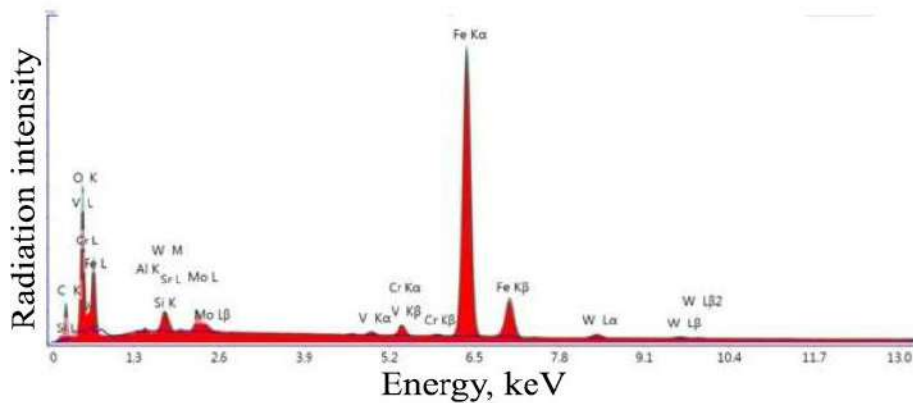


Fig. 6. X-ray spectral microanalysis of P6M5 powder at point 1

According to the results of the presented generalized data, it was established that the main elements in the powder obtained by the method of electroerosion dispersion of tool high-speed steel of the P6M5 brand (GOST 19265-73) in distilled water are: oxygen, iron, carbon, molybdenum and tungsten [8, 9].

It was established that when using stainless steel AISI 420 as a control (ball), after multiple passes over the tested surface of the experimental samples (substrates made of 30XHSA steel), the following occurs on the corresponding friction path:

- 100 m - intensive wear of the counterbody;
- 200 m – intensive wear of the counterbody;
- 500 m - intensive wear of the counterbody.

The results of tribological tests of samples using different friction paths are presented in Fig. 7, a-c.

The results of tribological tests of the friction surface of samples made of steel 30 HDSA, as well as electrospark coatings from BRS, indicate a high coefficient of friction of the latter. It was also noted that a jump occurs during tests of tribological samples from BRS. In this case, this is due to high roughness ($R_a = 2.14 \mu\text{m}$) and wear is characterized by smoothing of hard protrusions on the surface of the sample (Fig. 7, a-c) [10-12].

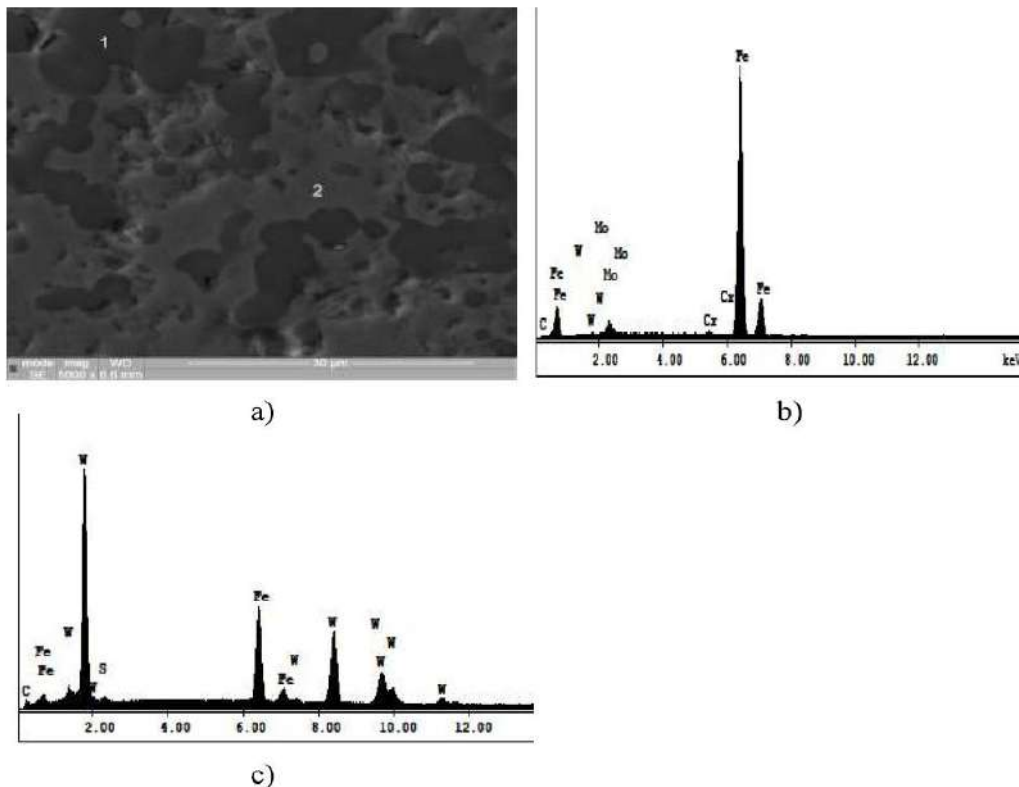


Fig. 7. The results of tribological tests of samples with different friction paths:
a - 100 m; b - 200 m; c - 500 m

The optical image of the wear spot of the counterbody (ball) after passes over the investigated surface of the experimental samples (electrospark coatings from BRS and substrate from 30KhGSA steel) is presented in Fig. 8, a-d.

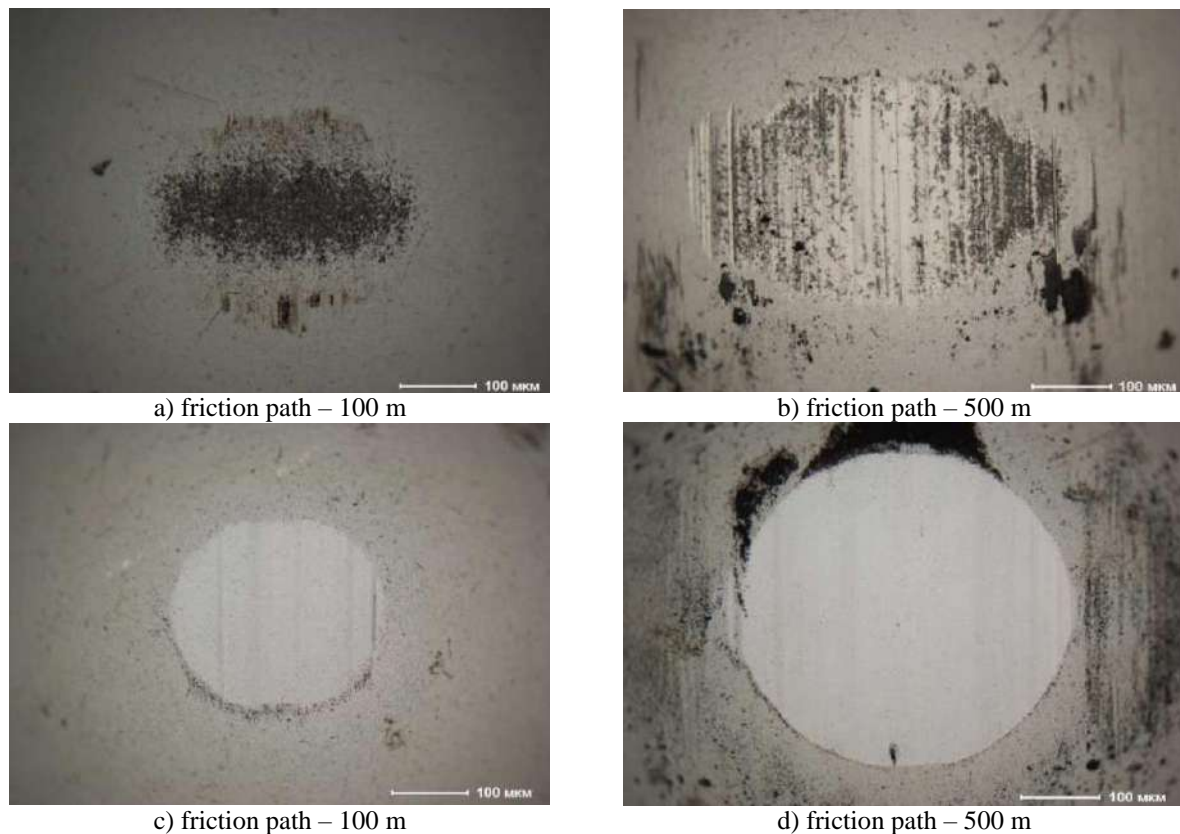


Fig. 8. Optical image of the wear spot of the counterbody (ball) after passes over the investigated surface of the experimental samples: electrospark coatings from BRS (a, b); substrates made of steel 30KHSA (c, d)

The optical image of the wear spot showed that when using stainless steel AISI 420 steel as a control (ball) [13], after multiple passes over the tested surface of the experimental samples (electrospark coatings with BRS), the following occurs on the corresponding friction path:

- 100 m - adhesion of sample wear products to the counterbody;
- 200 m - adhesion of sample wear products to the counterbody;
- 500 m - partial wear of the counterbody and sticking of wear products of the sample on the counterbody.

It was experimentally established that the roughness of samples with electrospark coating is $R_z 13.2 \mu\text{m}$ ($R_a 2.14 \mu\text{m}$).

It was experimentally established that electrospark coatings obtained with electrode material from electroerosion powders of high-speed steel have a thickness from 19.07 microns to 31.42 microns.

Conclusions

1. The proposed technology can be used to restore a wide range of parts for cars, tractors and other machines.

2. Experimentally determined dependences of the influence of the properties of electroerosive materials on the properties of electrospark coatings of restored car parts. It is shown that the content of nano-sized particles in the electrode material contributes to the improvement of the physical and mechanical properties of electrospark coatings. In particular, the average value of the microhardness of the electrospark coating (4.36 HV), obtained by the electrode material from electroerosion powders of high-speed steel, is greater than the microhardness of the substrate (2.09 HV) by up to 2.1 times.

3. Experimentally determined dependences of the properties of electrospark coatings on the service life of restored car parts. It is shown that the resource of the shafts of turbocompressors restored according to the recommended technology is higher than the resource of new shafts by an average of 1.5 times.

4. Experimentally established rational modes of applying wear-resistant coatings to worn shafts of turbocompressors, which provide the necessary complex of physical and mechanical properties of the coating and the given resource of the shafts as a whole (rotation frequency of the part, min - 1 - 50; electrode feed, mm/min - 0.4 ... 0.5).

5. The characteristics of wear resistance of electrospark coatings of turbocompressor shafts obtained using electroerosion nanomaterials were studied. It is shown that the average value of the coefficient of friction (μ) in the electrospark coating was 0.146 instead of 0.486 without coating, which is 3.3 times lower.

References

1. Archard J.F. Contact and rubbing of flat surfaces. *J Appl Phys* 1953; 24: 981–988.
2. Lai F.Q., Qu S.G., Yin L.M., et al. Design and operation of a new multifunctional wear apparatus for engine valve train components. *Proc IMechE, Part J: J Engineering Tribology* 2018; 232: 259–276.
3. Lewis R., Dwyer-Joyce R.S. Wear of diesel engine inlet valves and seat inserts. *Proc IMechE, Part D: J Automobile Engineering* 2002; 216: 205–216.
4. Worthen R.P., Rauhen D.G. Measurement of valve temperatures and strain in a firing engine. SAE paper 860356, 1986.
5. Forsberg P., Debord D., Jacobson S. Quantification of combustion valve sealing interface sliding – a novel experimental technique and simulations. *Tri Int* 2014; 69: 150–155.
6. Mascarenhas L.B., Gomes J.D., Beal V.E., et al. Design and operation of a high temperature wear test apparatus for automotive valve materials. *Wear* 2015; 342–343: 129–137.
7. Marchenko D.D., Matvyeyeva K.S. Improving the contact strength of V-belt pulleys using plastic deformation. *Problems of Tribology. Khmelnsky, 2019. Vol 24. No 4/94 (2019). S. 49–53. DOI: <https://doi.org/10.31891/2079-1372-2019-94-4-49-53>.*
8. Chun K.J., Kim J.H., Hong J.S. A study of exhaust valve and seat insert wear depending on cycle numbers. *Wear* 2007; 263: 1147–1157.
9. Marchenko D.D., Matvyeyeva K.S. Investigation of tool wear resistance when smoothing parts. *Problems of Tribology. Khmelnsky, 2020. Vol 25. No 4/98 (2020). S. 40–44. DOI: <https://doi.org/10.31891/2079-1372-2020-98-4-40-44>*
10. Dykha A.V., Marchenko D.D., Artyukh V.A., Zubiekhina–Khaiiat O.V., Kurepin V.N. Study and development of the technology for hardening rope blocks by reeling. *Eastern–European Journal of Enterprise Technologies. Ukraine: PC «TECHNOLOGY CENTER». 2018. №2/1 (92) 2018. pp. 22–32. DOI: <https://doi.org/10.15587/1729-4061.2018.126196>.*
11. Blum M., Jarczyk G., Scholz H., et al. Prototype plant for the economical mass production of TiAl-valves. *Mat Sci Eng A-Struct* 2002; 329–331: 616–620.
12. Dykha A.V., Marchenko D.D. Prediction the wear of sliding bearings. *International Journal of Engineering and Technology (UAE). India: “Sciencepubco–logo” Science Publishing Corporation. Publisher of International Academic Journals. 2018. Vol. 7, No 2.23 (2018). pp. 4–8. DOI: <https://doi.org/10.14419/ijet.v7i2.23.11872>.*
13. Marchenko D.D., Artyukh V.A., Matvyeyeva K.S. Analysis of the influence of surface plastic deformation on increasing the wear resistance of machine parts. *Problems of Tribology. Khmelnsky, 2020. Vol 25. No 2/96 (2020). S. 6–11. DOI: <https://doi.org/10.31891/2079-1372-2020-96-2-6-11>.*

Марченко Д.Д., Матвєєва К.С. Підвищення зносостійкості відновлених деталей автомобілів шляхом застосування електроіскрових покриттів

У роботі науково обгрунтовано застосування ефективною технології для відновлення зношених деталей автомобілів шляхом застосування нових електроіскрових покриттів на основі електроерозійних наноматеріалів. Розроблена технологія відрізняється технологічної гнучкістю, дешевизною, простотою, не вимагає використання дорогих та дефіцитних матеріалів та обладнання, а також відповідає вимогам екологічної безпеки. Пропонована технологія може бути використана для відновлення широкої номенклатури деталей автомобілів, тракторів та інших машин. Експериментально встановлені залежності впливу властивостей електроерозійних матеріалів на властивості електроіскрових покриттів відновлених деталей автомобілів. Показано, що зміст нанорозмірних частинок в електродному матеріалі сприяє покращенню фізико-механічних властивостей електроіскрових покриттів. Експериментально встановлені залежності впливу властивостей електроіскрових покриттів на ресурс відновлених деталей автомобілів. Показано, що ресурс валів турбокомпресорів, відновлених за рекомендованою технологією вище ресурсу нових валів у середньому в 1,5 рази. Експериментально встановлені раціональні режими нанесення зносостійких покриттів на зношені вали турбокомпресорів, що забезпечують необхідний комплекс фізико-механічних властивостей покриттям та заданий ресурс валам в цілому (частота обертання деталі, хв - 1 - 50; подача електрода, мм/хв - 0,4 ... 0,5). Вивчено характеристики зносостійкості електроіскрових покриттів валів турбокомпресорів, отриманих з використанням електроерозійних наноматеріалів. Показано, що середня значення коефіцієнта тертя у електроіскрового покриття склало 0,146 замість 0,486 без покриття, що в 3,3 рази нижче. За результатами виробничих випробувань встановлено, що тривалість роботи турбокомпресора, з відновленим методом електроіскрової обробки наноструктурним електродом валом, у 2,1 рази збільшилася по порівнянні з новим промислово виготовленим валом. Так, при введенні абразивного матеріалу, що містить фракцію розміром 0,1...0,4 мм час роботи турбокомпресора з відновленим валом становило 12,8 годин, а час роботи турбокомпресора з новим валом без зносу номінального розміру становило 8,1 год.

Ключові слова: зносостійкість, електроіскрові покриття, відновлення, деталі автомобілів, наноматеріали.



Investigation of the properties of coatings obtained by electric arc spraying

A. Lopata^{*1}, I. Smirnov¹, M. Holovashchuk², V. Lopata³

^{*1}National Technical University of Ukraine "Igor Sikorsky Kyiv Polytechnic Institute," Kyiv, Ukraine

²National Transport University, Kyiv, Ukraine

³E.O. Paton Electric Welding Institute of the National Academy of Sciences of Ukraine

*E-mail: lopata-sasha@ukr.net

Received: 19 January 2022; Revised: 20 February 2023; Accept: 08 March 2023

Abstract

The paper considers possibilities to increase the wear resistance, corrosion resistance, and service life for parts of machines and mechanisms via their hardening and renovating using electric arc coatings characterized by high density, adhesion strength, and micro hardness. Also, the possibility of controlling the properties of restored surfaces owing to choice of the related equipment with required structure and characteristics in order to prolong the service life of machinery parts is shown. The right choice of equipment for spraying makes it possible to increase the speed and temperature of the spraying gas and particles, reduce the droplet diameter, increase the density and reduce the oxidation of coatings. The influence of spray factors such as the flow rate and pressure of working gases, composition of combustion mixture, spraying distance, dispersion of the spray, properties of wire material, etc. on the properties of the coatings obtained has been investigated.

Key words: coatings, wear resistance, adhesion strength, electric arc spraying

Introduction. The state of the problem and the purpose of the research. In the practice of restoring and hardening parts through the use of hardening protective coatings, extensive experience has been accumulated in the application of coatings by methods of gas-thermal spraying (GTS) [1,2]. The reasonability of using GTS is evidenced by the appearance of a number of special firms for manufacture of equipment and materials for spraying, for example, Metko, Wall Cobmonoy Corp. Linde Div., Union Carbide Corp. *et al.* [3]. The produced domestic and foreign GTS units [1,2], spray materials [3], and published recommendations have made it possible to solve a series of items related to the repair, restoration, and prolongation of the service life of parts [1,2].

In the development of techniques for restoration of parts, it is necessary, of all the possible GTS methods (Table 1) [1,2], to choose such one that provides the longest service life of a part and the lowest cost of its recovery as well as can be fairly versatile, simple, and easy to implement [3]. When choosing a method for GTS, it is necessary to consider the basic conditions for high-quality coating formation [4]:

- 1) thermal effects on the part must prevent the phase or structural transformations in the base metal;
- 2) participation of the base metal in the coating must be negligible;
- 3) in the contact zone, no relaxation process capable to change its phase composition and structure should arise.

Table 1

Characteristics of spraying modes

Parameter	Spraying mode			
	Electric arc	Gas flame	Plasma	Detonation
Efficiency, kg/h	3 - 31	1 -10	0.5 - 8.0	0.1- 6.0
Coefficient of material consumption	0.8 -0.9	0.8 -0.95	0.4 -0.9	0.3 - 0.6
Adhesion strength, MPa	to 40	to 50	to 60	to 200
Temperature of part heating, °C	100-150	100-150	150 -200	100-150



From the standpoint of these conditions, the use of electric arc spraying (EAS) is promising [4,5]. In the world practice of hardening, recovery, and anticorrosion protection, EAS has become widespread as the most technologically advanced and productive method (productivity is 3-4 times that for flame spraying) [4,5]. EAS is widely used in the European countries and displaces the traditional gas-flame method [3]. This is due to the simplicity of the equipment, the availability of energy source for metal melting, higher thermal efficiency, which reaches 57% compared to 13 and 17% for gas and flame spraying [4,5]. The quality of EAS coatings are practically the same as that of coatings produced by plasma and detonation methods, and the coating-to-base adhesion strength is greater than in the case of flame spraying. In [4,5], information is given about the advantages of EAS over surfacing in terms of labor input and consumption of electrode material: duration of surfacing is 1 h 10 min and wire consumption 1.3 kg, while for EAS these parameters are 24 min and 0.95 kg, respectively.

The equipment on which coating is performed is relatively simple and light and can be moved fairly quickly (Fig. 1). The part dimensions do not limit the use of EAS [4,5]. This method is effective and economical in the manufacture and renovation of parts in the conditions of repair enterprises and small workshops with a single production [4,5].



Fig. 1. The electric arc spraying process

Despite the large number of innovations concerning EAS, researches on the improvement of this method and required equipment are actively being carried out and has become aimed at activating the spray process using various techniques, methods, and devices. The spray process activation is the basis for improving the technology and equipment for deposition of high-density wear-resistant layers. In practice, the following procedures for spray process activation have been implemented [1-7]:

- intensification of mixing working gases;
- provision of sprayed particles and the substrate with additional energy via heating them;
- diminution of the sprayed particles size;
- activation of the particle and the substrate surfaces by mechanical methods (increase in roughness) or by reduction of oxides;
- increase in the enthalpy of the spray flux by introducing thermo-reactive components;
- coating with the use of external effects (ultrasonic waves, electromagnetic fields, etc.);
- heat treatment or chemical heat treatment of coatings, etc.

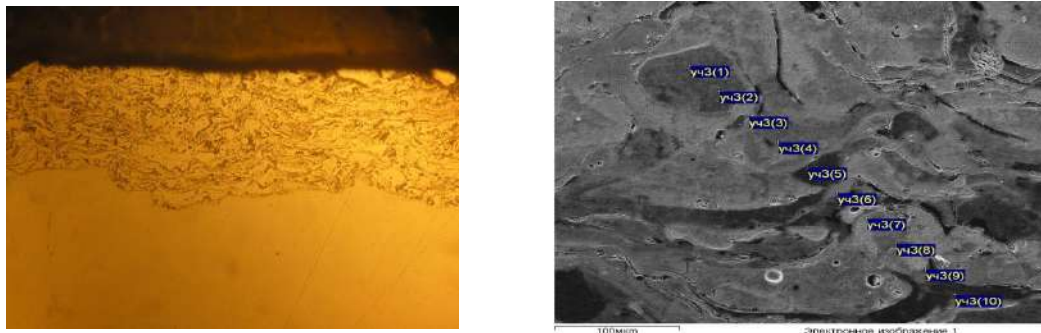
Preheating of the substrate was established to lead to decreasing the rates of crystallization, cooling of falling particles, and developing their chemical interaction with the substrate. As a consequence, adhesion strength increases. However, in the case of heating above 500 K, the rate of oxide formation increases and adhesion strength decreases. Moreover, preheating to 500 K is impossible when thin-walled parts are coated because of unavoidable thermal deformation, and this operation is undesirable in restoring parts that operate under alternating or cyclic loads (as fatigue cracks grow under heating). The use of activation techniques which intensify heat exchange processes in the "jet-particle" system and increase the dynamic parameters of particles, and allows reducing the wire particle size or of those that allow modifying (strengthening) the sprayed layer seems to be most expedient means [8-10].

The aim of the work - was set up to increase the wear resistance and service life of parts *via* combining EAS coatings characterized by high density, adhesion strength, and microhardness due to the activation of the spray process and nitriding of the coatings sprayed.

Study of the spraying process and the influence of its factors on the properties of EAS coatings.

The EAS process coating is the result of the following physicochemical interactions: the air flow with the wire melt and the formation of a jet of sprayed particles; transformation of the kinetic energy of the sprayed particles into the work of deformation during their mechanical contact with the part surface, and the transfer of internal (thermal) energy from the particles to the part. On the part surface, a coating layer is formed (Fig. 2), the properties of which depend on the characteristics of physicochemical processes listed above.

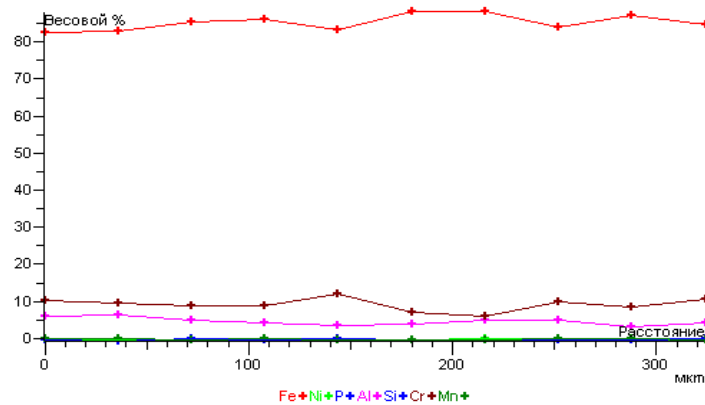
The study of the microstructure was carried out on unetched and etched sections using a light microscope "MeF-3" company "Reichert" (Austria) at a magnification of '100, '200, '500. Photos of microstructures are attached (Fig. 2). The study was also carried out on a CamScan scanning electron microscope (Oxford Instruments, England) with an X-ray energy dispersive analyzer (Fig. 2). The morphology (topography) of the coating surface was studied in the mode of reflected electrons at an accelerating voltage of 10–20 kV. The resolution of this SEM is 70 Å. Two types of studies were used: the spectrum from the surface of a thin section and the structure of the surface in combination with Y-modulation, i.e. - slow scanning of the electron beam along the line with the registration of X-ray radiation for each element with and the construction of concentration distribution curves. In addition, spot X-ray microanalysis was carried out according to the program of quantitative analysis. The research results are presented in tables (Fig. 2). The color in the photograph determines the concentration: black - the complete absence of the element, white - 100% presence, transitional colors indicate an intermediate concentration. In the second case, we obtain the distribution of three or more elements at the same time, while each of the elements is assigned a conditional color. All other colors are formed when the three main colors are superimposed and indicate the joint presence of elements in one or another part of the sample, and the concentration in this case is determined by the density of the color. The application of this research program gives very good results for understanding the mechanisms of diffusion processes.



x 200

(b) x250

Спектр	Al	Si	P	Cr	Mn	Fe	Ni
уч3(1)	6.23	0.32	0.10	10.58	0.26	82.56	0.15
уч3(2)	6.69	0.37	0.20	9.97	0.20	82.92	0.05
уч3(3)	5.27	0.12	0.21	9.09	0.06	85.25	0.01
уч3(4)	4.45	0.12	0.04	9.12	0.23	86.12	0.09
уч3(5)	3.98	0.21	0.04	12.47	0.05	83.36	0.04
уч3(6)	4.09	0.15	0.14	7.26	0.10	88.40	0.15
уч3(7)	5.32	0.08	0.10	6.19	0.04	88.20	0.27
уч3(8)	5.26	0.22	0.09	10.21	0.20	83.99	0.02
уч3(9)	3.59	0.20	0.03	8.88	0.16	87.07	0.07
уч3(10)	4.44	0.27	0.21	10.75	-0.14	84.59	0.12



g)

Fig. 2. Microstructure of EAS coatings from wire from powder wire FMI-2 (a, b) and distribution of alloying element (g)

Studies of the effect of the average particle size of spray wires from 40Kh13, 12Kh18N10T, nichrome and powder wire FMI-2 on the physico-mechanical properties of coatings revealed (Fig. 3) that coatings made from steel wires show a decrease in adhesion with increasing porosity, whereas nichrome does not obey this rule. As seen in the figure, the curve of accumulated weight wear of tempered steel has a characteristic stage of running-in and a steady wear stage with almost linear dependence of the weight wear on the friction path. For EAS coatings, the stages of steady wear periodically alternate with the relatively short-term stages of accelerated wear, i.e., wear of EAS coatings is pronouncedly cyclical. The highest averaged weight wear rate was 0.39 mg/m (Table 2).

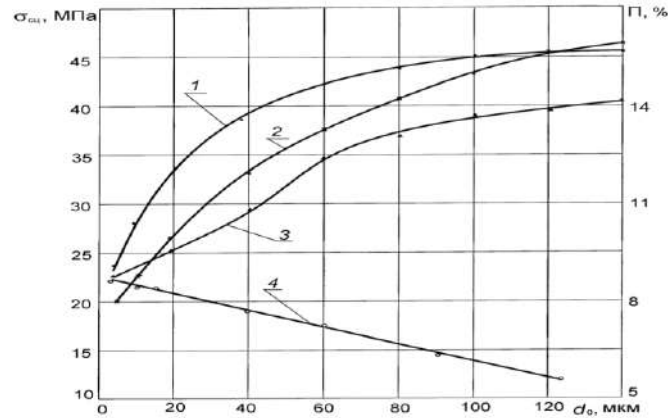


Fig. 3. The effect of the average size of sprayed wire particles of powder wire FMI-2 (1) and of steels 40Kh13, Kh18H10T (2, 3), and nichrome (4) on the adhesion strength (1, 2, 4) and porosity (3) of coatings

Table 2

Wear rate and coefficient of dry friction for EAS coatings and tempered powder wire FMI-2

Material	Wear rate, mg/m	Coefficient of friction
Powder wire FMI-2	0.12	0.82 – 0.93
EAS coating	0.27	0.83 – 0.96
EAS coating	0.39	0.94 – 1.02

Accelerated tribological tests of samples with EAS coatings from powder wire FMI-2 were conducted on an upgraded machine of the 2070 SMT-1 type. Upon spraying, an irregular coating structure was formed *via* layered stacking of molten steel droplets (Fig. 5). Such a structure provides damping of elastic excitations caused by friction. After the tribological tests, no noticeable wear of EAS coatings was detected for 9 h.

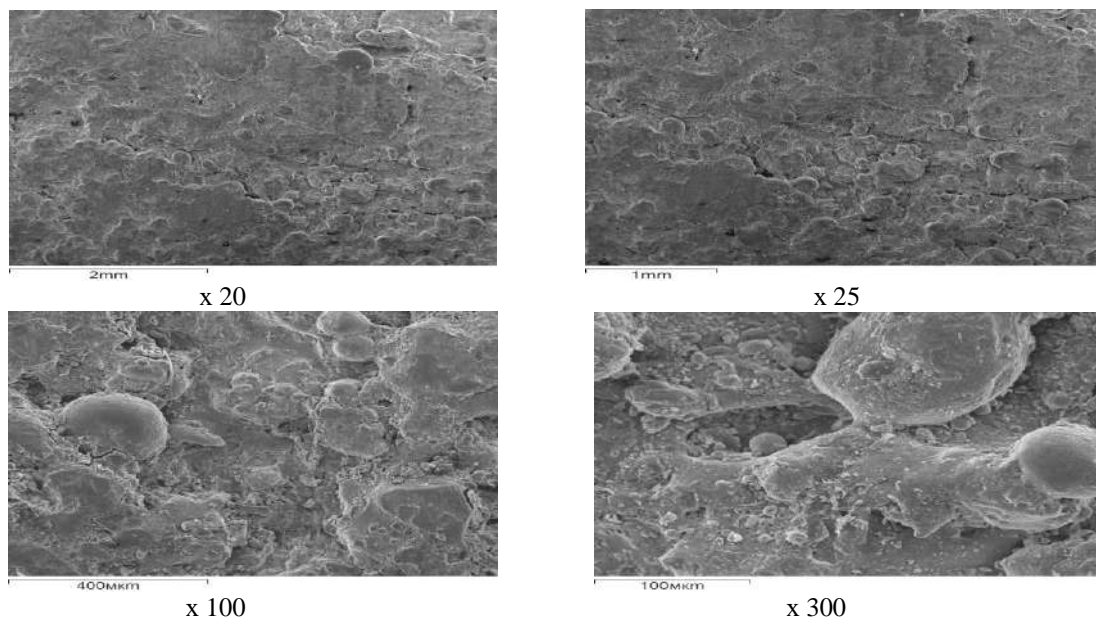


Fig. 5. Surface topography of EAS coating after 9 h testing obtained with a scanning electron microscope
Control of structure formation processes in sprayed coatings

A number of researchers have noted that the structure of coatings obtained by spraying the same wire material by different modes can differ not only in the number of pores, but also in the phase composition [1-7]. This paper presents the results of studies of the structural features of EAS coatings. As spray materials, FMI-2 powder wires with a diameter of 2 mm were used. Spraying was performed using an apparatus for EAS in the following modes:

- mode 1: spraying of metal melted in an electric arc with a reactive jet of combustion products of propane/air mixture with an excess of propane (reducing atmosphere);
- mode 2: spraying of metal melted in an electric arc with a reactive jet of combustion products of the propane/air mixture with an excess of air (oxidizing atmosphere);
- mode 3: spraying of metal melted in an electric arc with a fast air jet.

To improve the adhesion of coatings to a steel 3 substrate, an intermediate layer from powder wire FMI-2 was created. The velocity of molten particles was 120–130 m/s (modes 1 and 3) and 400–500 m/s (modes 1 and 2). The sizes of the particles from which the coatings were formed fell in the range of 5–40 μm . The dominant amount of oxides was formed as a result of the molten particles/air contact. In the work, the effect of the spraying air flow rate on the amount of oxygen in the coatings obtained by EAS (mode 3) was studied (Fig. 6). Here the oxygen content in EAS coatings was 2.5–3 times that in gas-flame ones (Fig. 6), with achieving the maximum concentration 3.8% at flow rates of about 0.5 m^3/min . An XRD analysis (diffractometer DRON-3.0, monochromatic $\text{CoK}\alpha$ radiation, $V = 30 \text{ kV}$, $I = 10 \text{ mA}$) revealed that the phase composition of the coatings includes: α -phase (martensite), γ -phase (austenite), oxides Fe_3O_4 , $\gamma\text{-Fe}_2\text{O}_3$ (traces), and Cr_2O_3 (traces) (Fig. 6).

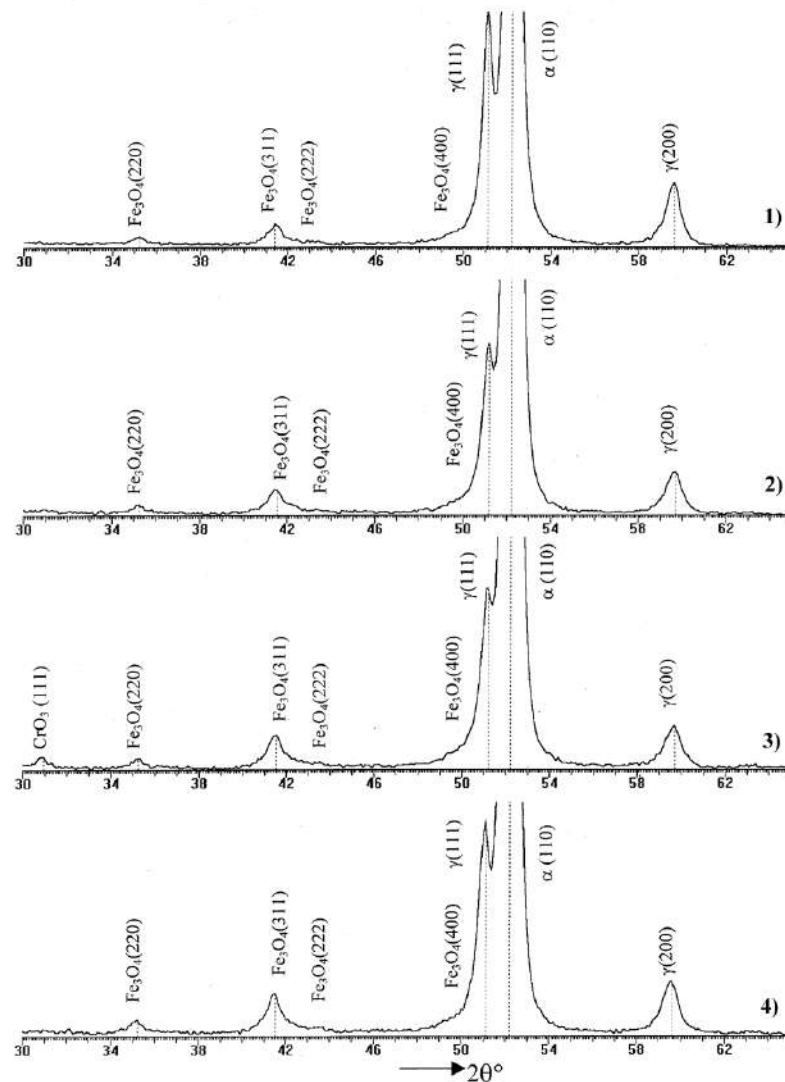


Fig. 6. Fragments of XRD patterns ($\text{CoK}\alpha$) from surface layers of gas-thermal coatings obtained under modes 1-4

The hardness of the coatings obtained using various spray schemes was within the HV range of 2800 - 3500 MPa. Activation of EAS (AEAS) in a reducing atmosphere leads to the formation of dense coatings with a porosity of 2 - 5% and hardness $\text{HV} = 3000 \text{ MPa}$, characterized by low content of residual austenite ($V_\gamma \approx 20 \text{ vol}\%$)

and oxides. The lattice parameters of martensite and austenite are $a_{\alpha}=0.2875$ nm and $a_{\gamma}=0.3592$ nm, respectively. AEAS by a reactive jet with an excess of air provides the formation of a layer with a porosity of 2 - 5% and hardness $HV = 3500$ MPa, characterized by substantial content of oxidation products. The content of residual austenite in the coating is $V_{\gamma} \approx 20$ Vol. %. The lattice parameters of martensite and austenite are $a_{\alpha}=0.2875$ nm and $a_{\gamma}=0.3592$ nm, respectively. Coatings obtained by spraying with air had a hardness of $HV=3200$ MPa and a residual austenite content of $V_{\gamma} \approx 18$ vol% at the porosity 6–8%. The XRD data fixed the highest concentration of oxidation products in the coating after EAS with air. Lattice parameters were $a_{\alpha}=0.2875$ nm and $a_{\gamma}=0.3596$ nm for martensite and austenite, respectively.

The results of the study of the phase composition and hardness of coatings from powder wire FMI-2 indicate the influence of the deposition technique on the structure and properties of the layer obtained. A distinctive feature of deposited layers is the presence of an anomalously large amount of residual austenite (up to 30 vol%) and oxides. Generally, the content of residual austenite in hardened powder wire FMI-2 does not exceed 3 - 5 vol% [11-13].

One of the reasons for the appearance of the “austenitic effect” in coatings is a higher concentration of alloying elements (chromium and carbon) owing to the complete dissolution of chromium carbides during melting of the wire and saturation of the molten droplets with carbon from the propane flame. This is confirmed by the absence of $Cr_{23}C_6$ carbide particles in the coating. While analyzing the causes of austenite stabilization in the layer, one should keep in mind that under spraying surface layers are heated to 500–670 K. As a result, the sprayed coating undergoes isothermal aging at 520–670 K during its formation and cooling, which promotes thermal stabilization of austenite [1-7]. A factor that increases the stability of austenite in the sprayed layers is saturation of the molten droplets with carbon during melting and spraying with propane flame (Table 3).

Table 3

The influence of the composition of combustion mixture forming the spray on the carbon and oxygen contents in EAS coatings from powder wire FMI-2

Technique of spraying	Air/propane volume ratio in mixture	Oxygen content in coatings, %	Carbon content in coatings, %
1	(Gas flame) propane/oxygen ratio 1/4	1.3	0.6
2	(AEAS) 18	1.4	0.5
3	(AEAS) 30	2.2	0.4
4	(AEAS) clean air	3.3 – 3.5	0.4

The low velocity of molten steel particles and high concentration of carbon-containing propane in the combustion products contribute to a deeper saturation of molten droplets with carbon. These circumstances are associated with a high content of residual austenite in coatings obtained by the gas flame procedure (technique 1).

The smaller amount of austenite in coatings obtained by AEAS in the reducing atmosphere of the spray torch (technique 2) is due to the higher flight velocity of the molten particles, which is characteristic for this technique. In this case, the processes of diffusion saturation of the droplets with carbon from the reducing atmosphere of the products of propane/air mixture combustion do not have enough time to complete (flight time of molten droplets in the atmosphere of combustion products is not more than $5 \cdot 10^{-4}$ s), and the content of residual austenite in the layer decreases to ~ 20 vol%.

An increase in the oxygen concentration in the mixture is not accompanied by change in the amount of residual austenite in the coating obtained under conditions of supersonic velocities of molten particles (technique 3) and at relatively low particle velocities (technique 4). In both cases, the content of residual austenite in the layer does not exceed 20 vol%. The carried-out studies made it possible to conclude that for EAS there are such regimes and steels that can provide the formation of a large amount of metastable austenite in the coatings, which during the performance of the tribocoupling will turn into martensite. The experiments established a relation between the temperature of the beginning of martensitic transformation, T_M , for the wire material and the amount of metastable austenite formed in the resultant coating (Table 4) [1 -7].

In steels of group 1, as well as in corrosion-resistant martensitic steels, the temperature T_M is within 550 - 700 K. When spraying wires from these steels, the volume content of metastable austenite reaches 45%.

In the case of spraying wires from steels of the first two groups, the preservation of a large amount of metastable austenite can be prescribed to the high rate of crystallization of steel particles in the course of forming the sprayed layer and slowing down its cooling rate in the martensitic transformation region. The decrease in austenite stability in coatings from steels of the third group, sprayed over 2500 K, is explained by the effect of manganese and chromium contained in the steel on the temperature range of its martensitic transformation. Thus, a decrease in the manganese content from 5% to 1% leads to an increase in the temperature from 270 to 470 K [1-7]. In this regard, one of the possible ways to increase the T_M temperature is reduction in the chromium or manganese content in the austenitic phase of steels by oxidizing it during spraying.

Table 4

Metastable austenite content in EAS coatings obtained by spraying various steel grades

Group of steels	Steel grade	Temperature T_M , K	Temperature of heating under spraying, K	Content of austenite in coating Vol %
1	09G2S, 40KhN, 40Kh13 FMI-2	550–700	1700-2000 2100-2500 > 2600	25-45 17-20 < 6
2	9KhS, Kh12MF, 9Kh12, Kh6VF, 35KhNM, 40KhFVA, 65G	420–540	1700-2100 2200-2500 > 2500	15- 25 8 -12 < 6
3	08Kh18N10, 12Kh18N10T, 110G13	70–110	1700-2000 2000-2500 > 2500	95 - 98 90 - 95 90 - 95

Conclusions

The present work recommends to increase the wear resistance, corrosion resistance, and service life of parts *via* hardening and renovating them using combined EAS coatings characterized by high density, adhesion strength, and microhardness due to activation of the spraying process. It has been shown that by properly choosing design parameters and characteristics of equipment for EAS, it is possible to control the properties of restored surfaces in order to increase the service life of SMM parts. The right choice of equipment for spraying will allow one to increase the speed and temperature of the jet of spraying gas and molten particles, decrease the droplet diameter, increase the density, and reduce the oxidation of coatings. Moreover, the phase composition and microhardness of coatings obtained by spraying wires from austenitic and martensitic steel were investigated. The presence of an abnormally large amount of residual austenite (to 50 vol%) in coatings from martensitic steel was established. Studies of the resistance to fatigue failure showed that coatings deposited by EAS of wires provide a slight decrease in the fatigue strength limit to 10–13% (for comparison, coatings obtained by vibro-arc surfacing reduce the fatigue limit by 35–40%). In the course of tribological tests, the wear of sprayed coatings was established to be cyclical. The cyclicity of weight wear of sprayed coatings is associated with the degradation of their surface layer under friction, described in terms of physical mesomechanics of solids.

References

- Ageev M.S., Volkov Yu.V., Chigrai S.L. Protective and hardening coatings in ship building and repair. Science Bulletin KhDMA. Kherson: №2 (13). 2015. P.110-124.
- Ageev M.S. Volkov Yu.V., Chigrai S.L. Welding and related processes in ship building. Water Transport. Kyiv: KGAVT, №2 (24), 2015. P. 15-26.
- Kharlamov Yu.A. Thermal spraying of coatings and ecological compatibility of production, operation and repair of machines. Heavy engineering. №2. 2000. P. 3-10.
- Ageev M.S. Kozhevnikova E.E, Lopata V.N. Restoration of ship pump shafts using a combined method of applying protective coatings. Science Bulletin KhDMA. Kherson: №2 (13). 2015, P. 4-16.
- Kozhevnikova E.E., Ageev M.S., Chigrai S.L. Increasing the life of ship pumps based on combined restoration technology. Coll. of papers Water Transport. Kyiv: KGAVT, №2 (24). 2015. P. 57-70.
- Brusilo Yu.V. Choice of equipment for hardening and restoring parts of piston engines by arc spraying. Aerospace Engineering and Technology. Kharkiv: №4 (71), 2010. P. 38-42.
- L.A. Lopata, N.A. Medvedeva, T.M. Tunik, S.G. Saliy Improvement of sprayed coatings. World of Engineering and Technologies. 8 (54), 2005. P. 54-56.
- Matveishin E.N. Deposition of layers with high adhesion strength by methods of arc metallization. Automatic welding. 8. 2000. P. 20-22.
- Karp I.N., Petrov S.V., Rudoi A.P. Installation for arc metallization in a supersonic flow of natural gas combustion products. Welding Production, 2, 1991. P. 22-23.
- Vilage B., Rupprecht K., Pokhmurskaya A. Features of gas-thermal spraying with flux-cored wires. Automatic welding. №10. 2011. P. 26-30.
- V.I. Pokhmursky, M.M. Student, V.S. Pikh Protective and restorative electric metallization of coatings from cored wires. New processes and equipment for gas-thermal and vacuum coating: Coll. of papers "Electric welding". Kyiv: 1990. P. 66 - 69.
- Student M.M. Development of old and new electrometallic coatings to cover powder darts: Thesis. Lviv: 1998. 18 p.
- Pokhmurska G.V., Dovgunik V.M., Student M.M. Wear resistance of laser-modified electric arc coatings from cored wire FMI-2. FKhMM № 4. 2003. P. 61-64.

Лопата О.В., Смирнов І.В., Головащук М.В., Лопата В.М. Дослідження властивостей покриттів, отриманих електродуговим напиленням

У роботі запропоновано підвищувати зносостійкість, корозійну стійкість та термін служби деталей машин та механізмів при їх зміцненні та реновації ЕДН-покриттями з високою щільністю, міцністю зчеплення та мікротвердістю за рахунок активації процесу напилення. У роботі розглянуто можливість за рахунок вибору конструктивних параметрів та характеристик обладнання для ЕДН керувати властивостями відновлених поверхонь з метою підвищення ресурсу деталей машин. Правильний вибір конструкції обладнання для напилення дозволить збільшити швидкість і температуру струменя газу і частинок, що транспортуються, зменшити діаметр крапель, підвищити щільність і знизити окислюваність покриттів. В роботі досліджено вплив факторів процесу напилення: витрат та тиску робочих газів, складу паливної суміші, дистанції напилення, дисперсності розпилення, матеріалу дроту та ін. на властивості ЕДН-покриттів.

Ключові слова: покриття, зносостійкість, міцність зчеплення, електродугове напилення.



The regularity of the change in the coefficient of friction of the coupling of "shaft-sleeve" parts using polymeric materials

V.V. Aulin*, S.V. Lysenko, A.V. Hrynkiv, A.A. Tykhyi, O.V. Kuzyk, O.M. Livitskyi

Central Ukrainian National Technical University, Ukraine

**E-mail: AulinVV@gmail.com*

Received: 25 January 2022; Revised: 25 February 2023; Accept: 15 March 2023

Abstract

For the conjugation of samples and parts of the "shaft-sleeve" type, from the theoretical and experimental points of view, the laws of the change of the coefficient of friction for the combined polymer-metal material and coating were considered. Based on the law of energy conservation and transformation in the friction zone, expressions for estimating friction coefficients for polymer coatings and combined polymer-metal materials were obtained, taking into account the properties of thermal conductivity and elasticity and the geometric dimensions of the polymer and metal components. The consistency of the patterns of change in the friction coefficient has been clarified in tribocouplings of samples and parts from load and sliding speed in modes without lubrication and at extreme friction. To substantiate the effective operation of tribocoupling of parts made of combined polymer-metal materials, a criterion was introduced - the coefficient of wear, which is used to evaluate the tribological efficiency. It is shown that the obtained experimental results do not contradict the theoretical justification.

Key words: polymer-metal material, coefficient of friction, load, sliding speed, tribocoupling of samples and parts, non-equilibrium state, elasticity, deformation, wear coefficient

Introduction

The use of tribocouplers of samples and parts made of combined polymer-metal materials depends on the polymer material, the formation of the metal component, the coating technology, properties and geometric characteristics of the polymer and metal components.

During the operation of tribocoupled parts, the intensity of wear and the coefficient of friction are important. Designing combined polymer-metal materials and coatings, they try to significantly reduce the intensity of wear and optimize the friction coefficient for a specific tribocoupling. There is no criterion by which it is possible to evaluate the effective operation of tribocoupling of parts made of combined polymer-metal material and coatings. It is important to control the value of the coefficient of friction by varying the geometric dimensions, properties of the components of the combined polymer-metal material, operating modes and load-speed characteristics.

Literature review

To effectively increase the durability of machine systems and units, tribo-coupling of parts made of polymer and polymer-metal materials is used [1-3]. But at the same time, it is necessary to solve the problem of optimal geometric dimensions, technologies for forming stress coatings in materials, intensity of their wear, development of methods for evaluating the efficiency and reliability of such tribocouplers [4,5].

It should be noted that when implementing such an operational property of materials as their wear resistance, the task is complicated due to the significant dependence of stresses on the ratio of constituent polymer-metallic materials, sizes, shapes of their constituents, as well as structural features of conjugated parts and properties of the working (technological) environment [6,7].

The authors of works [8-10] the main cause of destructive processes in the surface layers of half-dimensional materials are contact stresses and deformations that arise under the influence of loads on the tribocoupling of parts. This requires a detailed study of the features in the surface layers of the tribojoint materials of



the parts. Studying the features of combined polymer-metal materials in the process of tribocoupling of parts allows us to approach unsolved problems from a single point of view. The use of physical and mathematical models [11,12] is appropriate. Attempts to compare the wear resistance and stressed and deformed state of the surface layers of such coatings on parts were made in [1].

The relationship between the wear process of combined polymer-metal materials and their tribological properties is given in works [13,14]. The results of studies of wear resistance with polymer and polymer-metal coatings show that in the first case it is lower than in the second due to faster equalization of contact pressure. The phenomenon of spontaneous establishment and maintenance of a stationary mode of wear was also revealed [1,15,16].

The existing results of studies of combined polymer-metal materials [17-20] do not allow to evaluate the effectiveness of the tribocoupling of parts according to the intensity of wear, and there is a need to relate them to the types of contacts and contact conditions.

Purpose

The purpose of this work is to identify the patterns of change in the friction coefficient of tribocouplers of parts made of combined polymer-metal materials and with applied polymer and polymer-metal coatings and to propose a criterion for their tribological efficiency in operation.

Results

Research results indicate that the heat resistance of the combined polymer-metal coating (PMeC) is higher than that of pure polymer (PC). This makes it possible to develop the formation of polymer-metal coatings as a technological process to increase the wear resistance and heat resistance of the range of parts that work as sliding bearings in machines.

For polymer materials, there is a fairly clear relationship between friction coefficients and temperature in the contact zone: lower temperatures correspond to lower values of the friction coefficient and vice versa. The temperature arising as a result of friction changes the elastic and strength properties of the polymer surface layers of tribocouples of samples and parts. This affects the change of the actual contact area of the surfaces and the force of friction, and therefore the coefficient of friction.

The temperature change observed in the friction zone is due to more intensive heat removal by combined polymer-metal coatings compared to pure polymer ones.

In the case of a combined polymer-metal coating (fig. 1), its two components should be considered: metal with a width a , height – h and polymer – with a width of b . Thermal conductivity of metal material – λ_3 . The thickness of the polymer coating over the metal component is δ_1 .

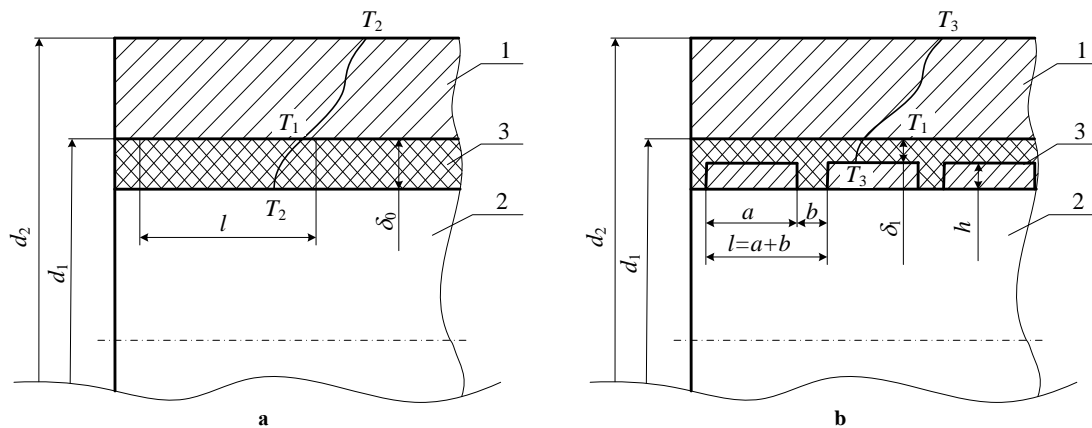


Fig. 1. Scheme of tribocoupling of parts "shaft-sleeve with polymer (a) and combined polymer-metal (b) coatings: 1 - sleeve; 2 - shaft; 3 - coating

Heat flows through the components of the combined polymer-metal coating of the cylindrical surface have the form:

– for the polymer component:

$$Q_p = (1 - \gamma)(1 - \beta) \frac{2\pi b \lambda_2 (T_1 - T_2)}{\ln \frac{d_1}{d_1 - 2h_1 - 2\delta_1}}; \quad (1)$$

– for the metal component:

$$Q_{Me} = (1 - \gamma)(1 - \beta) \frac{2\pi a \lambda_3 (T_1 - T_2)}{\ln \frac{d_1}{d_1 - 2h_1 - 2\delta_1}}, \quad (2)$$

where γ – the coefficient that takes into account part of the heat dissipated through the bushing friction surfaces;

β – the coefficient that takes into account part of the heat dissipated in the triboconjugation of samples and parts;

λ_2 – thermal conductivity of the polymer.

The flow of heat removed from the friction zone by the combined polymer-metal coating is equal to:

$$Q_{MeP} = \frac{(1 - \gamma)(1 - \beta)2\pi(T_1 - T_2)}{\ln \frac{d_1}{d_1 - 2h - 2\delta_1}} (b\lambda_2 + a\lambda_3). \quad (3)$$

We compare the heat flows Q_P and Q_{MeP} assuming that $h + \delta_1 = \delta_0$:

$$\frac{Q_{MeP}}{Q_P} = \frac{b\lambda_2 + a\lambda_3}{(a + b)\lambda_2}. \quad (4)$$

After some transformations (4) can be represented in the form:

$$\frac{Q_{MeP}}{Q_P} = 1 + \frac{a(\lambda_3 - \lambda_2)}{(a + b)\lambda_2}. \quad (5)$$

Since $\lambda_2 \ll \lambda_3$, then $\frac{Q_{MeP}}{Q_P} \gg 1$, that is, the process of heat removal is significantly intensified by the

combined polymer-metal material in comparison with the polymer one.

An increase in the relative sliding speed of the contacting tribocoupling of parts causes an increase in the temperature in the friction zone, which can affect both the mechanical properties of materials and the nature of the entire complex of physico-chemical processes. Based on the law of conservation of energy in the mode of steady friction, when the surfaces of the contacting parts are worn, the temperature in the contact zone can be calculated using the expression:

$$T_1 = \frac{k}{\lambda_1 + \lambda_2} \frac{f_p V N}{I \cdot r}, \quad (6)$$

where k – is a coefficient ranging from 0.25 to 0.32;

I – mechanical heat equivalent ($I = 43.57$ kcal/J);

r – the radius of the contact spot;

V – sliding speed;

λ_1, λ_2 – thermal conductivity coefficients of contacting bodies;

f_p – the coefficient of friction of the polymer surface.

For a polymer-metal material, expression (6) has the form:

$$T_1 = \frac{k(a + b)}{(\lambda_1 + \lambda_3)a + (\lambda_1 + \lambda_2)b} \frac{f_{MeP} V N}{I \cdot r}, \quad (7)$$

where f_{MeP} – the coefficient of friction of the combined polymer-metal surface.

The expression for determining the step of the metal component in the combined polymer-metal coating is obtained using the law of conservation of thermal energy when it is removed through a cylindrical surface:

$$(1 - \gamma) \frac{2\pi(a + b)\lambda_1(T_1 - T_2)}{\ln \frac{d_2}{d_1}} = \frac{(1 - \beta)2\pi(T_1 - T_2)}{\ln \frac{d_1}{d_1 - 2h - 2\delta_1}} (b\lambda_2 + a\lambda_3). \quad (8)$$

After some transformations of equation (8), we obtain:

$$\frac{(a + b)\lambda_1(1 - \gamma)}{\ln \frac{d_2}{d_1}} = \frac{(1 - \beta)(\lambda_2 b + \lambda_3 a)}{\ln \frac{d_1}{d_1 - 2(\delta_1 + h)}}. \quad (9)$$

Assuming that in the first approximation we have:

$$\ln \frac{d_2}{d_1} = \ln \left(1 + \frac{d_2 - d_1}{d_1} \right) \approx \frac{d_2 - d_1}{d_1}; \quad (10)$$

$$\ln \frac{d_1}{d_1 - 2(\delta_1 + h)} = \ln \left(1 + \frac{2(\delta_1 + h)}{d_1 - 2(\delta_1 + h)} \right) \approx \frac{2(\delta_1 + h)}{d_1 - 2(\delta_1 + h)}, \quad (11)$$

and also taking into account these expressions in equation (9), we have:

$$\frac{(a+b)\lambda_1(1-\gamma)d_1}{d_2 - d_1} = \frac{(1-\beta)(\lambda_2 b + \lambda_3 a)}{2(\delta_1 + h)} [d_1 - 2(\delta_1 + h)]. \quad (12)$$

Having entered the variables ϕ_1 in ϕ_2 equation (12), we have:

$$b = \frac{\lambda_3 \phi_1 - \lambda_1 \phi_2}{\lambda_1 \phi_2 - \lambda_2 \phi_1} a, \quad (13)$$

$$\text{where } \phi_1 = (1-\beta)(d_1 - 2(\delta_1 + h))(d_2 - d_1). \quad (14)$$

$$\phi_2 = 2d_1(1-\gamma)(\delta_1 + h). \quad (15)$$

Taking into account the thermophysical characteristics of the material of the sleeve and the materials covering the cylindrical surface, as well as the geometric parameters of the parts and the coating, it is possible to calculate the technological parameter b of the combined polymer-metal material on the renewable cylindrical surface of the part for this tribocoupling of parts. The formation of combined polymer-metal materials on a cylindrical surface not only increases the speed of heat removal from the friction zone, but also improves the anti-friction properties of the mating surfaces.

From a theoretical point of view, let's consider the change of such an energy characteristic in the tribocoupling of "shaft-sleeve" parts as the coefficient of friction. We obtain an expression for the coefficient of friction for polymer and polymer-metal materials, based on the law of conservation of energy, taking into account the work of friction forces and the process of heat removal from the friction zone.

For a polymer coating, the work of friction forces can be calculated using the formula:

$$A_{mp_p} = \Omega f_p d_1 \left(\frac{N \delta E_1 E_2 d_1 (a+b)}{(d_1 - \delta) [E_1 (1 - \mu_2)^2 + E_2 (1 - \mu_1)^2]} \right)^{1/2}, \quad (16)$$

where Ω – the coefficient that takes into account the nature of the movement of the tribocoupling of parts ($\Omega = 7,9$ - for rotational movement; $\Omega = 3,2d_{\max}^2$ – for oscillating movement);

μ_1, μ_2, E_1, E_2 – are Poisson's ratios and modulus of elasticity, respectively, of the material of the shaft and sleeve.

Taking into account (16), in the law of energy conservation and transformation, we have:

$$\Omega f_p d_1 \left(\frac{N \delta E_1 E_2 d_1 (a+b)}{(d_1 - \delta) [E_1 (1 - \mu_2)^2 + E_2 (1 - \mu_1)^2]} \right)^{1/2} = (1-\beta) \frac{K 2\pi (a+b) \lambda_2 (T_1 - T_2)}{\ln \frac{d_1}{d_1 - 2\delta_1}} + \gamma \frac{2\pi (a+b) \lambda_1 (T_1 - T_2)}{\ln \frac{d_2}{d_1}}, \quad (17)$$

where K – a coefficient that takes into account the material of the coupling parts and the presence of a lubricating medium.

From the obtained equation (17), it is possible to determine the coefficient of friction for the "shaft-sleeve" tribocoupling with a uniform polymer coating of the cylindrical surface of the shaft:

$$f_p = \frac{K 2\pi (a+b)^{1/2} (T_1 - T_2) \left[(1-\beta) \lambda_2 / \ln \frac{d_1}{d_1 - 2\delta_1} + \gamma \lambda_1 / \ln \frac{d_2}{d_1} \right]}{\Omega d_1 \left(\frac{N \delta E_1 E_2 d_1}{(d_1 - \delta) [E_1 (1 - \mu_2)^2 + E_2 (1 - \mu_1)^2]} \right)^{1/2}}. \quad (18)$$

For a combined polymer-metal material on a section of a cylinder with a length of $l = a + b$, the work of friction forces can be calculated by the formula:

$$A_{MeP} = f_{MeP} d_1 \Omega (a+b) \left(\frac{N \delta E_1}{d_1 (d_1 - \delta)} \right)^{1/2} \times \left[\left(\frac{b E_2}{E_1 (1 - \mu_2)^2 + E_2 (1 - \mu_1)^2} \right)^{1/2} + \left(\frac{a E_3}{E_1 (1 - \mu_3)^2 + E_3 (1 - \mu_1)^2} \right)^{1/2} \right], \quad (19)$$

where E_3, μ_3 – are the modulus of elasticity and Poisson's ratio of the metal component of the combined

polymer-metal material, respectively.

Using (3) in the law of energy conservation and transformation, we have:

$$f_{MeP} d_1 \Omega (a+b) \left(\frac{N \delta E_1}{d_1 (d_1 - \delta)} \right)^{1/2} \cdot \left[\left(\frac{b E_2}{E_1 (1 - \mu_2)^2 + E_2 (1 - \mu_1)^2} \right)^{1/2} + \left(\frac{a E_3}{E_1 (1 - \mu_3)^2 + E_3 (1 - \mu_1)^2} \right)^{1/2} \right] =$$

$$= \frac{K 2 \pi \gamma (a+b) \lambda_1 (T_1 - T_2)}{\ln \left(\frac{d_2}{d_1} \right)} + \frac{2 \pi (1 - \beta) (T_1 - T_2)}{\ln \left(\frac{d_1}{d_1 - 2h - 2\delta_1} \right)} (b \lambda_2 + a \lambda_3) \quad (20)$$

From equation (20), it is possible to determine the coefficient of friction for couplings of samples and parts made of a combined polymer-metal material:

$$f_{MeP} = \frac{K \cdot 2 \pi (T_1 - T_2)}{d_1 \Omega \sqrt{\frac{N \delta_1 E_1}{d_1 (d_1 - \delta_1)}}} \cdot \frac{\left[\frac{\gamma (a+b) \lambda_1}{\ln \left(\frac{d_2}{d_1} \right)} + \frac{(1 - \beta) (b \lambda_2 + a \lambda_3)}{\ln \left(\frac{d_1}{(d_1 - 2h) - 2\delta_1} \right)} \right]}{\left(\frac{b E_2}{E_1 (1 - \mu_2)^2 + E_2 (1 - \mu_1)^2} \right)^{1/2} + \left(\frac{a E_3}{E_1 (1 - \mu_3)^2 + E_3 (1 - \mu_1)^2} \right)^{1/2}} \quad (21)$$

By substituting the mechanical and thermophysical characteristics of the materials of the conjugated parts, the coatings applied to them, the geometric dimensions, the components of the combined polymer-metal material, as well as the specified characteristics of the coatings into expressions (18) and (21), one can make sure that $f_{MeP} < f_P$. This indicates an improvement in the antifriction properties of polymer-metal materials and coatings.

Triboconjugation of samples and parts may be brought out of equilibrium under the influence of external friction conditions, random occurrences of natural inclusions on contacting surfaces, relaxation phenomena in combined polymer-metal materials and coatings, development of physico-chemical processes in the area of antifriction contact, etc. The process of deviation from the equilibrium state in them is described by the equation:

$$d \xi_{Me} = (I_{aMe} - I_{aP}) dL_{mp}, \quad (22)$$

where ξ_{Me} – the excess deformation of the polymer compared to the deformation of the metal;

I_{aMe}, I_{aP} – intensity of metal and polymer wear.

By integrating the differential equation (22), it can be shown that the tribosystem of the conjugations of parts returns to equilibrium, that is, it is stable:

$$I_{aMe} - I_{aP} = (I_{aMe} - I_P) \exp \left[L_{mp} \frac{(I_{aMe} - I_{aP})}{\xi_{Me} - \xi_{MeP}} \right], \quad (23)$$

where $I_{aMe} - I_P$ – the deviation from the initial value of the difference in intensity of metal and polymer wear;

$\xi_{Me} - \xi_{MeP}$ – the corresponding deviation of the excess deformation of the polymer.

Expression (23) shows that as the friction path increases, L_{mp} the wear intensities of metal and polymer asymptotically converge. The expression is obtained on the assumption that in a fairly small zone the equilibrium point $I_{aMe} - I_P$ depends linearly on the amount of deformation of the metal ξ_{Me} . Disturbing factors, without affecting the performance of tribocoupled parts, can lead to a temporary increase in the intensity of wear of the coupled surfaces. Due to the optimal choice of parameters a and b , this phenomenon can be minimized.

One of the indicators of the properties of materials to resist wear in the process of friction is the wear coefficient K_u , which is equal to:

$$K_u = \frac{u_h}{P_k L_{mp}}, \quad (24)$$

where u_h – linear wear;

P_k – nominal contact pressure;

L_{mp} – friction path.

The wear coefficient links the strength, speed and structural parameters of the couplings of parts taking into

account their operation. For coupling parts of the "shaft-sleeve" type, the wear factor has the form:

$$K_u = \frac{4l^2 u_{h1} \left(u_{h1} + \frac{d_1}{2} \right) \sin \varphi}{(d_1 + \delta) L_{mp} N}, \quad (25)$$

where l – is the length of the cylindrical surface;

u_{h1} – value of the maximum linear wear of the sleeve;

L_{mp} – friction path;

N_p – load reaction;

δ – nominal clearance of the bearing;

φ – half of the contact angle, determined by the expression:

$$\varphi = \arcsin \left[\frac{N_p l}{2\pi} \left(\frac{1 + \mu_1}{E_1} + \frac{1 + \mu_2}{E_2} \right) \left(\frac{d_1 + \delta}{d_1} \right) \right]^{1/2} + \arccos \left[1 - \frac{d_1 + \delta - u_{h1} - u_{h2}}{d_1 \left(\frac{\delta}{u_{h1} + u_{h2}} + 1 \right)} \right], \quad (26)$$

where the first term is the constant value of the contact angle, determined by the plastic deformation of the materials of the coupling parts, and the second term is the value of the contact angle, which depends on the wear of the sleeve and shaft;

u_{h2} – value of the maximum linear wear of the shaft.

Expression (26) for a uniform polymer coating of a shaft with length $l = a + b$, takes the form:

$$\varphi_p = \arcsin \left[\frac{N(a+b)}{2\pi\delta} \left(\frac{1 + \mu_1}{E_1} + \frac{1 + \mu_2}{E_2} \right) \left(\frac{d_1 + \delta}{d_1} \right) \right]^{1/2} + \arccos \left[1 - \frac{d_1 + \delta - u_{h1} - u_{h2}}{(d_1 - 2\delta_0) \left(\frac{\delta}{u_{h1} + u_{h2}} + 1 \right)} \right], \quad (27)$$

and for a combined polymer-metal coating:

$$\varphi_{MeP} = \arcsin \left[\frac{N}{2\pi\delta} \left(\frac{1 + \mu_1}{E_1} (a+b) + \frac{1 + \mu_2}{E_2} b + \frac{1 + \mu_3}{E_3} a \right) \left(\frac{d_1 + \delta}{d_1} \right) \right]^{1/2} + \arccos \left[1 - \frac{d_1 + \delta - u_{h1} - u_{h2}}{(d_1 - 2\delta_1 - 2h) \left(\frac{\delta}{u_{h1} + u_{h2}} + 1 \right)} \right] \quad (28)$$

Having experimentally determined on the friction machine the wear values u_{h1} and u_{h2} , and also, knowing the dimensions of the conjugated samples and parts and the mechanical parameters of their materials, according to the expression (25), taking into account (27) and (28), it is possible to estimate the coefficient of wear and draw a conclusion about the expediency of using combined polymer-metal coatings in the restoration of parts and their tribological efficiency.

Experimental studies of the influence of the specific load and sliding speed on the friction coefficient in the triboconjugation of samples have shown that the use of polymeric materials in coatings allows to significantly increase the antifriction properties of working surfaces.

Theoretical estimates of the coefficient of friction, carried out according to formulas (18), (21), lead to a similar conclusion. The results of experimental and theoretical studies of the coefficient of friction without lubrication and in extreme friction modes for different surfaces under the same test conditions are given in table 1.

The analysis of the data presented in Table 1 shows that the coefficient of friction of PC is 1.2...1.3 times lower than that of a purely polymer coating and 1.6...2.1 times lower than the coefficient of friction of cast iron and steel without lubrication.

The value of the friction coefficients in the contact zone of triboconjugation of materials ($P=1.0$ MPa, $V = 0.5$ m/s) according to experimental data and theoretical features

Surface	Coefficient of friction, f_{mp}			
	Experimental data		Theoretical evaluations	
	without lubrication	marginal friction	without lubrication	marginal friction
PC	0.302	0.244	0.280	0.220
PMeC	0.263	0.197	0.240	0.180
Cast iron CH18	0.543	0.320	-	-
Steel 45	0.447	0.286	-	-

In conditions of friction without lubrication, the value of the coefficient of friction decreases significantly due to the formation of polymer films and the increase in their density and thickness. The reduction of the friction coefficient in the presence of lubrication is associated with the facilitation of the process of deformation of the surface layers of the friction pairs.

On the basis of the obtained results, it can be noted that RS are distinguished by the specific feature of forming films and maintaining their density and thickness in the process of friction.

Tables 2 and 3 show the change in the coefficient of friction of various surfaces without lubrication and in the limit friction mode depending on the specific load.

Table 2

Dependence of the coefficient of friction of surfaces without lubrication on the specific load ($V = 0.5$ m/s)

Surface	Coefficient of friction, f_{mp}			
	Specific load, MPa			
	0.5	1.0	1.5	2.0
PC	0.350	0.302	0.287	0.254
PMeC	0.302	0.263	0.243	0.213
Cast iron CH18	0.497	0.543	0.675	0.720
Steel 45	0.421	0.447	0.574	0.628

Table 2

Dependence of the surface friction coefficient at the limit friction on the specific load ($V=0.5$ m/s)

Поверхня	Coefficient of friction, f_{mp}			
	Specific load, MPa			
	0.5	1.0	1.5	2.0
PC	0.280	0.244	0.183	0.165
PMeC	0.210	0.197	0.120	0.113
Cast iron CH18	0.397	0.320	0.201	0.196
Steel 45	0.354	0.286	0.213	0.174

The analysis of the data in tables 2, 3 shows that with an increase in the specific load, the friction coefficient decreases both in the case of friction without lubrication and in the case of marginal friction, which corresponds to theoretical estimates within the confidence interval.

Experimental data were compared with theoretical calculations. According to the calculation data, theoretical curves of the dependence of the coefficient of friction on the specific load were constructed for the combined polymer-metal and pure polymer coatings, which are presented in fig. 2 and fig. 3.

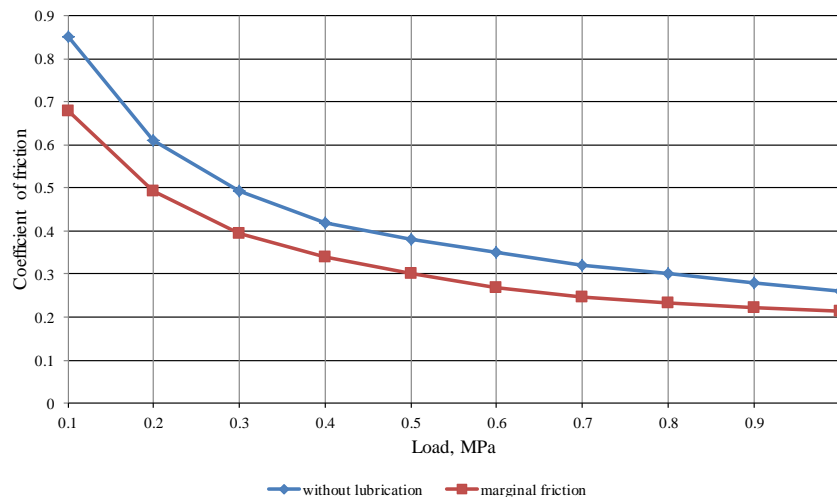


Fig. 2. Theoretical curves of the dependence of the coefficient of friction of the polymer coating (PC) on the specific load

The decrease in the coefficient of friction when the load increases indicates that the contact of the conjugated surfaces of the samples and parts in the considered range of loads is characterized by the condition of elastic contact.

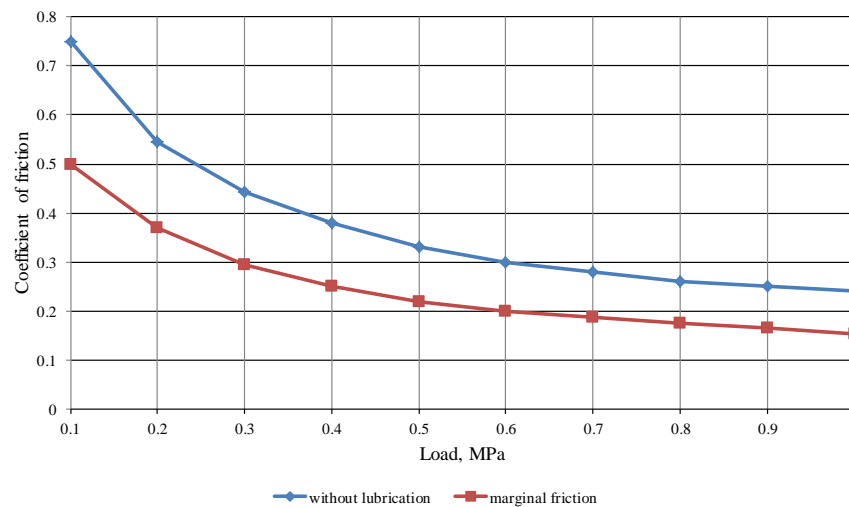


Fig. 3. Theoretical curves of the dependence of the coefficient of friction of the combined polymer-metal material (PMeC) on the specific load

At the limit friction of PMeC with an increase in load, an increase in surface cleanliness is also observed. The surface of the bushings working with combined polymer-metal coatings acquired a shiny polished appearance.

Experimental data on the dependence of the friction coefficients of various surfaces without lubrication and with extreme friction on the sliding speed are given in tables 4 and 5.

Table 4

Dependence of the friction coefficient on the sliding speed without lubrication at a specific pressure of $P=1.0$ MPa

Surface	Coefficient of friction, f_{mp}			
	Sliding speed, m/s			
	0.5	1.0	1.5	2.0
PC	0.28	0.42	0.45	0.37
PMeC	0.24	0.35	0.39	0.30
Cast iron CH18	0.54	0.71	0.68	0.62
Steel 45	0.45	0.67	0.61	0.55

Table 5

Dependence of the friction coefficient on the sliding speed at the limit of friction at a specific pressure of $P=1.0$ MPa

Surface	Coefficient of friction, f_{mp}			
	Sliding speed, m/s			
	0.5	1.0	1.5	2.0
PC	0.22	0.20	0.17	0.15
PMeC	0.18	0.16	0.13	0.09
Cast iron CH18	0.32	0.29	0.23	0.21
Steel 45	0.28	0.25	0.21	0.18

The regularity of the change in friction coefficients from the sliding speed for the combined polymer-metal coating under friction conditions without lubrication is illustrated in fig. 4, and at the limit of friction – fig. 5.

It can be seen that in conditions of friction without lubrication, the coefficient of friction changes in a complex way: when the sliding speed increases to 1.5 m/s, it increases, further increasing the sliding speed leads to a decrease in the value of the friction coefficient. The dependence of the friction coefficient on the sliding speed is, strictly speaking, the dependence of the friction coefficient on the temperature. As the sliding speed increases, the temperature on the friction surface increases, as a result of which the physical and mechanical properties of materials change, the area of actual contact increases, which is accompanied by an increase in frictional forces and, therefore, the friction coefficient. This corresponds to the increasing sections of the curve of the dependence of the coefficient of friction for PMeC in conditions of friction without lubrication on the speed of sliding (fig. 4).

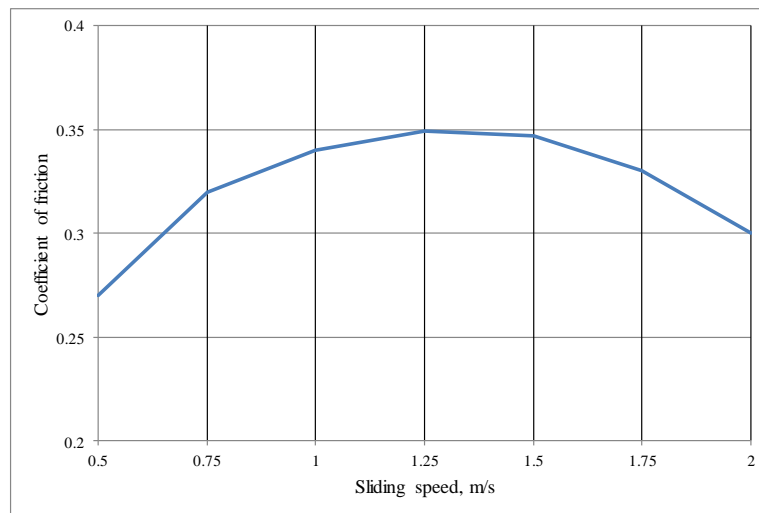


Fig. 4. Theoretical dependence of the PMeC friction coefficient on the sliding speed during friction without lubrication

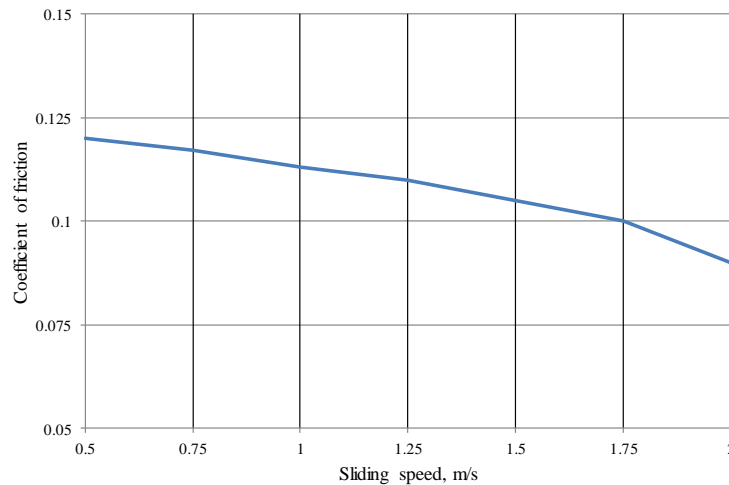


Fig. 5. Theoretical dependence of the PMeC friction coefficient on the sliding speed at the limit of friction

If in the zone of low sliding speeds (low temperature) a sufficient protective film does not have time to form, then with a further increase in speed (temperature), the intensity of film growth increases, its strength decreases, the nature of the film itself changes, and at the same time the shear resistance decreases, which reduces coefficient of friction. When the sliding speed increases, the plastic deformation does not have time to spread inward and is localized in a smaller volume. These features reduce the friction coefficient after the maximum.

Therefore, the transition from one type of violation of frictional bonds to another causes a change in the coefficient of friction and its transition through a maximum (fig. 4). At the limit of friction (fig. 5), the curve of the dependence of the coefficient of friction on the sliding speed has a decreasing character with increasing speed. The presence of an oil film on the friction surfaces changes the temperature regime, as well as the value of the friction forces due to the reduction of the area of direct contact of the friction surfaces.

As a result of experimental studies, it was found that combined polymer-metal coatings work better than pure polymer coatings. This is confirmed by theoretical justifications. As a result of temperature and deformation actions, the friction process of the combined polymer-metal material occurs in the presence of a polymer film with low shear resistance in the contact zone. This explains the decrease in the coefficient of friction. Triboconjugation of materials in operation, in the presence of a polymer, is accompanied by processes of interaction of mechanical destruction products with the metal surface. As a result of these interactions, polymer-metal compounds are formed, which also protect the contacting surfaces of tribo-bonding samples and parts from sticking. In addition, in the friction zone, the number of wear products between the friction surfaces decreases, as the polymer absorbs them from the friction surface, which also affects the reduction of wear intensity and the friction coefficient.

Conclusions

1. The coefficient of friction of PMeC is 1.2...1.3 times less than that of a pure polymer coating and 1.6...2.1 times less than the coefficients of friction of cast iron and steel without lubrication.
2. The decrease in the friction coefficient under the conditions of operation without lubrication is explained by the formation of polymer films on the surface with an increase in their density and thickness.
3. A criterion for evaluating the tribological efficiency of the combined polymer-metal material was

introduced, taking into account the strength, speed and structural parameters of the coupling of parts, taking into account their operating modes

4. The experimental data of the coefficient of friction obtained in the study agree positively with the theoretical calculations.

References

1. Aulin V.V. (2015). Trybofizychni osnovy pidvyshchennia znosostiikosti detalei ta robochykh orhaniv silskohospodarskoi tekhniki [dys. ... d-ra tekhn. nauk: 05.02.04]. 360 s.
2. Bondarenko V.P. (1987). Tribotekhnicheskie kompozityi s vyisokomodulnyimi napolnitelyami [K.: Nauk. dumka]. 232 s.
3. Kabat, O., Sytar, V., Derkach, O., Sukhyy, K. (2021). Polymeric composite materials of tribotechnical purpose with a high level of physical, mechanical and thermal properties [Chemistry and Chemical Technology, 15 (4)]. pp. 543-550.
4. Aulin, V., Lysenko, S., Hrynkiv, A., & Pashynskiy, M. (2022). Pokrashchennia trybolohichnykh kharakterystyk spriazhennia detalei "val-vtulka" polimernymy ta polimerno-kompozytsiinymy materialamy. [Problems of Tribology, 27(3/105)]. pp. 96-107.
5. Aulin V.V., Derkach O.D., Hrynkiv A.V., Makarenko D.O. (2021). Vyznachennia robochoi temperatury kompozytnykh elementiv rukhomykh ziednan v zoni tertia [Naukovyi visnyk Tavriiskoho derzhavnoho ahrotekhnolohichnoho universytetu: elektronne naukove fakhove vydannia. Vyp. 11, tom 1, stattia21].
6. Lan P X, Meyer J L, Economy J, Polycarpou A A. (2016). Unlubricated tribological performance of Aromatic Thermosetting Polyester (ATSP) coatings under different temperature conditions. [Tribol Lett 61(1)] p. 10.
7. Anni, I.A., Kaminskyj, M.S., Uddin, K.Z., Bacha, T.W., Singh, N.K., Stanzione, J.F., Haas, F.M., Koohbor, B. (2023) [Thermoplastic coating on fiber reinforced polymer composites by cold spray additive manufacturing. Materials Today Communications, 35, № 105650].
8. Lazarenko O.A., Vovchenko L.L., Ovsiienko I.V., Matsui L.Iu. (2018). Polimerni kompozyty nanovuhlets-metal: struktura i elektrychni vlastyvoli. [Kyiv-Vinnytsia: TOV «TVORY». 200 s.
9. Majid Hosseini, Abdel Salam Hamdy Makhlof. (2016). Industrial Applications for Intelligent Polymers and Coatings. [Springer International Publishing]. 710 s.
10. de With, G. (2018). Polymer coatings: a guide to chemistry, characterization, and selected applications. [Weinheim : Wiley-VCH Verlag]. 600 p.
11. Sirenko H.O., Sviderskyi V.P. (2016). Teplofizychni vlastyvoli polimernykh kompozytiv: monohrafiia [Za red. H.O. Sirenka. – Ivano-Frankivsk: Vyd. Suprun V.P.]. 292s.
12. Aulin V.V., Hrynkiv A.V., Smal V.V., Lysenko S.V. et al. (2021). Livitskyi Basic approaches and requirements for the design of tribological polymer composite materials with high-modulus fillers [Problems of Tribology, V. 26, No 4/102-2021]. pp. 51-60.
13. Derkach, O.D., Kabat O. S., Bezus R. M., Kovalenko V. L., Kotok V. A. (2018). Investigation of the influence of fullerene-containing oils on tribotechnical characteristics of metal conjunction [ARPN Journal of Engineering and Applied Sciences. VOL. 13 (14)]. pp. 4331-4336.
14. Kabat O., Sytar V., Derkach O., Sukhyy K. (2021). Polymeric composite materials of tribotechnical purpose with a high level of physical, mechanical and thermal properties [Chemistry & chemical technology. Vol. 15, No. 4]. pp. 543-550.
15. Berladir Kh. V., Budnyk O.A., Diadiura K.O. ta in. (2017). Naukovi osnovy rozrobky polimernykh kompozytsiinnykh materialiv trybotekhnichnoho pryznachennia na osnovi politetraforetylenu: monohrafiia. [Sumy : Sumskyi derzhavnyi universytet]. 176 s.
16. Yuan H, Yang S R, Liu X H, Wang Z F, Ma L M, Hou K M, Yang Z G, Wang J Q. (2017). Polyimide-based lubricating coatings synergistically enhanced by MoS₂@HCNF hybrid. [Composites Part A 102]. pp. 9-17.
17. Pan B L, Zhao J, Zhang Y Q, Zhang Y Z. (2012) Wear performance and mechanisms of polyphenylene sulfide/ polytetrafluoroethylene wax composite coatings reinforced by graphene. [J Macromol Sci Part B 51(6)]. pp. 1218-1227.
18. Buketov A.V. ta in. (2018). Vidnovlennia zasobiv transportu fulerenovmisnymy epoksykompozytamy : monohrafiia [Kherson : KhDMA]. 161 s.
19. Naffakh M., Diez-Pascual A.M., Marco C., Ellis G.J., Gomez-Fatou M.A. (2013). Opportunities and challenges in the use of inorganic fullerene-like nanoparticles to produce advanced polymer nanocomposites [Prog.Polym.Sci. V.38]. P. 1163–1231.
20. Kolosov O.Ye., Sivetskyi V.I., Sokolskyi O.L., Ivitskyi I.I., Kurylenko V.M. (2017). Materialy ta tekhnolohii dlia oderzhannia funktsionalnykh polimernykh kompozytsiinnykh materialiv [Naukovi notatky: mizhvuzivskyi zbirnyk (za haluziamy znan «Tekhnichni nauky»). Vyp. 58]. S. 184-192.

Аулін В.В., Лисенко С.В., Гриньків А.В., Тихий А.А., Кузик О.В., Лівіцький О.М.
Закономірність зміни коефіцієнта тертя спряження деталей "вал-втулка" з використанням полімерних матеріалів

Для спряження зразків і деталей типу "вал-втулка" з теоретичної та експериментальної точок зору розглянуто закономірності зміни коефіцієнта тертя для комбінованого полімерометалевого матеріалу і покриття. Виходячи із закону збереження і перетворення енергії в зоні тертя, отримано вирази для оцінки коефіцієнтів тертя для полімерних покриттів і комбінованих полімерометалевих матеріалів з урахуванням властивостей теплопровідності і пружності та геометричних розмірів полімерної та металевої складових. З'ясована узгодженість закономірностей зміни коефіцієнта тертя в трибоспряженнях зразків і деталей від навантаження і швидкості ковзання в режимах без змащення і при граничному терті. Для обґрунтування ефективної експлуатації трибоспряжень деталей з комбінованих полімерометалевих матеріалів введено критерій – коефіцієнт зносу, за яким оцінюють трибологічну ефективність. Показано, що отримані експериментальні результати не суперечать теоретичним обґрунтуванням.

Ключові слова: полімерометалевий матеріал, коефіцієнт тертя, навантаження, швидкість ковзання, трибоспряження зразків і деталей, нерівноважний стан, пружність, деформація, коефіцієнт зносу